Mitigation of the ϵ_K Fine-tuning Problem in the Randall-Sundrum Model

Diplomarbeit im Fachbereich Physik – **Raoul Malm**
May 2012

Institut für Physik

Staudingerweg 7, 55128 Mainz, Germany
Johannes-Gutenberg Universität Mainz

JOHANNES GUTENBERG
UNIVERSITÄT MAINZ

Contents

Introduction

When combining the Standard Model (SM) of elementary particle physics with general relativity for classical gravity, one can account for many of the observed phenomena in nature. Since both theories describe physics on largely separated energy scales, the electroweak scale M_{EW} and the Planck mass M_{Pl} differ by 16 orders of magnitude, one can ask for an explanation of this disparity. Lisa Randall and Raman Sundrum presented a solution to this Hierarchy Problem (HP) in 1998 [1], by supplementing four-dimensional space-time with one warped extra-dimension. Remarkably, their framework further admits an explanation for the hierarchical structure of the quark masses and mixing, which are treated within the SM just as input parameters. Hence, the actual Randall-Sundrum (RS) model represents a promising theory Beyond the Standard Model (BSM). Still each New Physics (NP) model has to pass already performed high-energy precision measurements, that are in tremendously well agreement with the SM predictions. Especially the flavor violating sector constitutes a high hurdle for many BSM theories, since they often involve new sources of flavor violation. However, the RS model provides an intrinsic mechanism to suppress Flavor-Changing Neutral Current processes. While the suppression is sufficient for many processes, there remains a single exception: the CP violating ϵ_K observable in K^0-$\bar{K}^0$ mixing.

This directly leads to the purpose of this thesis. In order to mitigate the tension between the theoretical and the experimental value of ϵ_K within the RS framework, we will present an extension of the Minimal RS model, that will include the proposal of a new colored gauge boson as well as a first treatment of the new Higgs sector. The discussion will be structured in the following way.

To lay the foundation for the subsequent chapters, we will briefly summarize the basic principles of quantum field theory and then proceed to the formulation of the Standard Model (chapter 1). Taking the modern view on the SM as an effective low-energy description of some more fundamental (unknown) theory, we will elaborate on the HPs and the issue of fine-tuning. Given the motivation to propose BSM theories, we will stick to the class of models that extend Minkowski space-time by additional spatial dimensions. After briefly reviewing some early ideas, we will focus on the proposal of Lisa Randall and Raman Sundrum and discuss a specific realization of their idea, referred to as the Minimal RS model, in more detail (chapter 2). All calculations in this framework will encompass tree-level diagrams, exchanging a five-dimensional gauge boson between two incoming and outgoing quarks. Thereby, the appearing five-dimensional boson propagator will play a key role and we will derive

a general expression that is applicable for bosonic particles with spin one (chapter 3). This will provide the necessary equipment to discuss K^0-$\bar{K}^0$ mixing in the RS model. Before, we will introduce the ϵ_K observable and link its definition to a calculable matrix element on the basis of an effective Hamiltonian. After a short consideration of this observable in the SM, we will switch to the RS model and derive an approximate formula for ϵ_K in order to locate the origin of the enhanced theoretical value when compared with the experimental measurement (chapter 4). To mitigate this tension, we will extend the strong gauge sector of the Minimal RS model, which leads to the introduction of a so called pseudo-axial gluon. After describing this proposal in detail, we will perform a numerical analysis and compare the ϵ_K prediction of the Minimal RS model with the one in the extended version (chapter 5). It will turn out that for a realistic extension, one has to modify the Higgs sector by introducing new color charged fields on both ends of the extra-dimension. After presenting the basic formulation within the RS framework (chapter 6), we will conclude and present an outlook for prospective work to be done.

1. The Standard Model of Particle Physics

The Standard Model is a mathematical description of elementary particles and their interactions via the strong, weak and electromagnetic forces. Being a quantum field theory, we shortly repeat the underlying principles in section 1.1 and discuss the issue of renormalization, on the basis of an example in Quantum Chromodynamics (QCD). After that, we proceed with the Lagrangian formulation of the SM in 1.2, which is nowadays viewed as a low energy description of a more fundamental (unknown) theory (sections 1.3 and 1.4). In this context, we will encounter several Hierarchy Problems, that motivate and guide the search for New Physics models.

1.1. Basic Principles

Since experimentalists measure cross sections or decay rates, we should start with the description of a scattering process [2]. The typical situation is, that several particles approach each other from a macroscopically large distance and then interact in a microscopically small region. What we need is an Hamiltonian, that can be decomposed into a free H_0 and an interaction part H_I,

$$H = H_0 + H_I \ . \tag{1.1}$$

The particles long before ($t \to -\infty$) or long after ($t \to +\infty$) the scattering process are non-interacting, free particle states. Therefore, they are eigenstates of H_0 and we denote them by $|\alpha\rangle_0$ and $|\beta\rangle_0$. The labels α and β summarize their properties like mass m, spin s, spin projection σ (helicity for massless particles) and further internal quantum numbers n (like electric charge Q_e),

$$\alpha = (m_1, s_1, \sigma_1, n_1; m_2, s_2, \sigma_2, n_2; ...) \tag{1.2}$$

and analogously for β. The interacting states of the scattering process must be eigenstates[1] of the full Hamiltonian H. We speak of them as the "in" and "out" states $|\alpha\rangle_{\text{in}}$ and $|\beta\rangle_{\text{out}}$, when they fulfill the formal conditions[2]

$$e^{-iHt}|\alpha\rangle_{\text{in}} = e^{-iH_0 t}|\alpha\rangle_0 \quad \text{for} \quad t \to -\infty, \tag{1.3}$$

$$e^{-iHt}|\beta\rangle_{\text{out}} = e^{-iH_0 t}|\beta\rangle_0 \quad \text{for} \quad t \to +\infty, \tag{1.4}$$

---

[1]To be manifest Lorentz invariant, we choose the Heisenberg picture, in which states do not change with time.

[2]Correctly, one has to work with well-behaved superpositions of states (wave-packets).

stating that when we observe[3] $|\alpha\rangle_{\text{in}}$, $|\beta\rangle_{\text{out}}$ at times $t \to -\infty$, $t \to +\infty$, we encounter the free particles described by the labels α and β. Now, we can define the object of interest, the probability amplitude for the transition $\alpha \to \beta$,

$$S_{\beta\alpha} = {}_{\text{out}}\langle\beta|\alpha\rangle_{\text{in}} = {}_0\langle\beta|S|\alpha\rangle_0, \tag{1.5}$$

which is one component of the general S-Matrix. Due to (1.3) and (1.4), the corresponding S-operator is given by $S = U(+\infty, -\infty)$, where

$$U(\tau, \tau_0) = e^{iH_0\tau} e^{-iH(\tau-\tau_0)} e^{-iH_0\tau_0} . \tag{1.6}$$

Differentiating (1.6) with respect to τ, we find that it obeys the following differential equation

$$i\frac{d}{d\tau}U(\tau, \tau_0) = H_I(\tau)U(\tau, \tau_0), \tag{1.7}$$

where $H_I(\tau) = e^{iH_0\tau} H_I e^{-iH_0\tau}$ is formulated in the interaction picture. At this stage, we can impose physical and sensible demands on the scattering matrix:

Poincaré-Invariance: In order to achieve a Poincaré[4] invariant S-matrix, we assume that we can write $H_I(\tau)$ as a position space integral over a scalar[5] density $\mathcal{H}_I(\vec{x}, \tau)$,

$$H_I(\tau) = \int d^3x \, \mathcal{H}_I(\vec{x}, \tau) . \tag{1.8}$$

Then, one can solve (1.7) and express the S-operator by

$$S = 1 + \sum_{n=1}^{\infty} \frac{(-i)^n}{n!} \int d^4x_1...d^4x_n \, T\left\{\mathcal{H}_I(x_1)...\mathcal{H}_I(x_n)\right\}, \tag{1.9}$$

which is known as the Dyson series. The solution (1.9) is almost in a manifest Poincaré invariant form, except for the time-ordering[6] of the Hamilton densities. Due to the definition of T, we can solve this issue by demanding that $\mathcal{H}_I$ commutes at all space-like points

$$[\mathcal{H}_I(x), \mathcal{H}_I(y)] = 0 \quad \text{for} \quad (x-y)^2 < 0, \tag{1.10}$$

which is referred to as a causality condition. Note, that throughout this thesis, we use the signature $(+, -, -, -)$ for the Minkowski metric $\eta_{\mu\nu}$.

---

[3] The operators e^{-iHt} and e^{-iH_0t} perform a time-translation of the observer coordinate system.

[4] We refer to proper and orthochronous Lorentz-transformations Λ^μ_ν with additional space-time translation a^μ, such that coordinates transform by $x'^\mu = \Lambda^\mu_\nu x^\nu + a^\mu$.

[5] Given a unitary Poincaré transformation $U_0(\Lambda, a)$, this states $U_0(\Lambda, a)\mathcal{H}(x)U_0^{-1}(\Lambda, a) = \mathcal{H}(\Lambda x + a)$.

[6] For $n = 2$, the definition is $T\{\mathcal{H}_I(x_1)\mathcal{H}_I(x_2)\} \equiv \theta(x_1^0 - x_2^0)\mathcal{H}_I(x_1)\mathcal{H}_I(x_2) + \theta(x_2^0 - x_1^0)\mathcal{H}_I(x_2)\mathcal{H}_I(x_1)$. The cases $n > 2$ can be generalized in an obvious way.

Unitarity: Beginning with a state $|\alpha\rangle$ at $t \to -\infty$, the probability to find it, after the scattering process, in any other state at $t \to +\infty$ must sum up to 1,

$$1 = \sum_\beta S_{\beta\alpha} = \sum_\beta {}_0\langle\beta|S|\alpha\rangle_0 \quad \Rightarrow \quad S^\dagger S = 1, \tag{1.11}$$

which leads to a unitary S-operator. Together with (1.7), this means that the time-evolution operator is unitary and therefore H must be hermitian. This makes $\mathcal{H}_I$ a real scalar density.

Cluster Decomposition Principle: Distant experiments should lead to uncorrelated results. From this statement one can reason (chapter four in [2]), that it is sensible to construct $\mathcal{H}_I$ out of creation and annihilation field-operators. This leads one to use quantum fields

$$\psi_l(x) = \sum_\sigma \int \frac{d^3p}{(2\pi)^3 2p^0} \left[e^{-ipx} u_l(\vec{p}, \sigma) a(\vec{p}, \sigma) + v_l(\vec{p}, \sigma) e^{ipx} v_l(\vec{p}, \sigma) a^{c\dagger}(\vec{p}, \sigma) \right], \tag{1.12}$$

where $a(\vec{p}, \sigma)$ is an annihilation operator for particles, while $a^{c\dagger}(\vec{p}, \sigma)$ creates antiparticles. The coefficients u_l and v_l depend on the representation of the Lorentz group. Concerning the SM fields, we will encounter scalars ($u_l = v_l = 1$), vectors ($u_l = u_\mu, v_l = v_\mu$) and Dirac spinors ($u_l = u_\alpha, v_l = v_\alpha$).

Typically, one formulates quantum field theories in terms of Lagrangians, since this has advantages concerning the implementation of further internal symmetries. When we decompose the Lagrangian $\mathcal{L} = \mathcal{L}_0 + \mathcal{L}_I$, we can effectively replace $\mathcal{H}_I = -\mathcal{L}_I$ in (1.9).

In order to fulfill the above-mentioned demands on the S-matrix[7], the Lagrangian must be hermitian, Lorentz invariant and has to be constructed out of quantum fields. In the past, people further demanded the criterion of renormalizability that effectively reduced the number of possible terms in $\mathcal{L}$. Although this viewpoint has changed during the last three decades, we repeat the steps of reasoning and the idea behind renormalization in general, by giving a short example.

Renormalization

Nowadays, we associate with each quantum field theory an energy cutoff Λ, up to which the theory is assumed to be valid. This gives us a natural regulator to cutoff ultraviolet infinities, that would arise from integration over the complete four-momentum space inside loops of Feynman diagrams. The idea of renormalization is then to express all observable quantities like cross sections or decay amplitudes

---

[7]The first part of this section just intended to repeat the basic principles and to motivate the use of quantum fields. There are still some caveats in the line of reasoning, that are discussed in [3].

in terms of physical parameters, like masses or couplings. But, these are not the so called "bare" parameters that appear in the Lagrangian. For instance, we can consider the (partial) QCD Lagrangian

$$\mathcal{L}_B = \bar{q}_B(i\gamma^\mu\partial_\mu - m_B)q_B - g_{s,B}\,\bar{q}_B\gamma^\mu\frac{\lambda_a}{2}q_B\,G^a_{B,\mu}, \tag{1.13}$$

where the subscript B labels the bare quantities like the quark field q_B, the mass m_B, the strong coupling $g_{s,B}$ and the gluon field G_B. Quantum corrections in form of loop diagrams will shift these parameters. As an example, we want to consider the one-loop self energy diagram of the quark in fig. 1.1. We know, that this diagram exhibits a singularity when one does not cutoff the momentum integration in the loop. But, instead of using a sharp cutoff as a regulator, we make use of dimensional regularization, where the dimension of space-time is slightly changed to $4 - 2\epsilon$ with $\epsilon \ll 1$. This alters the canonical mass dimension of the quark fields and the gluon field, such that we have to introduce an energy scale μ to render the interaction in (1.13) with the correct dimension. The renormalized or physical quantities can then be defined via

$$q_B = Z_2^{1/2}q, \qquad G^a_{\mu,B} = Z_3^{1/2}G^a_\mu, \qquad g_{s,B} = Z_g\mu^\epsilon g_s, \qquad m_B = Z_m m, \tag{1.14}$$

where Z_2, Z_3, Z_g and Z_m are called renormalization constants. With these, we can decompose $\mathcal{L}_B$ into a renormalized Lagrangian $\mathcal{L}_R$ and a counter-term Lagrangian $\mathcal{L}_{CT}^{(1)}$,

$$\mathcal{L}_R = \bar{q}(i\gamma^\mu\partial_\mu - m)q - g_s\mu^\epsilon\,\bar{q}\gamma^\mu\frac{\lambda_a}{2}q\,G^a_\mu \tag{1.15}$$

$$\mathcal{L}_{CT}^{(1)} = (Z_2-1)\bar{q}i\gamma^\mu\partial_\mu q - (Z_2 Z_m - 1)m\bar{q}q - (Z_g Z_2 Z_3^{1/2} - 1)g_s\mu^\epsilon\,\bar{q}\gamma^\mu\frac{\lambda_a}{2}q\,G^a_\mu \tag{1.16}$$

such that $\mathcal{L}_B = \mathcal{L}_R + \mathcal{L}_{CT}^{(1)}$. This procedure is referred to as the counter-term method. Now, we can calculate the self-energy diagram using $\mathcal{L}_R$ and then add the tree level contribution coming from $\mathcal{L}_{CT}$, yielding [4]

$$-i\Sigma_{ab}(p) = \frac{g_s^2}{12\pi^2\epsilon}(-\not{p} + 4m)\delta_{ab} + [(Z_2-1)\not{p} - (Z_2 Z_m - 1)m]\delta_{ab} + \text{finite terms}\,. \tag{1.17}$$

We see, that we can absorb the appearing singularities (for $\epsilon \to 0$) by adjusting the renormalization constants Z_2 and Z_m,

$$Z_2 = 1 - \frac{g_s^2}{12\pi^2\epsilon} + \mathcal{O}(g_s^4), \qquad\qquad Z_m = 1 - \frac{g_s^2}{4\pi^2\epsilon} + \mathcal{O}(g_s^4)\,. \tag{1.18}$$

So, by redefining the quark field and the mass, we obtain a finite expression for the self-energy diagram. Furthermore, the counter-term in (1.16) is sufficient and does not involve new sorts of operators, than are already present in $\mathcal{L}_B$.
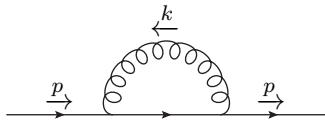
Figure 1.1.: Quark self-energy graph.

In general, when proceeding with a two loop diagram, one has to calculate the relevant diagram using $\mathcal{L}_R + \mathcal{L}_{CT}^{(1)}$ and then construct a new counter-term $\mathcal{L}_{CT}^{(2)}$, that cancels appearing singularities. Iterating this procedure for arbitrary loop orders, one speaks of a renormalizable theory when all introduced counter-terms $\mathcal{L}_{CT}^{(n)}$ involve the same operators as appear in $\mathcal{L}_B$. A necessary condition can be inferred by using power counting of the internal momenta in a Feynman diagram. It turns out [5], that operators Q_i with canonical mass dimension greater than four lead to divergencies in Feynman diagrams that can not be absorbed by counter-terms having the same structure as $\mathcal{L}_B$.

In case of D space-time dimensions, the necessary condition for renormalizability can be expressed as $[Q_i] \leq D$. When we write each term in the Lagrangian as $g_i Q_i$ with coupling g_i, this can be transformed in a statement about the coupling. In natural units, $\hbar = c = 1$, the action $S = \int d^D x \, \mathcal{L}(x)$ is dimensionless, therefore the Lagrangian must have mass dimension D, $[\mathcal{L}] = D$. Thus, it is necessary that the coupling has no negative canonical mass dimension, $[g_i] \geq 0$.

For a long time, one demanded that the renormalizability condition $[g_i] \geq 0$ must be fulfilled by any realistic quantum field theory. The reason given is that the new counter-terms (infinitely many) introduce new couplings, that have to be measured in experiments and therefore spoil the predictivity of the theory. But, this viewpoint has changed due to the interpretation of QFTs as effective field theories (EFTs) rather than fundamental theories, where one would set $\Lambda \to \infty$. In fact, an EFT is less but still predictive since each non-renormalizable operator gets suppressed by powers of the cutoff Λ, effectively reducing its contributions on physical processes with energies $E \ll \Lambda$. But before elucidating the concept of EFTs (in 1.4), we proceed with the construction of the SM Lagrangian .

1.2. The SM Lagrangian

First, we need to specify the quantum field content to start with. Concerning the matter fields, we introduce spin zero (Higgs field) and spin 1/2 (quarks, leptons) fields and assign them quantum numbers under the global SM group

$$G_{\text{SM}} = SU(3)_c \times SU(2)_L \times U(1)_Y, \tag{1.19}$$

that are listed in tab. 1.1. At this stage, we have to write down all terms, constructed from the fields, that form real Lorentz scalars and that are singlets under the global SM group. But, we further need to include force mediating particles, which have spin one. This can be done by demanding all terms to be locally gauge invariant, enhancing G_{SM} to a gauge group. With these requirements, the most general Lagrangian is an infinite sum of operators Q_i times coefficients C_i,

$$\mathcal{L} = \sum_{i=0}^{\infty} C_i Q_i = C_0 + \mathcal{L}_{\mathrm{SM}} + \sum_{\{i|[Q_i]\geq 5\}} C_i Q_i \qquad (1.20)$$

The first term is just a constant and has no physical meaning as long as we do not include gravity. We will say more about this in section 1.4. The second part in (1.20) contains all operators with mass dimension[8] $[Q_i] \leq 4$ and is what we usually refer to as the SM Lagrangian $\mathcal{L}_{\mathrm{SM}}$. We restrict our discussion here to this selection of operators, since higher dimensional operators with $[Q_i] \geq 5$ are suppressed, see section 1.4.

Focusing on the SM Lagrangian, the strategy is to write down all terms with symmetry invariant operators of dimension $[Q_i] \leq 4$. For the next steps, it is convenient to divide $\mathcal{L}_{\mathrm{SM}}$ into four parts

$$\mathcal{L}_{\mathrm{SM}} = \mathcal{L}_{\mathrm{FS}} + \mathcal{L}_{\mathrm{GBS}} + \mathcal{L}_{\mathrm{YS}} + \mathcal{L}_{\mathrm{HS}}, \qquad (1.21)$$

denoted as the fermion (FS), gauge boson (GBS), Yukawa (YS) and Higgs (HS) sector. Up to this stage, (1.21) does not contain any mass terms for the fermions or gauge bosons. A solution can be provided by the Higgs field Φ, taking a non-zero vacuum expectation value $\langle 0|\Phi|0\rangle$, which is known as the Higgs mechanism. Furthermore, $\mathcal{L}_{\mathrm{SM}}$ is augmented by a gauge-fixing part $\mathcal{L}_{\mathrm{GF}}$ and Faddeev-Popov ghosts in $\mathcal{L}_{\mathrm{FPG}}$, which have to be included when properly quantizing gauge fields.

Based on this overview, we will go step by step through the terms and mechanisms in the following subsections.

Fermion Sector

The Lorentz group admits two inequivalent representations for describing spin $1/2$ particles. We denote the corresponding $(1/2, 0)$ Weyl spinor by χ_f and the $(0, 1/2)$ spinor by ξ_f, which are both two-component objects. Instead of working with them directly, we use a four component version

$$f_L = \begin{pmatrix} \chi_f \\ 0 \end{pmatrix}, \qquad\qquad f_R = \begin{pmatrix} 0 \\ \xi_f \end{pmatrix}, \qquad (1.22)$$

with a suitable notation, that is adjusted to construct Dirac spinors later on. But a priori, f_L and f_R describe two distinct fermion particles. Therefore we can assign

---

[8]The SM is defined on four-dimensional space-time, so $D = 4$.

SM Fields	$SU(3)_c$	$SU(2)_L$	$U(1)_Y$	I_3	Q_e
$(u_L, d_L), (c_L, s_L), (t_L, b_L)$	**3**	**2**	$1/6$	$(1/2, -1/2)$	$(2/3, -1/3)$
u_R, c_R, t_R	**3**	**1**	$2/3$	0	$2/3$
d_R, s_R, b_R	**3**	**1**	$-1/3$	0	$-1/3$
$(\nu_{eL}, e_L), (\nu_{\mu L}, \mu_L), (\nu_{\tau L}, \tau_L)$	**1**	**2**	$1/6$	$(1/2, -1/2)$	$(0, -1)$
e_R, μ_R, τ_R	**1**	**1**	$2/3$	0	-1
$\Phi = (\Phi^1, \Phi^2)$	**1**	**2**	$1/2$	$(1/2, -1/2)$	$(1, 0)$
Gauge Fields	G_μ^a	W_μ^i	B_μ		

Table 1.1.: Quantum numbers of the SM fields. The fermion fields are ordered in genera-tions/families. The $SU(2)_L$ eigenvalues of $\tau^3 = \sigma^3/2$ are denoted by the isospin I_3 component, while Q_e represents the electric charge in units of $e = |e|$.

them different quantum numbers under $G_{\rm SM}$, as listed in tab. 1.1. We collect the left-chiral $SU(2)_L$ (weak isospin) quark and lepton doublets and singlets[9] by

$$Q_L^n = \begin{pmatrix} u_L \\ d_L \end{pmatrix}, \begin{pmatrix} c_L \\ s_L \end{pmatrix}, \begin{pmatrix} t_L \\ b_L \end{pmatrix}, \qquad E_L^n = \begin{pmatrix} \nu_{eL} \\ e_L \end{pmatrix}, \begin{pmatrix} \nu_{\mu L} \\ \mu_L \end{pmatrix}, \begin{pmatrix} \nu_{\tau L} \\ \tau_L \end{pmatrix}, \qquad (1.23)$$

$$u_R^n = u_R, c_R, t_R, \qquad d_R^n = d_R, s_R, b_R, \qquad e_R^n = e_R, \mu_R, \tau_R, \qquad (1.24)$$

with "generation" or "family" index $n = 1, 2, 3$. Hence we can construct the gauge invariant kinetic Lagrangian

$$\mathcal{L}_{\rm FS} = \bar{Q}_L^n i\slashed{D} Q_L^n + \bar{E}_L^n i\slashed{D} E_L^n + \bar{u}_R^n i\slashed{D} u_R^n + \bar{d}_R^n i\slashed{D} d_R^n + \bar{e}_R^n i\slashed{D} e_R^n, \qquad (1.25)$$

where $\slashed{D} \equiv D_\mu \gamma^\mu$ and $\bar{Q}_L \equiv (Q_L)^\dagger \gamma^0$. The covariant derivate D_μ ensures that each term in $\mathcal{L}_{\rm FS}$ stays invariant under local transformation of $G_{\rm SM}$. In general, it is given by

$$D_\mu = \partial_\mu - igW_\mu^i \tau^i - ig'B_\mu Y - ig_s G_\mu^a T^a, \qquad (1.26)$$

where Y denotes the hypercharge of the matter field (D_μ is acting on) and $\tau^i = \sigma^i/2$, $T^a = \lambda^a/2$ are the generators[10] of the $SU(2)_L$ and $SU(3)_c$ groups respectively. It is further understood, that when D_μ is acting on any field ψ, it should only include the relevant gauge boson terms, where ψ has nontrivial quantum numbers under the gauge group.

---

[9] Concerning the neutrinos, we do not include a right-chiral one, since it would be a singlet under each of the groups and therefore does not interact with any of the other fields.

[10] They fulfill the commutator relation $[\tau^i, \tau^j] = i\epsilon^{ijk}\tau^k$ and $[T^a, T^b] = if^{abc}T^c$. The 2×2 Pauli matrices are given by $\sigma^1 = \begin{pmatrix} 0 & 1 \\ 1 & 0 \end{pmatrix}, \sigma^2 = \begin{pmatrix} 0 & -i \\ i & 0 \end{pmatrix}, \sigma^3 = \begin{pmatrix} 1 & 0 \\ 0 & -1 \end{pmatrix}$, while we use a common representation [5] in case of the Gell-Mann matrices λ^a, $a = 1, 2, ..., 8$.

For instance, we can consider the quark doublet Q_L^n, that transforms nontrivially under the complete SM group, therefore

$$D_\mu Q_L^n = \left(\partial_\mu - igW_\mu^i \tau^i - ig' B_\mu Y_{Q_L} - ig_s G_\mu^a T^a \right) Q_L^n, \qquad (1.27)$$

with hypercharge $Y_{Q_L} = 1/6$. Note, that we usually omit to write the $SU(2)_L$ and $SU(3)_c$ indices for the sake of clarity[11], while keeping in mind that τ^i acts in isospin space and T^a in color space. To guarantee that the term $\bar{Q}_L \not{D}_\mu Q_L$ in (1.25) stays invariant under the local transformations

$$U_I(x) = e^{i\theta_L^i(x)\tau^i}, \qquad U_Y(x) = e^{i\theta_Y(x)Y}, \qquad U_c(x) = e^{i\theta_c^a(x)T^a}, \qquad (1.28)$$

with space-time dependent functions $\{\theta_L^i(x)\}$, $\theta_Y(x)$ and $\{\theta_c^a(x)\}$, we have to demand that $D_\mu Q_L$ transforms like the field itself under each of the transformations, so in general $D'_\mu Q'_L = U(x) D_\mu Q_L$. This can only be accomplished, when the gauge fields do also transform in a suitable way. But instead of considering the finite transformations, it is more instructive to work out the behavior for infinitesimal transformation θ_I^i, θ_Y, $\theta_c^a \ll 1$, yielding then

$$B_\mu(x) \xrightarrow{U(1)_Y} B'_\mu(x) = B_\mu(x) + \frac{1}{g} \partial_\mu \theta_Y(x), \qquad (1.29)$$

$$W_\mu^i(x) \xrightarrow{SU(2)_L} W_\mu'^i(x) = W_\mu(x) + \frac{1}{g'} \partial_\mu \theta_L^i(x) + i\epsilon^{ijk} W_\mu^j(x)\theta_L^k(x), \qquad (1.30)$$

$$G_\mu^a(x) \xrightarrow{SU(3)_c} G_\mu'^a(x) = G_\mu(x) + \frac{1}{g_s} \partial_\mu \theta_c^a(x) + if^{abc} G_\mu^b(x)\theta_c^c(x) . \qquad (1.31)$$

Worth mentioning is that B_μ transforms as a singlet under the global $U(1)_Y$, which states that it carries no charge under this group (abelian case). A consequence is that there is no restriction on the coupling strength between B_μ and the matter fields, which is the reason why we can assign them different hypercharge values in tab. 1.1. This is different for the non-abelian $SU(2)_L$ and $SU(3)_c$ groups, where W_μ^i and G_μ^a transform in their respective adjoint representations[12]. For example, G_μ^a must couple with equal strength g_s (strong coupling) to each quark flavor, otherwise gauge invariance is lost.

Coming back to $\mathcal{L}_{FS}$, there are no more terms that respect the symmetry requirements. We may think of Lorentz invariant Majorana or Dirac mass terms

$$\frac{1}{2}m_f(\chi_f^T i\sigma_2 \chi_f + \text{h.c.}) \qquad \text{or} \qquad -m_f \bar{f}f = -m_f(\bar{f}_L f_R + \bar{f}_R f_L), \qquad (1.32)$$

---

[11]Otherwise, (1.27) reads

$$(D_\mu Q_L^n)^{i,\alpha} = \left(\partial_\mu \delta_{ij}\delta_{\alpha\beta} - igW_\mu^k \tau_{ij}^k \delta_{\alpha\beta} - ig' B_\mu Y_{Q_L}\delta_{ij}\delta_{\alpha\beta} - ig_s G_\mu^a T_{\alpha\beta}^a \delta_{ij} \right) (Q_L^n)^{j,\beta},$$

with isospin indices $i, j = 1, 2$ and color indices $\alpha, \beta = 1, 2, 3$.

[12]The generators of the adjoint representation can be constructed from the structure constants. In case of SU(2) and SU(3), we have $(\tau_{\text{adj}}^j)_{ik} = i\epsilon^{ijk}$ and $(T_{\text{adj}}^b)_{ac} = if^{abc}$ respectively.

but both are not singlets under $SU(2)_L$ or $U(1)_Y$ transformations. As mentioned earlier, we therefore introduce the Higgs field and make use of the related Higgs mechanism, which will be explained further below.

Gauge Boson Sector

Missing are the kinetic terms for the gauge bosons. They are given by the field strength tensors

$$B_{\mu\nu} = \partial_{[\mu} B_{\nu]}, \quad W^i_{\mu\nu} = \partial_{[\mu} W^i_{\nu]} + g' \epsilon^{ijk} W^j_\mu W^k_\nu, \quad G^a_{\mu\nu} = \partial_{[\mu} G^a_{\nu]} + g_s f^{abc} G^b_\mu G^c_\nu, \tag{1.33}$$

where the bracket [...] denotes an anti-symmetrization of the enclosed indices, for instance $\partial_{[\mu} B_{\nu]} = \partial_\mu B_\nu - \partial_\nu B_\mu$. With these, we can construct the following gauge invariant terms

$$\begin{aligned}
\mathcal{L}_{\text{BS}} = &-\frac{1}{4} W^i_{\mu\nu} W^{i\mu\nu} - \frac{1}{4} B_{\mu\nu} B^{\mu\nu} - \frac{1}{4} G^a_{\mu\nu} G^{a\mu\nu} \\
&+ g'^2 \frac{\Theta_W}{32\pi^2} W^i_{\mu\nu} \tilde{W}^{i\mu\nu} + g^2 \frac{\Theta_B}{32\pi^2} B_{\mu\nu} \tilde{B}^{a\mu\nu} + g_s^2 \frac{\Theta_G}{32\pi^2} G^a_{\mu\nu} \tilde{G}^{a\mu\nu},
\end{aligned} \tag{1.34}$$

where $\tilde{W}_{\mu\nu}, \tilde{B}_{\mu\nu}, \tilde{G}_{\mu\nu}$ are the dual field strengths, in general defined by $\tilde{F}_{\mu\nu} \equiv \frac{1}{2} \epsilon_{\mu\nu\rho\sigma} F^{\rho\sigma}$. Although each of the last three CP violating[13] terms in (1.34) can be rewritten as a total derivative of a current, this does not imply a priori that they give no contribution under the action integral. In fact, the answers are subtle and touch the subjects of anomalies, instantons and topology of gauge transformations [6], [5]. However, it turns out that Θ_W and Θ_B are not physical, while the strong Θ_G term is observable by measuring the electric dipole moment of the neutron (nEDM), yielding an upper bound of $\Theta_G \lesssim 10^{-11}$.

Further terms in (1.34) are not allowed, so we end up with massless spin one gauge bosons. The Higgs mechanism will also explain the occurrence of mass terms for the experimentally observed massive $W^\pm$ and Z bosons.

Gauge Fixing and Faddeev-Popov Ghosts

The freedom to perform gauge transformations without rendering the Lagrangian $\mathcal{L}_{\text{SM}}$ expresses, that the gauge fields are described by more degrees of freedom (DOF) than physical ones. While a Lorentz vector field admits four components, we know that massless and massive gauge bosons have two respectively three DOF according to their number of polarizations. For instance, we can consider the gluon field G^a_μ and make use of the path integral formalism[14]. Restricting on the free-field part, the

---

[13]This is due to the pseudotensor $\epsilon_{\mu\nu\rho\sigma}$, that flips its sign under a parity transformation.

[14]This formalism presents another way, besides the operator formalism, to quantize the theory and to develop perturbation theory. Note, that the path integral formalism involves classical fields for the bosons, while fermionic fields are represented by (anti-commuting) Grassmann valued fields.

generating functional reads

$$Z_0^G[J] = \int [dG_\mu^a] \, e^{i \int d^4x \left(-\frac{1}{4} \partial_{[\mu} G_{\nu]}^a \partial^{[\mu} G^{a\nu]} + J_\mu^a A^{a\mu} \right)}, \tag{1.35}$$

where $J_\mu^a(x)$ are so called Schwinger sources[15], introduced to create and destroy gluon particles. We can rewrite the gluon kinetic part in (1.35) to bring it into a bilinear form,

$$\int d^4x \left(-\frac{1}{4} \partial_{[\mu} G_{\nu]}^a \partial^{[\mu} G^{a\nu]} \right) = \frac{1}{2} \int d^4x \, G_\mu^a [\delta_{ab}(\eta^{\mu\nu} \partial^\alpha \partial_\alpha - \partial^\mu \partial^\nu)] G_\nu^b, \tag{1.36}$$

making use of a partial integration. The usual way to obtain the propagator is to perform a Gaussian integration of (1.35), for which we need to determine the inverse of the differential operator standing in between the fields G_μ^a (in (1.36)), such that

$$\delta_{ab}(\eta^{\mu\nu} \partial^\alpha \partial_\alpha - \partial^\mu \partial^\nu) D_{\nu\rho}^{G,bc}(x-y) = \delta_{ac} \, g_\rho^\mu \delta^4(x-y) \,. \tag{1.37}$$

One can show that the inverse does not exist, e.g. the operator has a zero eigenvalue when acting on $\partial_\nu g(x)$ for some smooth function $g(x)$.

Taking another view, gauge invariance leads to an overcounting of field configurations in $Z[J]$, that are related by gauge transformations. A procedure to reformulate the generating functional and divide out the infinite extra "volume" has been proposed by Faddeev and Popov [7]. Following their derivation, we can fix a gauge by adding the term

$$-\frac{1}{2\xi_G} G_\mu^a G^{a\mu} \tag{1.38}$$

to the Lagrangian with the gauge fixing parameter ξ_G and drop the redundant degrees of freedom in the functional measure. While the interaction in the abelian case does not change effectively, one has to introduce ghost fields, described by anti-commuting Grassmann fields $c_a(x)$ in the non-abelian case (see [5] for details). These fields violate the spin-statistic theorem and are therefore unphysical (non-observable), but need to be included in calculations, since they occur in internal loops. For our gluon example, the Faddeev-Popov Lagrangian reads

$$\mathcal{L}_{\text{FPG}}^G = c_a^\dagger \partial^\mu [\delta_{ab} \partial_\mu - g_s f_{abc} A_\mu^c] c_b \,. \tag{1.39}$$

In general, ghost fields couple only to the (non-abelian) gauge fields. However, in this thesis ghosts are not needed in the calculations and we refer to [8] for a complete citation within the Standard Model.

---

[15]When we perform a functional differentiation of $Z[J]$, we obtain the Green's functions that represent on-shell Feynman diagrams.

Yukawa Sector

When we introduce the Higgs field Φ, which is a scalar $SU(2)_L$ doublet with $Y_\Phi = 1/2$ (see tab. 1.1), one can write down Yukawa terms involving quark, lepton doublets and singlets. They are included in

$$\mathcal{L}_{\text{YS}} = -Y_d^{mn} \bar{Q}_L^m \Phi d_R^n - Y_u^{mn} \bar{Q}_L^m (i\sigma_2 \Phi^*) u_R^n - Y_e^{mn} \bar{E}_L^m \Phi e_R^n + \text{h.c.} , \qquad (1.40)$$

where $m, n = 1, 2, 3$ represent generation indices and $\boldsymbol{Y}_u$, $\boldsymbol{Y}_d$, $\boldsymbol{Y}_e$ are general, complex 3×3 matrices. Now, assume that the field operator Φ develops a nonzero vacuum expectation value (VEV) $\langle 0|\Phi|0\rangle \equiv \langle\Phi\rangle \neq 0$, then it is sensible to expand the Higgs field around this ground state. We will see below, that for the specific value of

$$\langle\Phi\rangle = \frac{1}{\sqrt{2}} \begin{pmatrix} 0 \\ v \end{pmatrix} , \qquad (1.41)$$

into (1.40), we obtain Dirac mass terms for the quarks and charged leptons. But first, we must discuss how such a nonzero VEV can be realized.

Higgs Sector & Mechanism

The Higgs Lagrangian is given by

$$\mathcal{L}_{\text{HS}} = (D_\mu \Phi)^\dagger (D^\mu \Phi) - V(\Phi) \quad \text{with} \quad V(\Phi) = -\mu^2 \Phi^\dagger \Phi + \lambda (\Phi^\dagger \Phi)^2 . \qquad (1.42)$$

Note, that the potential V is the most general potential respecting gauge symmetry and renormalizability. Due to the hermiticity condition, the couplings μ^2 and λ must be real. In order to allow for the VEV in (1.41), the potential must fulfill some requirements. It must be bounded from below to admit a stable ground state, enforcing $\lambda > 0$. However the sign of μ^2 is arbitrary, but we only obtain a nonzero minimum for $\mu^2 > 0$, which leads to the well known Mexican hat potential. Extremizing the potential, we find minima for the values $|\langle\Phi\rangle| = \mu/\sqrt{2\lambda}$, so (1.41) is just one possible VEV with $v = \mu/\sqrt{\lambda}$.

It is sensible to describe our theory out of the ground state, so we must expand Φ around its vacuum expectation value $\langle\Phi\rangle$. As a consequence, the symmetry properties of our Lagrangian $\mathcal{L}_\Phi$ depend on the transformation behavior of $\langle\Phi\rangle$ under the SM gauge group. While the VEV is obviously not affected by the $SU(3)_c$ group, it transforms nontrivially under infinitesimal $SU(2)_L$ and $U(1)_Y$ gauge transformations,

$$\frac{1}{\sqrt{2}} \begin{pmatrix} 0 \\ v \end{pmatrix} \xrightarrow{SU(2)_L \times U(1)_Y} \left[\mathbb{1} + \theta_L^i(x) \frac{\sigma^i}{2} + \theta_Y(x) \frac{1}{2} \right] \frac{1}{\sqrt{2}} \begin{pmatrix} 0 \\ v \end{pmatrix} \qquad (1.43)$$

We see that $\langle\Phi\rangle$ stays invariant only for $\theta_L^1 = \theta_L^2 = 0$ and $\theta_L^3 = \theta_Y$, giving rise to the unbroken electric charge generator $Q_e = \tau^3 + \frac{1}{2}$. Otherwise, we encounter three linear independent generators $I_1 \equiv \tau^1, I_2 \equiv \tau^2$ and $\tau^3 - \frac{1}{2}$, that do not leave the VEV invariant and are therefore called broken symmetry generators. One refers to this mechanism as a spontaneous symmetry breakdown (SSB) to the electromagnetic $U(1)_{Q_e}$ group,

$$SU(2)_L \times U(1)_Y \xrightarrow{\text{SSB}} U(1)_{Q_e} . \tag{1.44}$$

Accompanied with this breakdown is the existence of massless spinless bosons for each broken generator, which is a general statement of the Goldstone theorem in case of global and continuous symmetry groups. To see this in our case, we can parametrize Φ by

$$\Phi(x) = \frac{1}{\sqrt{2}} \begin{pmatrix} \phi_1(x) + i\phi_2(x) \\ v + \phi_3(x) + i\phi_4(x) \end{pmatrix}, \tag{1.45}$$

with real-valued scalar fields ϕ_1, ϕ_2, ϕ_3 and ϕ_4. Then we can develop the potential around the VEV, yielding up to the second order

$$V = V\Big|_{\langle\Phi\rangle} + \frac{1}{2}\mathcal{M}_{ij}\Big|_{\langle\Phi\rangle}\phi_i\phi_j + ..., \quad \text{with} \quad \mathcal{M}_{ij} \equiv \frac{\partial V}{\partial\phi_i\partial\phi_j} = \text{diag}(0, 0, 2\lambda v^2, 0), \tag{1.46}$$

where the first order term vanishes, since $\langle\Phi\rangle$ is an extreme value. We find, that the mass matrix (Hessian) $\mathcal{M}_{ij}$ has three zero eigenvalues and one mass eigenvalue $m_h = \sqrt{2\lambda}v$ for the $h(x) \equiv \phi_3(x)$ field. This massive scalar field describes the Higgs particle.

Note, that the potential V admits in fact a higher (accidental) global symmetry $SO(4)$, which has six generators. The VEV breaks this group to a remaining $SO(3)$ symmetry, that has three generators. Finally, we end up with the same number of three broken generators, responsible for the three zero eigenvalues of $\mathcal{M}$.

Since we deal with gauge groups in the SM, the fields ϕ_1, ϕ_2, ϕ_4 do not represent physical particles. They can be eliminated by a suitable gauge transformation (called the unitary gauge). Still, their degrees of freedom do not vanish, but are absorbed by the previously massless gauge bosons (two DOF), that will become massive (three DOF) after SSB. The derivation of the mass terms is performed next.

Gauge Boson Masses

Since the Higgs field couples only to the $SU(2)_L$ and $U(1)_Y$ gauge fields ($Y_\Phi = 1/2$), the covariant derivative (1.26) can be written in a convenient way,

$$D_\mu\Phi = [\partial_\mu - igW_\mu^1\tau^1 - igW_\mu^2\tau^2 - i(gW_\mu^3\tau^3 + \frac{g'}{2}B_\mu)]\Phi . \tag{1.47}$$

With this expression at hand, we can insert the VEV (1.41) into the kinetic part of the Higgs Lagrangian in (1.42), yielding

$$(D_\mu \Phi)^\dagger (D^\mu \Phi)\Big|_{\langle \Phi \rangle} = \frac{v^2 g^2}{8} [(W_\mu^1)^2 + (W_\mu^2)^2] + \frac{v^2}{8} (-g W_\mu^3 + g' B_\mu)^2 . \tag{1.48}$$

The masses of the two W bosons W_μ^1 and W_μ^2 can be directly read off, yielding

$$m_1^2 = m_2^2 = \frac{v^2 g^2}{4}, \tag{1.49}$$

while the mixed term on the right-hand side of (1.48) has to be diagonalized first. We can rewrite this term by

$$\frac{v^2}{8} (-g W_\mu^3 + g' B_\mu)^2 = \frac{v^2}{8} \begin{pmatrix} W_\mu^3 & B_\mu \end{pmatrix} \begin{pmatrix} g^2 & -gg' \\ -gg' & g'^2 \end{pmatrix} \begin{pmatrix} W_\mu^3 \\ B_\mu \end{pmatrix}$$

$$= \frac{1}{2} \begin{pmatrix} Z_\mu & A_\mu \end{pmatrix} \begin{pmatrix} m_Z^2 & 0 \\ 0 & 0 \end{pmatrix} \begin{pmatrix} Z_\mu \\ A_\mu \end{pmatrix} = \frac{1}{2} m_Z^2 Z_\mu Z^\mu, \tag{1.50}$$

where we used in the penultimate step the orthogonal transformations

$$Z_\mu = \cos\theta_W W_\mu^3 - \sin\theta_W B_\mu, \qquad A_\mu = \sin\theta_W W_\mu^3 + \cos\theta_W B_\mu, \tag{1.51}$$

with the mixing angle $\tan\theta_W = g'/g$, which is generally referred to as the Weinberg angle. After diagonalization, we obtain a massive and a massless boson

$$m_Z^2 = \frac{v^2(g^2 + g'^2)}{4}, \qquad\qquad m_A^2 = 0 . \tag{1.52}$$

which are identified with the Z boson and the photon A. The missing mass term for the photon is in fact a consequence of the SSB in (1.44), after which the Lagrangian $\mathcal{L}_{\text{SM}}$ remains still invariant under local phase-transformations $U(1)_{Q_e}$. Here, concerning the Higgs field, the electric charge generator reads $Q_e = \tau^3 + Y_\Phi = \text{diag}(1,0)$, whose eigenvalues denote that Φ^1 is positively charged and Φ^2 is the neutral component. It is further convenient to rewrite

$$W_\mu^1 \tau^1 + W_\mu^2 \tau^2 = \frac{1}{\sqrt{2}} (W_\mu^+ \tau^+ + W_\mu^- \tau^-), \qquad W_\mu^\pm = \frac{1}{\sqrt{2}} (W_\mu^1 \mp W_\mu^2), \tag{1.53}$$

since each of the matrices $\tau^\pm = \tau^1 \pm \tau^2$ is closed under commutation with the charge generator[16]. Finally, we can express the general covariant derivative (1.26) in terms of mass eigenstates and identify $e \equiv g' \cos\theta_W$, yielding

$$D_\mu = \partial_\mu - i \frac{g}{\sqrt{2}} (W_\mu^+ \tau^+ + W_\mu^- \tau^-) - i \frac{g}{\cos\theta_W} Z_\mu (\tau^3 - \sin^2\theta_W Q_e)$$

$$- ie A_\mu Q_e - i g_s G_\mu^a T^a . \tag{1.54}$$

----

[16]This means $[\tau^+, Q] = -\tau^+$ and $[\tau^-, Q] = \tau^-$.

The electric charge generator is given for $SU(2)_L$ doublets by $Q_e = \tau^3 + Y$ and in case of singlets by $Q_e = Y$. For instance, $Q_e = \mathrm{diag}(2/3, -1/3)$ for the quark doublets Q_L^n. Inserting (1.54) into $\mathcal{L}_{\mathrm{FS}}$, we obtain

$$\mathcal{L}_{\mathrm{FS}} = \bar{Q}_L^n i\slashed{\partial} Q_L^n + \bar{E}_L^n i\slashed{\partial} E_L^n + \bar{u}_R^n i\slashed{\partial} u_R^n + \bar{d}_R^n i\slashed{\partial} d_R^n + \bar{e}_R^n i\slashed{\partial} e_R^n$$
$$+ g(W_\mu^+ J_W^{+\mu} + W_\mu^- J_W^{-\mu} + Z_\mu J_Z^\mu) + e A_\mu J_{\mathrm{em}}^\mu, \tag{1.55}$$

with the charged and neutral weak currents $J_W^{\pm\mu}$, J_Z^μ and the electromagnetic current J_{em}^μ, given by

$$J_W^{+\mu} = \frac{1}{\sqrt{2}}(\bar{\nu}_L^n \gamma^\mu e_L^n + \bar{u}_L^n \gamma^\mu d_L^n), \qquad J_W^{-\mu} = \left(J_W^{+\mu}\right)^\dagger, \tag{1.56}$$

$$J_Z^\mu = \frac{1}{\cos\theta_W}\Big[\bar{\nu}_L^n \gamma^\mu \left(\frac{1}{2}\right) \nu_L^n + \bar{e}_L^n \gamma^\mu \left(-\frac{1}{2} + \sin^2\theta_W\right) e_L^n + \bar{e}_R^n \gamma^\mu \left(\sin^2\theta_W\right) e_R^n$$
$$+ \bar{u}_L^n \gamma^\mu \left(\frac{1}{2} - \frac{2}{3}\sin^2\theta_W\right) u_L^n + \bar{u}_R^n \gamma^\mu \left(-\frac{2}{3}\sin^2\theta_W\right) u_R^n$$
$$+ \bar{d}_L^n \gamma^\mu \left(-\frac{1}{2} + \frac{1}{3}\sin^2\theta_W\right) d_L^n + \bar{d}_R^n \gamma^\mu \left(\frac{1}{3}\sin^2\theta_W\right) d_R^n \Big], \tag{1.57}$$

$$J_{\mathrm{em}}^\mu = \bar{e}\gamma^\mu(-1)e + \bar{u}\gamma^\mu\left(+\frac{2}{3}\right)u + \bar{d}\gamma^\mu\left(-\frac{1}{3}\right)d. \tag{1.58}$$

Note, that all fermion fields in (1.55) are still gauge eigenstates. Parity P and charge C is violated in both weak currents, since the interactions do not couple with equal strength between left-chiral and right-chiral fields. A maximal violation occurs in the charged sector and for the neutrinos, since here are only left-chiral particles (right-chiral antiparticles) involved. The combined operation CP is conserved by both weak interactions, but this will change when we rotate to the mass eigenstates of the fermion fields.

Fermion Masses

Returning to our Yukawa terms in (1.40), we can insert the VEV (1.41) and obtain

$$\mathcal{L}_{\mathrm{YS}} \ni -\frac{v}{\sqrt{2}} Y_d^{mn} \bar{d}_L^m d_R^n - \frac{v}{\sqrt{2}} Y_u^{mn} \bar{u}_L^m u_R^n - \frac{v}{\sqrt{2}} Y_e^{mn} \bar{e}_L^m e_R^n + \mathrm{h.c.}, \tag{1.59}$$

where the fermion fields are gauge eigenstates. To work with mass eigenstates, we have to diagonalize the 3×3 complex Yukawa matrices $\boldsymbol{Y}_u$, $\boldsymbol{Y}_d$ and $\boldsymbol{Y}_e$. This can be done via biunitary transformations [5], i.e. for each of the matrices there exist unitary matrices $\boldsymbol{U}_u$, $\boldsymbol{U}_d$, $\boldsymbol{U}_e$ and $\boldsymbol{W}_u$, $\boldsymbol{W}_d$, $\boldsymbol{W}_e$ such that

$$\boldsymbol{U}_u^\dagger \boldsymbol{Y}_u \boldsymbol{W}_u = \mathrm{diag}(y_u, y_c, y_t), \qquad \boldsymbol{U}_d^\dagger \boldsymbol{Y}_d \boldsymbol{W}_d = \mathrm{diag}(y_d, y_s, y_b),$$
$$\boldsymbol{U}_e^\dagger \boldsymbol{Y}_e \boldsymbol{W}_e = \mathrm{diag}(y_e, y_\mu, y_\tau), \tag{1.60}$$

with real diagonal entries denoted as Yukawa couplings. So, when we transform to the quark and lepton mass eigenstates via

$$u_L \to \boldsymbol{U}_u \cdot u_L, \qquad d_L \to \boldsymbol{U}_d \cdot d_L, \qquad e_L \to \boldsymbol{U}_e \cdot e_L, \qquad \nu_L \to \boldsymbol{U}_e \cdot \nu_L,$$
$$u_R \to \boldsymbol{W}_u \cdot u_R, \qquad d_R \to \boldsymbol{W}_d \cdot d_R, \qquad e_R \to \boldsymbol{W}_e \cdot e_R, \tag{1.61}$$

their masses are given by the VEV of the Higgs field and the Yukawa couplings,

$$m_q = \frac{y_q\, v}{\sqrt{2}} \quad \text{for} \quad q = u, d, c, s, t, b\,, \qquad m_l = \frac{y_l\, v}{\sqrt{2}} \quad \text{for} \quad l = e, \mu, \tau\,. \qquad (1.62)$$

Flavor Content

The neutral currents are invariant under the transformations in (1.61), therefore J_Z^μ, J_{em}^μ remain the same with fermion fields in their mass basis. Affected are the charged quark currents, $J_W^{+\mu}$ in (1.56) gets replaced by

$$J_W^{+\mu} = \frac{1}{\sqrt{2}}\big(\bar{\nu}_L^n \gamma^\mu e_L^n + (U_u^\dagger U_d)^{mn} \bar{u}_L^m \gamma^\mu d_L^n\big)\,. \qquad (1.63)$$

The unitary 3×3 matrix in between the up- and down-type quarks is termed as the CKM matrix after Cabibbo, Kobayashi and Maskawa [9], [10],

$$\boldsymbol{V} = \boldsymbol{U}_u^\dagger \boldsymbol{U}_d = \begin{pmatrix} V_{ud} & V_{us} & V_{ub} \\ V_{cd} & V_{cs} & V_{cb} \\ V_{td} & V_{ts} & V_{tb} \end{pmatrix}, \qquad (1.64)$$

which is in general not diagonal. Since, its non-diagonal components can allow for quark transitions that change flavor but not the electric charge, we speak of the Flavor-Changing Neutral Currents (FCNCs) $J_W^{+\mu}$ and $J_W^{-\mu}$. For instance, when describing the transition from a down- to an up-quark, we have to use for the Feynman vertex rule the entry V_{ud}, and V_{ud}^* in case of the reverse transition. It is convenient to parametrize $\boldsymbol{V}$ in a way, that only includes physical degrees of freedom. Any complex 3×3 matrix has 18 real parameters, while imposing the unitarity condition $(\boldsymbol{V}^\dagger \boldsymbol{V})_{mn} = \delta_{mn}$ reduces them to three rotation angles and six complex phases. Since the quark phases are unphysical, we can redefine them

$$u^m \to e^{i\phi_{u_m}} u^m, \quad d^n \to e^{i\phi_{d_n}} d^n \qquad \Rightarrow \qquad V_{mn} \to e^{-i(\phi_{u_m} - \phi_{d_n})} V_{mn}, \qquad (1.65)$$

such that their phase differences eliminate five of the CKM phases. This leaves us with one physical complex phase, which is the only parameter that violates CP in the SM. This can be seen by means of the charged weak currents for the quarks, which transform under a CP transformation by

$$\bar{u}_L \gamma^\mu \boldsymbol{V} d_L W_\mu^+ + \bar{d}_L \gamma^\mu \boldsymbol{V}^\dagger u_L W_\mu^- \xrightarrow{\boldsymbol{CP}} \bar{d}_L \gamma^\mu \boldsymbol{V}^{\dagger *} u_L W_\mu^- + \bar{u}_L \gamma^\mu \boldsymbol{V}^* d_L W_\mu^+\,. \qquad (1.66)$$

Both sides do not coincide, unless $\boldsymbol{V}$ is real or the physical phase vanishes. One common parametrization, which is also used by the Particle Data Group (PDG) [11], is given by

$$\boldsymbol{V} = \begin{pmatrix} c_{12}c_{13} & s_{12}c_{13} & s_{13}e^{-i\delta} \\ -s_{12}c_{23} - c_{12}s_{23}s_{13}e^{i\delta} & c_{12}c_{23} - s_{12}s_{23}s_{13}e^{i\delta} & s_{23}c_{13} \\ s_{12}s_{23} - c_{12}c_{23}s_{13}e^{i\delta} & -c_{12}s_{23} - s_{12}c_{23}s_{13}e^{i\delta} & c_{23}c_{13} \end{pmatrix}, \qquad (1.67)$$

where $s_{ij} \equiv \sin\theta_{ij}$ and $c_{ij} \equiv \cos\theta_{ij}$ and δ is the CP violating phase. To bring (1.64) into this standard parametrization, we can use four phase rotations in (1.65) to make V_{ud}, V_{us}, V_{cb} and V_{tb} real and the remaining one to adjust the condition

$$\text{Im}\, V_{ub} = \frac{\sqrt{|V_{ud}|^2 + |V_{us}|^2}}{|V_{cb}|}\, \text{Im}\, V_{cs} \,. \tag{1.68}$$

Experimentally, one finds hierarchies $s_{12} \ll s_{23} \ll s_{13}$, therefore it is convenient to define

$$s_{12} \equiv \lambda, \qquad s_{23} \equiv A\lambda^2, \qquad s_{13} \equiv A\lambda^3(\rho - i\eta), \tag{1.69}$$

and to expand (1.67) in terms of $\lambda \approx 0.23$, yielding the approximate Wolfenstein parametrization [12],

$$\boldsymbol{V} = \begin{pmatrix} 1 - \lambda^2/2 & \lambda & A\lambda^3(\rho - i\eta) \\ -\lambda & 1 - \lambda^2/2 & A\lambda^2 \\ A\lambda^3(1 - \rho - i\eta) & -A\lambda^2 & 1 \end{pmatrix} + \mathcal{O}(\lambda^4) \,. \tag{1.70}$$

This representation highlights the hierarchical structure of the CKM matrix. Here, we see that a CP violation is associated with $\eta \neq 0$. Instead of working with ρ and η, it is convenient to work with convention independent quantities $\bar\rho$ and $\bar\eta$, that are defined by

$$\bar\rho + i\bar\eta = -\frac{V_{ub}^* V_{ud}}{V_{cb}^* V_{cd}}, \tag{1.71}$$

and related to the Wolfenstein parameters via $\bar\rho = \rho(1 - \lambda^2/2)$ and $\bar\eta = \eta(1 - \lambda^2/2)$ up to order $\mathcal{O}(\lambda^4)$. The experimental values for λ, A, $\bar\rho$, $\bar\eta$ can be found in the appendix B.1.

Parameter Counting

We have shown explicitly above, that we can infer from the three Yukawa matrices 13 physical real parameters, composed of nine quark/lepton masses and four parameters describing the CKM matrix. The same result can also be achieved by global symmetry considerations, see [13] and [14]. When we neglect the Yukawa Lagrangian in $\mathcal{L}_{\text{SM}}$, we can perform global unitary transformations of the quark/lepton $SU(2)_L$ doublets and singlets separately in generation space[17], leading to the enlarged symmetry group

$$G_Y = U(3)_{Q_L} \times U(3)_{u_R} \times U(3)_{d_R} \times U(3)_{E_L} \times U(3)_{e_R}, \tag{1.72}$$

which has $5 \times 9 = 45$ generators. The corresponding transformation matrices can be parametrized by 15 angles and 30 phases, denoted as $N_{G_Y} = (15, 30)$. Now, we add

---

[17]For instance, the quark doublet transforms by $Q_L^m \xrightarrow{U(3)_{Q_L}} U_{Q_L}^{mn} Q_L^n$ for $\boldsymbol{U}_{Q_L} \in U(3)_{Q_L}$.

$\mathcal{L}_Y$ and introduce the quark and lepton Yukawa matrices $\boldsymbol{Y}_{u,d,l}$, which are general 3×3 complex matrices. They give rise to 27 new complex parameters, classified by $N_Y = (27, 27)$. As a consequence of adding the Yukawa terms, the symmetry of $\mathcal{L}_{\text{SM}}$ is reduced to simultaneous phase transformations of all quark fields and to separate phase transformations of each lepton generation[18], summarized by the subgroup

$$H_Y = U(1)_B \times U(1)_e \times U(1)_\mu \times U(1)_\tau, \qquad (1.73)$$

with $N_{H_Y} = (0, 4)$. The corresponding quantum numbers are the baryon number ($1/3$ for each quark) and family lepton numbers (1 for e, μ, τ). They are in fact accidental symmetries of $\mathcal{L}_{\text{SM}}$, since they have not been imposed a priori, when constructing the SM Lagrangian. Now, we can use the $N_{G_Y} - N_{H_Y}$ broken generators to eliminate unphysical parameters in the Yukawa matrices. Finally, the remaining physical parameters can be calculated to

$$N_{\text{phys}} = N_Y - (N_{G_Y} - N_{H_Y}) = (27, 27) - [(15, 30) - (0, 4)] = (12, 1), \qquad (1.74)$$

which distribute among the six quark masses, three charged lepton masses, three mixing angles and the one CP violating phase of the CKM matrix[19].

Including also the physical parameters in $\mathcal{L}_{\text{FS}}$, $\mathcal{L}_{\text{BS}}$ and $\mathcal{L}_{\text{HS}}$, the SM relies on 18 physical parameters

- 3 gauge couplings: g, g', g_s

- 2 from Higgs sector: m_h, v

- 13 from Flavor sector: (m_u, m_c, m_t), (m_d, m_s, m_b), (m_e, m_μ, m_τ), 3 mixing angles and 1 CP violating phase,

that have to be adjusted properly to fit the experiments.

1.3. Concept of an Effective Field Theory

We start with a quantum field theory in D space-time dimensions, that incorporates a fundamental energy scale Λ_0[20]. Being interested in the physics at some lower scale $E \ll \Lambda_0$, we choose a cutoff $\Lambda < \Lambda_0$ and divide the fields ϕ of the theory into low- and high-frequency modes

$$\phi(x) = \phi_L(x) + \phi_H(x) . \qquad (1.75)$$

---

[18]The SM Lagrangian stays invariant under the quark transformations $q \xrightarrow{U(1)_B} e^{i\frac{1}{3}\theta_B} q$ and lepton transformations $l \xrightarrow{U(1)_l} e^{i\theta_l} l$ for $l = e, \mu, \tau$.

[19]Repeating the considerations with two fermion generations, leads to $N_{\text{phys}} = (12, 12) - ((5, 15) - (0, 3)) = (7, 0)$, including four quark and two lepton masses and one Cabibbo angle for quark mixing.

[20]Good expositions about the concept of EFTs and its relation to renormalization can be found in [15], [16], [17] and [18].

The field ϕ_L contains the Fourier modes with frequencies $w < \Lambda$, while ϕ_H contains the remaining modes with frequencies $w > \Lambda$. Since, we want to describe a low-energy theory, the propagating particles must be described by low-frequency fields ϕ_L. In terms of the path integral formalism, we therefore introduce only source fields $J(x)$ for ϕ_L, yielding the generating functional

$$Z[J_L] = \int [d\phi_L][d\phi_H]\, e^{iS(\phi_L,\phi_H)+i\int d^D x J(x)\phi_L(x)}, \tag{1.76}$$

where $S(\phi_L, \phi_H) = \int d^D x\, \mathcal{L}(x)$ denotes the complete action. Consequently, we can perform the integral over the high-frequency fields and shuffle their contribution into a new effective (Wilsonian) action, defined by

$$e^{iS_\Lambda(\phi_L)} \equiv \int [d\phi_H] e^{iS(\phi_L,\phi_H)} \,. \tag{1.77}$$

This action $S_\Lambda(\phi_L)$ depends explicitly on the choice of Λ, that separates the low- and high-frequency modes. It involves an integration over ϕ-modes with $w > \Lambda$, therefore as long as $E \ll \Lambda$ one can expand (1.77) in terms of local operators composed of light fields, yielding

$$S_\Lambda(\phi_L) = \int d^D x\, \mathcal{L}_{\text{eff}}^\Lambda(x) \qquad \text{with} \qquad \mathcal{L}_{\text{eff}}^\Lambda(x) = \sum_i^\infty C_i(\Lambda)\, Q_i(\phi_L(x)), \tag{1.78}$$

which is referred to as the operator-product expansion (OPE). The effective Lagrangian $\mathcal{L}_{\text{eff}}^\Lambda$ is then given by an infinite sum of local operators Q_i multiplied by the so called Wilson coefficients C_i. Note, that since the OPE depends on Λ, so do the Wilson coefficients as well as the operators through the fields ϕ_L. Furthermore, each operator Q_i that respects the symmetry of the theory must appear in the sum (1.78).

At first sight, the infinite number of coefficients C_i seems to render the theory non-predictive. But, this can be resolved, when we estimate the Wilson coefficients using naive-dimensional analysis. By assumption, there is only one fundamental scale Λ_0 that can be used to give each Wilson coefficient its corresponding mass dimension. Defining $\gamma_i \equiv -[C_i] \equiv [Q_i] - D$, we conclude that $C_i = c_i \Lambda_0^{-\gamma_i}$ with dimensionless couplings c_i. Unless there is a special mechanism at work (like a symmetry), we expect that any dimensional number c_i in our theory is of $\mathcal{O}(1)$. This is essentially the statement behind the "naturalness principle". On the basis of this principle, we can estimate the contribution of a given operator Q_i to a process of low energy $E \ll \Lambda < \Lambda_0$. We expect $\int d^D x\, Q_i \sim E^{\gamma_i}$, so that the ith term in (1.78) is of order

$$c_i \left(\frac{E}{\Lambda_0}\right)^{\gamma_i} = \begin{cases} \mathcal{O}(1), & \gamma_i = 0 \\ \ll 1, & \gamma_i > 0 \\ \gg 1, & \gamma_i < 0 \end{cases}, \tag{1.79}$$

which allows for a classification of operators. The main contributions arise from relevant ($\gamma_i < 0$) and marginal ($\gamma_i = 0$) operators, while the series of irrelevant ($\gamma_i > 0$) operators can be truncated depending on the precision goal of the calculation[21]. Thus, the low energy physics depends only on a finite number of couplings, rendering it predictive.

1.4. The SM as an EFT & Motivation for New Physics

On the basis of the previous section, we can think of the SM as a low energy description of a more fundamental (unknown) theory with a characteristic energy $\Lambda_{\mathrm{NP}} \sim \Lambda_0$. With this New Physics scale, we can write down the effective Lagrangian (compare with (1.20))

$$\mathcal{L}_{\mathrm{eff}} = c_0 \, \Lambda_{\mathrm{NP}}^4 + \mathcal{L}_{\mathrm{SM}} + \sum_{\{i \mid \gamma_i \geq 1\}} \frac{c_i}{\Lambda_{\mathrm{NP}}^{\gamma_i}} \, Q_i, \tag{1.80}$$

where c_i are dimensionless couplings and $\gamma_i \equiv [Q_i] - 4$.

In spite of the notation, the irrelevant terms in (1.80) are in fact interesting, since they can give us information about the primary theory. For instance, there is only one dimension five operator that respects the symmetries of the SM. It is given by[22] $(\bar{E}_L^{n,c} i\sigma_2 \Phi)(E_L^n i\sigma_2 \Phi) + $ h.c. with a coefficient, suppressed by one power of Λ_{NP}. When the Higgs field attains its VEV, this term gives rise to a Majorana mass for the neutrinos, $m_\nu \sim v^2 / \Lambda_{\mathrm{NP}}$. Thus, the Standard Model does predict neutrino masses and when comparing them with the experiment value, this would imply $\Lambda_{\mathrm{NP}} \sim \mathcal{O}(10^{14}\,\mathrm{GeV})$. This is also not far away from the grand unified theory (GUT) scale, where the strong and electroweak gauge couplings approximately unify.

Another important energy scale is given by the Planck mass $M_{\mathrm{Pl}} \sim 10^{19}\,\mathrm{GeV}$, where gravity is expected to become strong, such that it can not be neglected in particle interactions anymore. When we include gravity into the SM, we can think of it as being the low energy theory of some quantum gravity theory with $\Lambda_{\mathrm{NP}} \sim M_{\mathrm{Pl}}$. Consequently, the first expansion term in (1.80) has a physical meaning, since it contributes to the cosmological constant. Naturally, we expect it to scale like M_{Pl}^4, but this deviates by more than 120 orders of magnitude compared with the observed value. This is known as the cosmological constant problem. So, on the basis of the naturalness principle, we encounter a Hierarchy Problem (HP). Regarding $\mathcal{L}_{\mathrm{SM}}$, there are two further HPs, that strongly motivate the search for New Physics models:

---

[21]Here, we used the modern nomenclature for the classification. In the old-fashioned language, they refer to super-renormalizable, renormalizable and non-renormalizable operators.

[22]Here, n refers to the generation index and $E_L^{n,c} = i\gamma^2 (E_L^n)^*$ is the conjugate of the lepton doublet E_L^n. The given operator in the text is then both Lorentz and gauge invariant, but does break the (accidental) lepton symmetry in (1.73).

Gauge Hierarchy Problem: Before EWSB, the Lagrangian $\mathcal{L}_{\mathrm{SM}}$ is composed of marginal operators except for the (relevant) Higgs field mass term $\mu^2 \Phi^\dagger \Phi$ in (1.42). Due to the naturalness principle, we expect a value of $\mu^2 \sim \Lambda_{\mathrm{NP}}^2$. Relating this to the Higgs mass, it states that the bare parameter $m_{h,B} = 2\mu/\sqrt{\lambda} \sim \Lambda_{\mathrm{NP}}$ scales with the New Physics energy. Being a bare parameter in the Lagrangian, we have to consider quantum corrections to it. One loop corrections from fermions or bosons turn out to be quadratically sensitive on
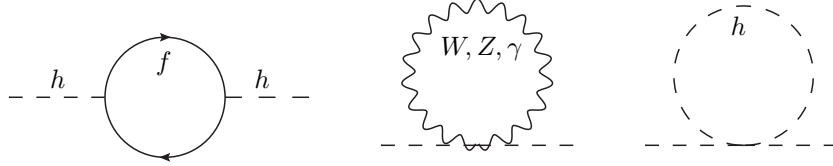
the cutoff scale (which is set to Λ_{NP}), yielding a mass shift of $\Delta m_h^2 \sim \Lambda_{\mathrm{NP}}^2$. Thus, we can only stabilize a low value of the (physical) Higgs mass $m_h^2 = (m_{h,B}^2 + \Delta m_h^2) \sim (100\,\mathrm{GeV})^2$, when finely tuning the counter-terms with high precision. For instance, considering $\Lambda_{\mathrm{NP}} \sim M_{\mathrm{Pl}}$, one would have to tune two numbers over 33 orders of magnitude.

So, the New Physics model should present a mechanism to explain the hierarchy between Λ_{NP} and the electroweak scale $M_{\mathrm{EW}} \sim v$.

Yukawa Hierarchy Problem: The operators in $\mathcal{L}_Y$ are marginal ones, so we expect complex $\mathcal{O}(1)$ numbers for the components of the dimensionless Yukawa matrices $\boldsymbol{Y}_u$, $\boldsymbol{Y}_d$ and $\boldsymbol{Y}_l$. When we rotate into the mass basis, this must further hold for the Yukawa couplings y_{q_i} and y_{l_i}, that set the fermion masses via (1.62). Concerning the quarks, they read $m_{q_i} = y_{q_i} v/\sqrt{2}$. While the top quark coupling $y_t \sim 1$ is natural, the remaining couplings are several orders of magnitude smaller according to the approximate mass ratios

$$m_d/m_s/m_b = 1/10^2/10^3 \qquad \text{and} \qquad m_u/m_c/m_t = 1/10^3/10^5 \ . \qquad (1.81)$$

The SM does not give an explanation (mechanism) for these mass splittings. Note, that in contrast to the Higgs mass, quantum corrections to the fermion masses are at most logarithmically depending on the cutoff scale Λ_{NP}. Therefore, we are not confronted here with a fine-tuning problem. The reason lies in the chiral gauge structure of the SM[23].

Another manifestation of the hierarchies in the quark sector is given by the pattern of the CKM matrix, see the Wolfenstein parametrization in (1.70), which has components differing up to three orders in magnitude.

---

[23] In the limit of vanishing masses $m_f \to 0$, left- and right-chiral fermions in the SM are independent non-interacting particles, prohibiting any non-zero mass corrections. Consequently, self-energy loop diagrams are proportional to $m_f \ln \Lambda_{\mathrm{NP}}$ (see [19]). Thus, it is the chiral gauge symmetry that protects fermion masses from large corrections.

Furthermore, we have no rationale for the unnatural small value for Θ_G in (1.34) or a viable mechanism to set it to zero. This is known as the strong CP puzzle. Besides the above mentioned HPs, there are more open questions, e.g. what is dark matter or dark energy and how can we provide a mechanism, that can account for the baryon asymmetry in the universe.

Before ending this section and proceeding with the Randall-Sundrum Model, we want to say some more words about the issue of fine-tuning, since it will play a major role in the analysis of the ϵ_K problem:

Fine-tuning: Barbieri and Giudice introduce in [20] a measure for fine-tuning of an observable $O(\bar{a})$, that depends on several parameters $\bar{a} = (a_i)$. They propose to calculate the quantity

$$\Delta_i(O, \bar{a}) \equiv \left| \frac{a_i}{O(\bar{a})} \frac{\partial O(\bar{a})}{\partial a_i} \right|, \tag{1.82}$$

so that the percentage variation of one parameter a_i leads to a Δ_i times larger variation of $O(\bar{a})$. For example, imposing $\Delta_i < 10$ means to tolerate cancellations in $O(\bar{a})$ of at most one order of magnitude.

Let us calculate the fine-tuning measure for the one-loop top-quark contribution to the Higgs mass, where Λ shall denote the fixed momentum cutoff. Here, the observable is

$$m_h^2 = m_{h,B}^2 + \Delta m_h^2(\Lambda, y_t) \quad \text{with} \quad \Delta m_h^2(\Lambda, y_t) = \frac{3y_t}{4\pi^2}\Lambda^2 \text{ [8]}, \tag{1.83}$$

and depends on the top-quark Yukawa coupling y_t. Applying (1.82), we obtain $\Delta_{y_t}(m_h^2, y_t) = 2\,\Delta m_h^2/m_h^2$, which gives a huge fine-tuning value around 10^{33} in case of $\Lambda \sim M_{\text{Pl}}$. Taking another point of view, we can also demand Δ_{y_t} to be less than 10, which is often used as an acceptable fine-tuning value in literature, and then derive an upper bound for the cutoff-scale, yielding

$$\Lambda^2 < \frac{20\pi^2}{3y_t^2}m_h^2 \approx \left(\frac{8.1m_h}{y_t} \right)^2. \tag{1.84}$$

Setting $y_t = \sqrt{2}\,m_t/v \approx 1$ and $m_h = 125\,\text{GeV}$ for concreteness, the bound is approximately $\Lambda \lesssim 1\,\text{TeV}$. Following the EFT concept, this would predict new particles (physics) in the one TeV range. But, the bound is probably already excluded by collider experiments.

There are two major objections in using a definite measure for fine-tuning. The first one is that (1.82) is only one possible choice of measure, since there is no unique and valid procedure how to deal with fine-tuning. Furthermore, each calculation depends on the reliability of the estimator Δ_i as well as on the personal choice where one sets the fine-tuning limit value.

Therefore, in this thesis we do not use a specific measure, but rather give everywhere an explanation, whenever we speak of fine-tuning.

2. The Minimal Randall-Sundrum Model

While the Standard Model describes quite successfully three of the fundamental forces, we have no quantized description of gravity. Still, we can treat gravity on the same footing as the other interactions. Writing down the Einstein-Hilbert action[1] $S = \int d^4x \sqrt{|g|} M_{\mathrm{Pl}}^2 R^{(4)}$, we can expand the metric $g_{\mu\nu} = \eta_{\mu\nu} + h_{\mu\nu}$ around the flat metric, where $h_{\mu\nu}$ is the (hypothetical) force mediating graviton field (spin-2 boson). In fact, this field couples with strength $1/M_{\mathrm{Pl}}$ to matter, demonstrating the weakness of gravity in relation to other forces and the notorious non-renormalizability of gravity interactions. The point is that when we want to combine the SM and gravity, we encounter two characteristic scales M_{EW} and M_{Pl}. The question arises, how we can explain and stabilize this vast hierarchy between the Planck and the electroweak scale (Gauge HP in section 1.4). The introduction of extra dimensions does provide a fruitful ground to solve this problem.

In section 2.1, we briefly mention some of the extra-dimensional ideas, which have influenced the formulation of the Randall-Sundrum model, that builds the basis for all our subsequent calculations and analyses. When discussing the actual implementation in section 2.2, we will see that this model further admits an explanation for the quark mass splittings (Yukawa HP). At the end of this chapter, subsection 2.2.5 presents the techniques to calculate tree-level diagrams for a two-quark process exchanging a gluon, which forms the basis for the remainder of this thesis.

2.1. Extra Dimensional Ideas

2.1.1. Nordström, Kaluza and Klein

Gunner Nordström discovered in 1914 that he could unite the physics of electromagnetism with his scalar gravity theory by postulating the existence of a fourth spatial dimension [21]. But his proposal[2] was generally overlooked, when Einstein formulated the correct theory of gravity shortly thereafter. Five years later, Theodor

---

[1] The Ricci scalar in four dimension is denoted by $R^{(4)}$ and the metric by $g_{\mu\nu}$.

[2] Nordström extended Maxwell's theory to five dimensions, $\mathcal{L} = -\frac{1}{4} F_{MN} F^{MN} - J_M A^M$, with the 5D el. magn. vector potential $A^M = (A^\mu, \phi/\sqrt{4\pi G})$ and current density $J^M = (J^\mu, \rho 4\pi G)$. Assuming A^M does not depend on the fifth coordinate, the 5D wave equation separates into standard Maxwell's and Nordström's gravitational wave equation $\Box \phi = -4\pi G \rho$.

Kaluza extended Einstein's relativity to five dimensions, but his model [22] faced two problems:

- The Extra Dimension (ED) had not been observed and

- Kaluza assumed without explanation a 5D metric, that was independent of the fifth dimension.

In 1926, Oscar Klein addressed these concerns by proposing a cylindrical universe with Kaluza's 5th dimension having a small radius r [23], which solved the first problem above. Furthermore, by introducing a compact ED one may choose periodic boundary conditions (BCs) for a 5D real massless scalar field[3] $\Phi(x_M)$, such that $\Phi(x_\mu, x_5) = \Phi(x_\mu, x_5 + 2\pi r)$, and perform a Fourier decomposition

$$\Phi(x_\mu, x_5) = \frac{1}{2\pi r} \sum_{n=-\infty}^{\infty} \phi_n(x_\mu) e^{-inx_5/r} \ . \tag{2.1}$$

The Fourier coefficients are functions, depending only on 4D coordinates, and therefore represent an infinite set of 4D scalars. In general, one speaks of a Kaluza-Klein (KK) decomposition. Inserting (2.1) into the five-dimensional scalar action and integrating out the fifth dimension yields,

$$S_\phi^{(5)} = \frac{1}{2} \int d^5x \, \partial_M \Phi \partial^M \Phi = \int d^4x \, \frac{1}{2} \partial_\mu \phi_0 \partial^\mu \phi_0 + \sum_{n=1}^{\infty} \left[\partial_\mu \phi_n \partial^\mu \phi_n - \frac{n^2}{r^2} \phi_n^2 \right], \tag{2.2}$$

giving rise to a massless scalar particle ϕ_0 (zero-mode) and a tower of scalars with masses, proportional to the inverse of the compactification radius, $m_n^2 = n^2/r^2$. Note, that this decomposition can be extended to tensor fields in general. For experimental energies smaller than the $1/r$ scale, one is allowed to truncate the massive fields. Coming back to Kaluza and his unification idea, the proposed x_5 independent metric can be recognized as the zero-mode part of the following 5D metric

$$G_{MN}(x_M) = \begin{pmatrix} g_{\mu\nu} + \Phi A_\mu A_\nu & \Phi A_\nu \\ \Phi A_\mu & \Phi \end{pmatrix} = \underbrace{\begin{pmatrix} g_{\mu\nu}^{(0)} + \phi_0 A_\mu^{(0)} A_\nu^{(0)} & \phi_0 A_\nu^{(0)} \\ \phi_0 A_\mu^{(0)} & \phi_0 \end{pmatrix}}_{G_{MN}^{(0)}(x_\mu)} + \text{massive modes},$$

$$\tag{2.3}$$

since the tower of massive modes would depend on the fifth dimension, see (2.1). This resolves the second objection of Kaluza's model. Inserting (2.3) into the 5D action of general relativity and performing the integration along x_5 gives

$$S^{(5)} = \frac{1}{\kappa^2 r} \int d^5x \sqrt{|G^{(0)}|} R^{(5)} = \int d^4x \sqrt{|g|} \left[\frac{1}{\kappa^2} R^{(4)} + \frac{1}{4} \phi_0 F_{\mu\nu} F^{\mu\nu} - \frac{1}{6\kappa^2 \phi_0^2} \partial_\mu \phi_0 \partial^\mu \phi_0 \right], \tag{2.4}$$

where $R^{(4)}$ is the four-dimensional Ricci scalar and $|G| = \det(G_{MN})$. Choosing $\kappa = 16\pi G$ and $\phi_0 = -1$, the action (2.4) becomes the familiar one of general relativity together with electromagnetism.

---

[3]Throughout this thesis, capital Latin letters take on the values 0,1,2,3,5 and Greek ones 0,1,2,3.

2.1.2. Arkani-Hamed, Dimopolous, Dvali

As a potential solution to the Gauge HP, mentioned in section 1.4, Nima Arkani-Hamed, Savas Dimopolous and Gia Dvali (ADD) proposed Large Extra Dimensions [24] in 1998. They considered n spatial extra dimensions, each compactified with radius R and volume $V_n \sim R^n$. The basic idea is to confine all SM fields to a four-dimensional hyperspace, called brane, while gravity flux lines may extend in all dimensions, referred to as bulk. This will modify Newton's gravity law for two test objects with masses m_1 and m_2, separated by a distance r. For distances much smaller than the scale of the extra dimensions, $r \ll R$, their flux lines spread out as in a (4+n)-dimensional non-compact space, thus the potential behaves like

$$V(r) \sim -\frac{m_1 m_2}{M_{\mathrm{Pl}(4+n)}^{n+2}} \frac{1}{r^{n+1}} \qquad (r \ll R), \tag{2.5}$$

where $M_{\mathrm{Pl}(4+n)}$ is the (4+n)-dimensional Planck mass. On the other hand, if the objects are placed at distances $r \gg R$, the flux lines connecting both masses have to reside on the 4D brane, intuitively explaining the $1/r$ behavior, therefore

$$V(r) \sim -\frac{m_1 m_2}{M_{\mathrm{Pl}(4+n)}^{n+2} R^n} \frac{1}{r} \qquad (r \gg R). \tag{2.6}$$

Comparing (2.6) with Newton's gravity law, the four-dimensional Planck mass M_{Pl} is determined by

$$M_{\mathrm{Pl}}^2 \sim M_{\mathrm{Pl}(4+n)}^{n+2} R^n. \tag{2.7}$$

So, one can use the volume of the extra dimensions to explain the huge Planck scale in 4D, while allowing a fundamental Planck mass of the order of the electroweak scale, $M_{\mathrm{Pl}(4+n)} \sim M_{\mathrm{EW}}$. Thence one can solve (2.7) for the radius

$$R \sim \left(\frac{M_{\mathrm{Pl}}}{1\,\mathrm{TeV}}\right)^{2/n} \left(\frac{\hbar c}{1\,\mathrm{TeV}}\right) \left(\frac{1\,\mathrm{TeV}}{M_{\mathrm{EW}}}\right)^{1+\frac{2}{n}} \approx 2 \times 10^{\frac{32}{n}-16} \times \left(\frac{1\,\mathrm{TeV}}{M_{\mathrm{EW}}}\right)^{1+\frac{2}{n}} \mathrm{mm}, \tag{2.8}$$

which is then mainly dependent on the number n of extra dimensions. Three principal cases can be distinguished:

$\boldsymbol{n = 1}$ **:** One ED, with $R \sim 10^{13}\,\mathrm{m}$, would imply deviations from Newtonian gravity over solar distances, which is obviously excluded.

$\boldsymbol{n = 2}$ **:** This case where $R \sim 1\,\mathrm{mm}$ is interesting, since experiments are currently probing distances in the millimeter range and below.[4]

---

[4]Typically, experimental results are parametrized in terms of a Yukawa potential in addition to the Newtonian gravitational potential $V(r) = -\frac{m_1 m_2}{r}(1 + \alpha e^{-r/\lambda})$, with parameters α and λ (related to the compactification radius). Recent constraints for α and λ can be found in [25].

$n \geq 3$: Radii smaller than 100 nm are out of experimental reach for direct searches using gravitational methods and are therefore phenomenologically less interesting.

Apart from gravity law distortions, one may also expect energy violations in collider collisions, due to the disappearance or reappearance of particles from the extra dimensions.

Subsuming, ADD's model provides a solution to the Gauge HP, but introduces at the same time another hierarchy concerning the large volume V_n of the extra dimensions in relation to the weak scale M_{EW}. Since, assuming a natural radius $R \sim 1/M_{\mathrm{EW}}$, we have to demand $(M_{\mathrm{Pl}}/\mathrm{TeV})^{2/n}$ in (2.8) to be of $\mathcal{O}(1)$, which would require a large number n of extra dimensions.

2.1.3. Warped Extra Dimension

Unlike ADD's several large EDs, Lisa Randall and Raman Sundrum published in 1999 [1] an approach (RS1) to solve the Gauge Hierarchy Problem with one small extra dimension. Four-dimensional space-time gets extended by the compact orbifold $S^1/\mathbb{Z}_2$. The complete space then owes the metric

$$ds^2 = e^{-2kr|\phi|}\eta_{\mu\nu}dx^\mu dx^\nu - r^2 d\phi^2, \tag{2.9}$$

with compactification radius r, a positive constant k (related to the curvature) and the orbifold[5] coordinate $\phi \in [0, \pi]$. Attached to the fixed points are two 3-branes (a 4D hypersurface with one time and three spatial dimensions), one at $\phi = 0$, called "hidden" brane and one at $\phi = \pi$, referred to as "visible" brane, since all SM fields are confined to this one. We denote their 4D metrics as

$$g_{\mu\nu}^{\mathrm{hid}}(x_\rho) \equiv G_{\mu\nu}(x_\rho, 0) \qquad \text{and} \qquad g_{\mu\nu}^{\mathrm{vis}}(x_\rho) \equiv G_{\mu\nu}(x_\rho, \pi), \tag{2.10}$$

and see from (2.9) that $g_{\mu\nu}^{\mathrm{vis}}$ is suppressed by the square of the so called warp-factor $e^{-kr|\phi|}$. This is the crucial ingredient for warping the Planck scale down to the weak scale. The action for the Higgs field Φ, which is confined on the visible brane, reads

$$S_{\mathrm{vis}} \ni \int d^4x \sqrt{|g^{\mathrm{vis}}|} \left\{ g_{\mathrm{vis}}^{\mu\nu}(D_\mu\Phi)^\dagger(D_\nu\Phi) - \lambda \left(|\Phi|^2 - v_5^2/2 \right)^2 \right\}, \tag{2.11}$$

where $g_{\mathrm{vis}}^{\mu\nu}$ is the inverse to $g_{\mu\nu}^{\mathrm{vis}}$. In order to obtain a canonically normalized Higgs field, we perform a redefinition $\Phi \to e^{kr\pi}\Phi$, yielding

$$S_{\mathrm{vis}} \ni \int d^4x \left\{ \eta_{\mu\nu}(D^\mu\Phi)^\dagger(D^\nu\Phi) - \lambda \left(|\Phi|^2 - e^{-2kr\pi}v_5^2/2 \right)^2 \right\}, \tag{2.12}$$

which is the common 4D Higgs action with a redefined vacuum expectation value

$$v \equiv e^{-kr\pi}v_5 . \tag{2.13}$$

Assuming a fundamental scale of order the Planck mass, then $v_5 \sim M_{\mathrm{Pl}}$ can be exponentially reduced to the $M_{\mathrm{EW}} \sim v$ scale for $kr \approx 12$. Such a value can be stabilized by the Goldberger-Wise mechanism [26].

---

[5]More details on the orbifolding procedure will be given in section 2.2.1.

2.2. The Actual RS Model

This section describes the Minimal Randall-Sundrum model, which constitutes the framework for performing calculations in the subsequent chapters. It is mainly based on [27], [28] and [29], where one can find further details.

2.2.1. Structure & Setup

Let us start with a manifold M (in general non-compact) and a group G, that acts freely on M through representation maps $\tau_g : M \to M$ for each $g \in G$. Freely means that none of the maps has fixed points in M, except for the identity map τ_i. Identifying points $y_1, y_2 \in M$ that belong to the same orbit, i.e. $y_1 = \tau_g(y_2)$ for some $g \in G$, will construct the compactified manifold $C = M/G$. Now, we introduce another discrete group H, acting this time non-freely on C, with $\zeta_h : C \to C$ for $h \in H$. Therefore some transformations ζ_h have fixed points, resulting in singularities for the factorspace $O = C/H$, which is called an orbifold[6].

In the RS model, $M = \mathbb{R}$ and $G = \mathbb{Z}$ with $\tau_n(y) = y + 2\pi n$ constructs the unit circle S^1. Thereafter, $H = \mathbb{Z}_2$ with $\zeta_\pm(\phi) = \pm\phi$, $\phi \in S^1$ leads to the orbifold $S^1/\mathbb{Z}_2$ as depicted in figure 2.1.
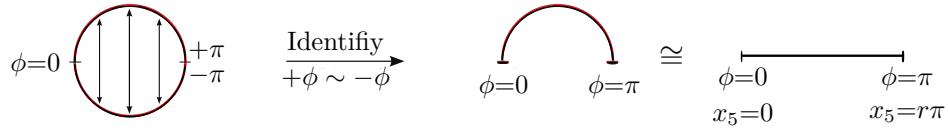

Figure 2.1.: Schematic representation of the orbifolding procedure (based on [32]).

Let us consider a general field $f(x_\mu, \phi)$, which is defined on the 4D space-time with coordinates x_μ and on the orbifold, parametrized by $\phi \in [0, \pi]$. Recapitulating the compactification and orbifolding steps above, we can additionally specify field transformations under the symmetry groups G and H,

$$f(x_\mu, \tau_n(y)) \equiv f(x_\mu, y + 2\pi n) = T_n f(x_\mu, y), \quad f(x_\mu, \phi) = Z_f f(x_\mu, -\phi). \quad (2.14)$$

Note that f shall be implicitly continued in accord with (2.14), when the inserted coordinate has an extended domain, e.g. for $y \in \mathbb{R}$ or $\phi \in [-\pi, \pi]$. All fields shall be 2π-periodic in the fifth dimension with $T_n \equiv 1$, which is referred to as an ordinary compactification. The $\mathbb{Z}_2$ symmetry is defined separately for each field ($Z_f = +1$ or $Z_f = -1$) and allows to solve the chirality problem, which is discussed in the following.

---

[6]A good treatment on the compactification and orbifolding procedure can be found in [30] and [31].

The Clifford algebra in five dimensions, $\{\Gamma_M, \Gamma_N\} = 2\,G_{MN}$, can be fulfilled by a set of five 4×4 Dirac matrices

$$\Gamma_\mu = \gamma_\mu \qquad \text{and} \qquad \Gamma_5 = i\gamma_5 = -\gamma_0\gamma_1\gamma_2\gamma_3, \qquad (2.15)$$

including γ_5, which is needed in 4D to build the operators projecting on left- and right-chiral spinors. Therefore, the 5D Lorentz group furnishes only one irreducible representation and it is not possible to define chiral fermions. As a resort, one can use the transformation behavior under the $\mathbb{Z}_2$, also called parity or orbifold, symmetry in (2.14). A fermionic field $Q(x_\mu, \phi)$ can always be splitted into a $\mathbb{Z}_2$ even and odd part

$$Q(x_\mu, \phi) = Q_L(x_\mu, \phi) + Q_R(x_\mu, \phi) \quad \text{with} \quad Q_{L/R}(x_\mu, \phi) = \pm Q_{L/R}(x_\mu, -\phi), \quad (2.16)$$

where we used a foresighted notation. As an example[7], we can perform a decomposition of the fermionic fields into simple trigonometric functions, yielding

$$Q_L(x_\mu, \phi) = \sum_{n=0}^{\infty} Q_L^{(n)}(x_\mu)\cos(n\phi), \qquad Q_R(x_\mu, \phi) = \sum_{n=0}^{\infty} Q_R^{(n)}(x_\mu)\sin(n\phi), \qquad (2.17)$$

with the familiar left and right-chiral spinors $Q_L^{(n)}$, $Q_R^{(n)}$ in four dimensions. Only a left-chiral zero-mode exists, which can be part of a $SU(2)_L$ doublet. The right-chiral singlets can be obtained by introducing an additional set of fermions $q^c(x_\mu, \phi)$, which can be decomposed analogous to (2.16) with reversed orbifold symmetries, allowing this time for a right-handed zero-mode.

The Minimal RS model is the simplest realization of the Randall-Sundrum idea, introduced in subsection 2.1.3. Four-dimensional Minkowskian space-time is supplemented by the previously discussed $S^1/\mathbb{Z}_2$ orbifold with a compactification radius r. For the fifth coordinate, we use $\phi \in [-\pi, \pi]$ or situationally the associated coordinate $x_5 = r\phi$, that has the proper mass dimension. We assume two existing 3-branes attached to the fixed points, one at $\phi = 0$, which is called UV (Planck) brane and one at $\phi = \pi$, denoted as IR (TeV) brane. The warped geometry of the model is expressed by the metric

$$ds^2 = e^{-2\sigma(\phi)}\eta_{\mu\nu}dx^\mu dx^\nu - r^2 d\phi^2, \qquad (2.18)$$

which is a general ansatz, respecting local 4D Lorentz invariance at each firm point in the extra dimension. Inserting (2.18) into the Einstein equations, derived from the 5D classical action (only gravity part)

$$S^{(5)} = \int d^5x \sqrt{|G|} \left\{ 2M_{\mathrm{Pl}(5)}^3 R^{(5)} - \Lambda^{(5)} - \delta(x_5)V_{\mathrm{UV}} - \delta(x_5 - r\pi)V_{\mathrm{IR}} \right\}, \qquad (2.19)$$

---

[7]Take a flat spatial extra dimension of size R and consider the 5D kinetic action for a massless fermion $S^{(5)} = \int d^4x R \int d\phi\, \bar{Q}i\partial_M \Gamma^M Q$, and use (2.16), (2.17) to integrate out ϕ, leading to $S^{(4)} = \pi R \int d^4x \left\{ \bar{Q}_L^{(0)} i\partial_\mu \gamma^\mu Q_L^{(0)} + \sum_{n=1}^{\infty} \bar{Q}^{(n)}(i\partial_\mu \gamma^\mu - n/R)Q^{(n)} \right\}$. Besides the left-chiral massless zero-mode, a massive tower of KK particles for each chirality is generated.

yields a solution for $\sigma(\phi) = kr|\phi|$ and $V_{\text{UV}} = -V_{\text{IR}} = 24M_{\text{Pl}(5)}^3 k$. Calculational details can be found in appendix A.1. The parameter k is related to the cosmological constant through $k^2 = -\Lambda^{(5)}/24M_{\text{Pl}(5)}^3$, enforcing a negative value of $\Lambda^{(5)}$. Such a space is of the anti de-Sitter type. Choosing the parameter set $(k, M_{\text{Pl}(5)}, 1/r) \sim M_{\text{Pl}}$ and the warp factor such that the product $kr \approx 12$, then the quantity

$$\epsilon \equiv e^{-kr\pi} = \frac{M_{\text{EW}}}{M_{\text{Pl}}} \approx 10^{-16} \tag{2.20}$$

can resolve the hierarchy between the electroweak and the Planck scale. Remaining is a small hierarchy, which can be expressed through the "volume" factor

$$L \equiv -\ln \epsilon = kr\pi \approx 37, \tag{2.21}$$

which is larger compared to its natural size of $\mathcal{O}(1)$. For the sake of completeness, we define here another important quantity,

$$M_{\text{KK}} \equiv k\epsilon, \tag{2.22}$$

that will represent the mass scale for the lowest modes of the KK particles.

Note further that the RS model is not expected to be a fundamental theory[8], but rather an effective field theory with a cutoff, that depends on the position in the extra-dimension ϕ. We naturally choose $\Lambda_{\text{UV}}(\phi) = e^{-kr|\phi|}M_{\text{Pl}}$, indicating that the typical scale on the UV brane is of order the Planck scale, while the natural cutoff at the IR brane is given by $\Lambda_{\text{UV}}(\pi) \sim \epsilon M_{\text{Pl}}$, lying in the TeV range. This implies that if we follow the original RS proposal (RS1) in [1] by localizing all fields on the IR brane, we can write down higher-dimensional operators contributing to FCNC processes or allowing for proton decay, which are only suppressed by some TeV scale. Therefore, it is sensible[9] to let the fields propagate into the complete five-dimensional space-time (bulk). Only the Higgs field stays confined on the IR brane, in order to keep the solution of the Gauge HP (see the end of section 2.2.2). So, we will perform a generalization of the remaining SM fields to five dimensions and promote G_{SM} to a bulk gauge group involving 5D gauge transformations. In this sense, we refer to our model as being "minimal" since we do not include further higher dimensional operators.

Before dealing with the particle content, we state the 5D metric representation, that will be used throughout this thesis,

$$G_{MN} = \begin{pmatrix} \eta_{\mu\nu} e^{-2kr|\phi|} & 0 \\ 0 & -1 \end{pmatrix}, \tag{2.23}$$

---

[8]Actually, we will see in (2.28) that the gauge couplings have negative mass dimension, implying that we have irrelevant interaction operators in the RS Lagrangian.

[9]In fact, it turns out that we will additionally obtain a geometrical explanation for the Yukawa hierarchy problem (see section 2.2.4).

which is obtained from (2.18) by inserting $\sigma(\phi) = kr|\phi|$. Furthermore, when we integrate over the fifth dimension (below), it is often convenient to switch to the *t*-notation, introduced in [33], $t = \epsilon e^{\sigma(\phi)}$. Some important relations, concerning the conversion from ϕ to t and vice versa are listed in the appendix A.2.

2.2.2. Gauge Boson & Higgs Sector

The extension of the SM bosonic action to five dimensions reads

$$S_{\mathrm{BS}}^{(5)} = \int d^4x\, r \int_{-\pi}^{\pi} d\phi \left[\mathcal{L}_{\mathrm{GBS}} + \mathcal{L}_{\mathrm{HS}} + \mathcal{L}_{\mathrm{GF}} + \mathcal{L}_{\mathrm{FPG}} \right], \tag{2.24}$$

where $\mathcal{L}_{\mathrm{GBS}}$ contains the kinetic terms for the 5D gauge boson fields W_M^i, B_M and G_M^a. Constructing field strength tensors analog to (1.33) in the SM, we find

$$\mathcal{L}_{\mathrm{GBS}} = \sqrt{|G|}\, G^{KM} G^{LN} \left(-\frac{1}{4} W_{KL}^i W_{MN}^i - \frac{1}{4} B_{KL} B_{MN} - \frac{1}{4} G_{KL}^a G_{MN}^a \right). \tag{2.25}$$

Note that the gauge bosons have mass dimension 3/2, in order to obtain a dimensionless action. Proceeding with $\mathcal{L}_{\mathrm{HS}}$, we will explain at the end of this section that the Higgs particle must be confined on the IR brane. Thus, we introduce a δ-function in front of the kinetic and potential terms, yielding

$$\mathcal{L}_{\mathrm{HS}} = \frac{\delta(|\phi| - \pi)}{r} \left[|D_\mu \Phi|^2 - V(\Phi) \right] \quad \text{with} \quad V(\Phi) = -\mu^2 |\Phi|^2 + \lambda |\Phi|^4. \tag{2.26}$$

The covariant derivative in five dimensions, compare with (1.26), reads in general

$$D_M = \partial_M - i g_5 W_M^i \tau^i - i g_5' B_M Y - i g_{s5} G_M^a T^a, \tag{2.27}$$

with dimensionful 5D couplings, related to the 4D ones by

$$\{ g_5,\, g_5',\, g_{s5} \} = \sqrt{2\pi r}\, \{ g,\, g',\, g_s \}. \tag{2.28}$$

Here we directly see that the 5D couplings have negative mass dimension, thus the interaction terms involve irrelevant operators showing directly that the Minimal RS model is an effective field theory. Proceeding with the Higgs field, we decompose it by

$$\Phi = \frac{1}{\sqrt{2}} \begin{pmatrix} -i\sqrt{2}\varphi^+ \\ v + h + i\varphi_3 \end{pmatrix} \quad \text{with} \quad \varphi^\pm = \frac{1}{\sqrt{2}}(\varphi^1 \mp i\varphi^2), \tag{2.29}$$

where $v = e^{-kr\pi} v_5 \approx 246\,\mathrm{GeV}$, as shown in section 2.1.3, with the bare VEV v_0 of order the Planck mass.

Before continuing, some remarks are needed concerning the treatment of the δ-function in (2.26). The range of integration along ϕ from $[-\pi, \pi]$ does not include

small open neighborhoods around π and $-\pi$ respectively, therefore the δ-function shall be understood as a limiting procedure

$$\delta(|\phi| - \pi) \equiv \lim_{\theta \to 0^+} \frac{1}{2} \left[\delta(\phi - \pi + \theta) + \delta(\phi + \pi - \theta) \right], \qquad (2.30)$$

where the δ-functions on the right-hand side are defined on the interval $[-\pi, \pi]$. The prefactor $1/2$ in (2.30) ensures a normalization on the orbifold interval $[0, \pi]$. As we will see later, appearing δ-functions in the Lagrangian are responsible for the boundary conditions of the fields. Due to the above limiting procedure, these conditions get shifted into the bulk, which is relevant in case of discontinuities[10]. In such cases, we use the notation $f(\pi^-) \equiv \lim_{\theta \to 0^+} f(\pi - \theta)$ and $f(-\pi^+) \equiv \lim_{\theta \to 0^+} f(-\pi + \theta)$ for a function $f(\phi)$ being discontinuous at $\phi = \pi$ and $\phi = -\pi$ respectively.

EWSB and Kaluza-Klein Decomposition

Next we decompose the gauge boson fields analog to the SM mass eigenstates in (1.51) and (1.53), yielding

$$W_M^{\pm} = \frac{1}{\sqrt{2}}(W_M^1 \mp i W_M^2), \qquad\qquad Z_M = \frac{1}{\sqrt{g_5^2 + g_5'^2}}(g_5 W_M^3 - g_5' B_M),$$

$$A_M = \frac{1}{\sqrt{g_5^2 + g_5'^2}}(g_5' W_M^3 + g_5 B_M) . \qquad (2.31)$$

In this basis, we obtain from the kinetic Higgs term in $\mathcal{L}_{\text{HS}}$ after SSB with $\langle \Phi^i \rangle = \delta_{i2} v / \sqrt{2}$ the following 5D mass parameters[11]

$$M_W = \frac{v g_5}{2}, \qquad\qquad M_Z = \frac{v \sqrt{g_5^2 + g_5'^2}}{2}, \qquad\qquad M_A = 0. \qquad (2.32)$$

Note that these parameters have mass dimensions of $3/2$, due to (2.28). They are not the physical masses, but they are related to them via the boundary conditions of the fields, see (2.37) below.

The gauge fixing part in (2.24) is chosen such, as to eliminate terms that mix vector μ- and scalar 5-components of the gauge bosons, which appear in $\mathcal{L}_{\text{GBS}}$. This can be achieved by the following gauge fixing Lagrangian

$$\mathcal{L}_{\text{GF}} = -\frac{1}{2\xi_G} \left(\partial^\mu G_\mu^a - \xi_G \left[\partial_5 e^{-2\sigma(\phi)} G_5^a \right] \right)^2 - \frac{1}{2\xi_A} \left(\partial^\mu A_\mu - \xi_A \left[\partial_5 e^{-2\sigma(\phi)} A_5 \right] \right)^2$$

$$- \frac{1}{2\xi_Z} \left(\partial^\mu Z_\mu - \xi_Z \left[\delta(|x_5| - r\pi) M_Z \varphi^3 + \partial_5 e^{-2\sigma(\phi)} Z_5 \right] \right)^2$$

$$- \frac{1}{\xi_W} \left| \partial^\mu W_\mu^+ - \xi_W \left[\delta(|x_5| - r\pi) M_Z \varphi^+ + \partial_5 e^{-2\sigma(\phi)} W_5^+ \right] \right|^2 . \qquad (2.33)$$

---

[10]This shift also eliminates possible boundary terms, coming from partial integrations of Lagrangian terms, thus enabling the hermiticity requirement of the Lagrangian.

[11]Note that these parameters are not strictly five dimensional ones, since they involve the 4D VEV.

A comprehensive treatment of gauge fixing and Faddeev-Popov ghosts in the Minimal RS model can be found in [28].

In the following part, we will integrate out the fifth dimension. Therefore, the 5D boson fields need to be decomposed, yielding

$$
G_\mu^a(x,\phi) = \frac{1}{\sqrt{r}} \sum_n G_\mu^{(n)a}(x)\chi_n^G(\phi), \qquad G_\phi^a(x,\phi) = \frac{1}{\sqrt{r}} \sum_n a_n^G \varphi_G^{(n)a}(x)\partial_\phi\chi_n^G(\phi),
$$

$$
A_\mu(x,\phi) = \frac{1}{\sqrt{r}} \sum_n A_\mu^{(n)}(x)\chi_n^A(\phi), \qquad A_\phi(x,\phi) = \frac{1}{\sqrt{r}} \sum_n a_n^A \varphi_A^{(n)}(x)\partial_\phi\chi_n^A(\phi),
$$

$$
Z_\mu(x,\phi) = \frac{1}{\sqrt{r}} \sum_n Z_\mu^{(n)}(x)\chi_n^Z(\phi), \qquad Z_\phi(x,\phi) = \frac{1}{\sqrt{r}} \sum_n a_n^Z \varphi_Z^{(n)}(x)\partial_\phi\chi_n^Z(\phi),
$$

$$
W_\mu^\pm(x,\phi) = \frac{1}{\sqrt{r}} \sum_n W_\mu^{\pm(n)}(x)\chi_n^W(\phi), \quad W_\phi^\pm(x,\phi) = \frac{1}{\sqrt{r}} \sum_n a_n^W \varphi_W^{\pm(n)}(x)\partial_\phi\chi_n^W(\phi),
$$

$$(2.34)$$

with 4D mass eigenstates $G_\mu^{(n)a}(x)$, etc. and corresponding profile functions $\chi_n^a(\phi)$ (with $a = G,\ A,\ Z,\ W$), fulfilling the orthonormality relations

$$
\int_{-\pi}^{\pi} d\phi\, \chi_m^a(\phi)\chi_n^a(\phi) = \delta_{mn} \ . \tag{2.35}
$$

Additionally, the profiles are chosen even under the orbifold symmetry, in order to allow for a zero-mode and reproduce the SM gauge bosons. As a consequence of 5D gauge invariance[12] (before EWSB), the scalar components[13] G_ϕ, A_ϕ, Z_ϕ and $W_\phi^\pm$ must have the opposite $\mathbb{Z}_2$ symmetry, therefore they are odd and vanish at the orbifold boundaries $\phi = -\pi, \pi$.

Inserting the decompositions (2.34) into the bosonic action and trying to perform the integration along ϕ, one finds that the profile χ_n^a must obey the equation of motion (EOM)

$$
-\frac{1}{r^2}\partial_\phi e^{-2\sigma}\partial_\phi\chi_n^a(\phi) = (m_n^a)^2\chi_n^a(\phi) - \frac{\delta(|\phi|-\pi)}{r}M_a^2\chi_n^a(\phi) \tag{2.36}
$$

with boundary conditions at the UV and IR brane, given by

$$
\partial_\phi\chi_n^a\Big|_0 = 0, \qquad\qquad \partial_\phi\chi_n^a\Big|_{\pi^-} = -\frac{rM_a^2}{2\epsilon^2}\chi_n^a(\pi^-) \ . \tag{2.37}
$$

Note that the condition at the IR brane implies a kink for the derivative of the profile $\partial_\phi\chi_n^a(\phi)$ at $\phi = -\pi, \pi$. Both boundary conditions are important, since one can derive from them the physical masses m_n^a.

---

[12]For instance, consider the infinitesimal gauge transformation of the five-dimensional photon field, $A_M(x,\phi) \to A_M'(x,\phi) = A_M(x,\phi) + \frac{1}{e}\partial_M\alpha(x,\phi)$, which is only consistent when A_μ and A_5 have opposite $\mathbb{Z}_2$ symmetries.

[13]The ϕ- and 5-component of a boson are related by the radius r, exemplary for the gluon this states $G_\phi = r\, G_5$.

What remains are the scalar fields, which can be decomposed in the basis of the 4D mass eigenstates of Z_ϕ and W_ϕ,

$$\varphi^\pm(x) = \sum_n b_n^W \varphi_W^{\pm(n)}(x), \qquad\qquad \varphi_3(x) = \sum_n b_n^Z \varphi_Z^{(n)}(x), \qquad (2.38)$$

with yet to be determined coefficients b_n^W and b_n^Z. Actually, there is only one possible choice,

$$a_n^a = -\frac{1}{m_n^a}, \qquad\qquad b_n^a = \frac{M_a}{\sqrt{r}} \frac{\chi_n^a(\pi^-)}{m_n^a}, \qquad (2.39)$$

that will give the desired form of the four-dimensional action (only quadratic terms)

$$\begin{aligned}
S_{\text{BS},2}^{(5D)} = \sum_n \int d^4x \Bigg\{ &-\frac{1}{4}G_{\mu\nu}^{(n)a}G^{(n)a\mu\nu} - \frac{1}{2\xi_G}(\partial^\mu G_\mu^{(n)a})^2 + \frac{(m_n^G)^2}{2}G_\mu^{(n)a}G^{(n)a\mu} \\
&-\frac{1}{4}F_{\mu\nu}^{(n)}F^{(n)\mu\nu} - \frac{1}{2\xi_A}(\partial^\mu A_\mu^{(n)})^2 + \frac{(m_n^A)^2}{2}A_\mu^{(n)}A^{(n)\mu} \\
&-\frac{1}{4}Z_{\mu\nu}^{(n)}Z^{(n)\mu\nu} - \frac{1}{2\xi_Z}(\partial^\mu Z_\mu^{(n)})^2 + \frac{(m_n^Z)^2}{2}Z_\mu^{(n)}Z^{(n)\mu} \\
&-\frac{1}{2}W_{\mu\nu}^{(n)+}W^{(n)-\mu\nu} - \frac{1}{\xi_W}(\partial^\mu W_\mu^{(n)+})(\partial^\mu W_\mu^{(n)-}) + \frac{(m_n^W)^2}{2}W_\mu^{(n)+}W^{(n)-\mu} \\
&+\frac{1}{2}\partial_\mu\varphi_G^{(n)a}\partial^\mu\varphi_G^{(n)a} - \frac{\xi_G(m_n^G)^2}{2}\varphi_G^{(n)a}\varphi_G^{(n)a} + \frac{1}{2}\partial_\mu\varphi_A^{(n)}\partial^\mu\varphi_A^{(n)} \\
&-\frac{\xi_A(m_n^A)^2}{2}\varphi_A^{(n)}\varphi_A^{(n)} + \frac{1}{2}\partial_\mu\varphi_Z^{(n)}\partial^\mu\varphi_Z^{(n)} - \frac{\xi_Z(m_n^Z)^2}{2}\varphi_Z^{(n)}\varphi_Z^{(n)} \\
&+\partial_\mu\varphi_W^{(n)+}\partial^\mu\varphi_W^{(n)-} - \xi_W(m_n^W)^2\varphi_W^{(n)+}\varphi_W^{(n)-} + \mathcal{L}_{\text{FPG}}^{(n)}\Bigg\} \\
&+\int d^4x \frac{1}{2}\left(\partial_\mu h\partial^\mu h + 2\lambda v^2 h^2\right).
\end{aligned} \qquad (2.40)$$

At this stage, it is necessary to check the conservation of the degrees of freedom concerning the gauge particles. The matching procedure shows that all (massive) KK modes of the gauge bosons, e.g. $Z_\mu^{(n\geq 1)}$, obtained their longitudinal degrees of freedom by absorbing the corresponding scalar modes, like $\varphi_Z^{(n\geq 1)}$. At the level of the zero-modes ($n = 0$), the photon and gluon remain massless while the W and Z bosons "eat" the scalars $\varphi^\pm$ and φ_3 to become massive, analogous to the SM. Now all degrees of freedom are distributed, although we have not considered zero-modes[14] of the scalar gauge bosons. But it turns out that such modes do not exist in our theory, which can be illustrated as follows. Before EWSB ($v \to 0$), the zero-modes

---

[14]To be precise, we understand under a zero-mode a massless particle having a constant profile, e.g. $A_\mu^{(0)}$, $G_\mu^{(0)}$, or a massive particle that would become massless when setting $v \to 0$, e.g. $W_\mu^{\pm(0)}$, $Z_\mu^{(0)}$.

would be flat and by imposing the requirement of being orbifold-odd need to vanish. When we slightly enhance v, we do not reintroduce a zero-mode, implying that they are also not existent in our theory after EWSB.

Bosonic Bulk Profiles

We proceed with the determination of the profile functions χ_n (suppressing label a) in equation (2.36). When we switch to t-notation it is convenient to define the dimensionless ratio $x_n \equiv m_n/M_{\mathrm{KK}}$. Based on this, (2.36) leads for the homogeneous part to the first order Bessel differential equation

$$\left(t^2 \frac{d^2}{dt^2} + t \frac{d}{dt} + (x_n t)^2 - 1 \right) \frac{\chi_n(t)}{t} = 0, \tag{2.41}$$

whose solution is a superposition of Bessel functions of the first and second kind,

$$\chi_n(t) = \frac{1}{N_n} t \left[J_1(x_n t) + \alpha_n Y_1(x_n t) \right] . \tag{2.42}$$

The parameters x_n and α_n can be determined from the boundary conditions (2.37). Taking the UV BC into account, the solution can be reformulated [27] as

$$\chi_n(t) = N_n \sqrt{\frac{L}{\pi}} \, t \, c_n^+(t) \quad \text{with} \quad c_n^+(t) = Y_0(x_n \epsilon) J_1(x_n t) - J_0(x_n \epsilon) Y_1(x_n t) . \tag{2.43}$$

The normalization constant N_n can be fixed via the orthogonality relation in (2.35), yielding

$$N_n = [c_n^+(1)]^2 + [c_n^-(1)]^2 - \frac{2}{x_n} c_n^+(1) c_n^-(1) - \epsilon^2 [c_n^+(\epsilon)]^2, \tag{2.44}$$

where we introduced

$$c_n^-(t) = \frac{1}{x_n t} \frac{d}{dt} [t c_n^+(t)] = Y_0(x_n \epsilon) J_0(x_n t) - J_0(x_n \epsilon) Y_0(x_n t) . \tag{2.45}$$

With this function, we can formulate both boundary conditions at the UV and IR brane in the following way,

$$c_n^-(\epsilon) = 0, \qquad\qquad x_n c_n^-(1^-) = -\frac{\tilde{g}^2 v^2}{4 M_{\mathrm{KK}}^2} L \, c_n^+(1^-), \tag{2.46}$$

where $\tilde{g}^2 = g^2$ for the W boson and $\tilde{g}^2 = g^2 + g'^2$ in case of the Z boson. Note that for the gluon and photon, the IR boundary condition in (2.46) gets replaced by $c_n^-(1) = 0$, giving rise to massless zero-modes $\chi_0 = 1/\sqrt{2\pi}$, which have to be added to the solutions in (2.43).

Reason for Confining the Higgs on the IR Brane

As a try, let the Higgs field propagate into the bulk. This alters the gauge boson EOM by replacing the δ-function in (2.36) with 1, changing the boundary conditions to

$$\partial_\phi \chi_n^a \Big|_{0^+} = 0, \qquad\qquad \partial_\phi \chi_n^a \Big|_{\pi^-} = 0, \qquad\qquad (2.47)$$

Moreover, the 4D VEV v, appearing in the mass parameters (2.32), is replaced by a ϕ-dependent vacuum expectation value $v(\phi) = e^{-2\sigma(\phi)} v_5$. For instance, let us consider a W boson with 5D mass $M_5 \equiv g_5 v_5 / 2$, whose EOM in t-notation,

$$\left(t^2 \frac{d^2}{dt^2} + t \frac{d}{dt} + (x_n t)^2 - \nu^2 \right) \frac{\chi_n(t)}{t} = 0, \qquad\qquad (2.48)$$

is now a Bessel differential equation with paramter $\nu \equiv \sqrt{1 + M_5^2 / k^2 r}$. Solving (2.48) and integrating along small neighborhoods around the boundaries, while taking (2.47) into account, induces for the bulk-Higgs scenario a zero-mode mass of

$$m_0^2 \approx \frac{M_5^2}{2\pi k r^2} = \frac{g^2 v_5^2}{4kr} \ . \qquad \text{(for a detailed calculation see [34])} \qquad (2.49)$$

As v_5 is naturally of order M_{Pl} and $m_0 \sim \mathcal{O}(100\,\mathrm{GeV})$, this reintroduces a strong fine-tuning issue and does not present a solution to the Gauge HP.

2.2.3. Fermion Sector

Next, we would like to write down the fermionic action in five dimensions. Since the RS space is curved, we have to generalize the Dirac operator $i\gamma^M \partial_M$ of flat spacetime. Therefore, one introduces the inverse vielbeins E_a^M and the spin covariant derivative $D_M \psi = (\partial_M - \frac{i}{4} \omega_M^{ab} \sigma_{ab}) \psi$ with the spin connection ω_M^{ab} and $\sigma_{ab} \equiv \frac{i}{2}[\gamma_a, \gamma_b]$. By means of these quantities, the following kinetic 5D Dirac Lagrangian

$$\mathcal{L}_{\mathrm{F}} = \sqrt{|G|} \left(E_a^M \bar{\psi} i \gamma^a D_M \psi \right) \qquad\qquad (2.50)$$

is invariant under general coordinate transformations of General Relativity as well as Lorentz transformations, see [35] for more details. Making (2.50) manifest hermitian by writing it in the form $\mathcal{O}_H = \frac{1}{2}(\mathcal{O} + \mathcal{O}^\dagger)$ and adding a explicit mass term yields after some calculation steps [33],

$$\mathcal{L}_{\mathrm{F}} = \sqrt{|G|} \left\{ E_a^M \left[\frac{i}{2} \bar{\psi} \gamma^a (\overrightarrow{\partial}_M - \overleftarrow{\partial}_M) \psi + \frac{\omega_{bcM}}{8} \psi \{\gamma^a, \sigma^{bc}\} \psi \right] - \mathrm{sgn}\phi\, m\bar{\psi}\psi \right\} \ . \quad (2.51)$$

We added the function $\mathrm{sgn}\,\phi$ in the $\bar{\psi}\psi$-term, to ensure an orbifold even mass term after the KK decomposition in (2.53), where even/odd fields will correspond to left/right-chiral fields at the 4D level. In case of the RS metric, the vielbeins are

determined to $E_a^M(\phi) = \mathrm{diag}(e^{\sigma(\phi)}, e^{\sigma(\phi)}, e^{\sigma(\phi)}, e^{\sigma(\phi)}, 1)$, while the spin connection will cancel in the fermionic Lagrangian (2.51), see the extra note to [36].

On the basis of the above mentioned, we can proceed with the quark sector including the kinetic terms, explicit mass terms and the Yukawa terms. The 5D Lagrangian is given by

$$\mathcal{L}_{\mathrm{FS}} = \sqrt{|G|}\Big\{ \bar{Q}i\Gamma^a E_a^M D_M Q - \mathrm{sgn}\phi\, \bar{Q}\boldsymbol{M}_Q Q + \sum_{q=u,d} \Big(q^c i\Gamma^a E_a^M D_M q^c - \mathrm{sgn}\phi\, \bar{q}^c \boldsymbol{M}_q q^c \Big)$$

$$- \delta(x_5 - r\pi)\left[\boldsymbol{Y}_u^{(5)} \bar{Q}\Phi d^c + \boldsymbol{Y}_d^{(5)} \bar{Q}i\sigma_2 \Phi^* u^c + \mathrm{h.c.} \right] \Big\}, \tag{2.52}$$

where $\boldsymbol{M}_{Q,q}$ are diagonal matrices[15] containing the real bulk masses. Following the discussion in [27], we normalize the up- and down-type Yukawa matrices $\boldsymbol{Y}_u^{(5)}$, $\boldsymbol{Y}_d^{(5)}$ by the curvature constant k, defining dimensionless 4D Yukawa matrices via $\boldsymbol{Y}_q = \boldsymbol{Y}_q^{(5)} k/2$ for $q = u, d$. Assuming the naturalness principle, we expect their complex entries to be of $\mathcal{O}(1)$. Concerning the notation in (2.52), $Q \equiv (Q^1, Q^2, Q^3)$ stands for a three-vector in generation space containing the $SU(2)_L$ doublets in flavor space $Q^n = (u^n, d^n)^\top$ for $n = 1, 2, 3$. Likewise the 5D singlets are subsumed by $q^c \equiv (q^{c,1}, q^{c,2}, q^{c,3})$ with $q = u, d$. Note that the quark fields have mass dimension two.

Kaluza-Klein Decomposition

The corresponding decomposition in 4D modes and profiles is given by

$$q_L(x,\phi) = \frac{e^{2\sigma}}{\sqrt{r}} \sum_{n=1}^{\infty} \boldsymbol{C}_n^{(Q)}(\phi) a_n^{(Q)} q_L^{(n)}(x), \quad q_L^c(x,\phi) = \frac{e^{2\sigma}}{\sqrt{r}} \sum_{n=1}^{\infty} \boldsymbol{S}_n^{(q)}(\phi) b_n^{(q)} q_L^{(n)}(x),$$

$$q_R(x,\phi) = \frac{e^{2\sigma}}{\sqrt{r}} \sum_{n=1}^{\infty} \boldsymbol{S}_n^{(Q)}(\phi) b_n^{(Q)} q_R^{(n)}(x), \quad q_R^c(x,\phi) = \frac{e^{2\sigma}}{\sqrt{r}} \sum_{n=1}^{\infty} \boldsymbol{C}_n^{(q)}(\phi) a_n^{(q)} q_R^{(n)}(x),$$

$$\tag{2.53}$$

where we set $q = u$, $Q = U$ for the up-sector and $q = d$, $Q = D$ for the down-sector. The fields q, q^c contain the three up- or down-type 5D flavor eigenstates[16], while $q^{(n)}$ represents a single chiral 4D Dirac spinor of mode n in the mass basis. For $n = 1, 2, 3$, they fit the SM quarks with masses m_1, m_2 and m_3. Higher modes can be grouped to form Kaluza-Klein modes[17], each containing six quarks due to the doubling of the 5D quark content. To allow for chiral 4D quarks, the q, q^c fields are splitted into an orbifold even and odd part, which is managed by the $\mathbb{Z}_2$ even (odd) profiles $\boldsymbol{C}_n^{Q,q}(\phi)$ $(\boldsymbol{S}_n^{Q,q}(\phi))$. For each mode n, these profiles are diagonal 3×3 matrices with components, depending on the different bulk mass parameters. In every term

---

[15]It is always possible to express the action in this bulk mass basis, see [27].

[16]In case of the up-sector, this means $q = u = (u^1, u^2, u^3)^\top$ and $q^c = u^c = (u^{c,1}, u^{c,2}, u^{c,3})^\top$.

[17]Exemplarily for the up-sector, $u^{(n)} = (\,\underbrace{u,\ c,\ t}_{\text{SM quarks}}\,, \underbrace{u^{(4)}, u^{(5)}, u^{(6)}, u^{(7)}, u^{(8)}, u^{(9)}}_{\text{1. KK mode}}, ...)\,.$

of (2.53), they get multiplied with three-vectors $a_n^{(q,Q)}$ or $b_n^{(q,Q)}$, which contain the information about 4D flavor mixing, e.g. in the limit of vanishing Yukawa entries, the a- and b-vectors approach unit vectors.

Note that due to gauge invariance, the components of the $SU(2)_L$ doublets have the same profiles, such that $C_n^U \equiv C_n^D$ and $S_n^U \equiv S_n^D$. Still, the a- and b-vectors are in general different for $Q = U, D$. We agree upon, that Q shall only be replaceable by U, D in case of the profiles and flavor vectors but stay fixed in other cases of appearance.

Inserting the KK decompositions into the action (2.52), and comparing it to the desired four-dimensional one

$$S_{\text{FS}}^{(5)} \ni \sum_{q=u,d} \sum_{n=1}^{\infty} \int d^4x \left\{ \bar{q}^{(n)} i \not{\partial} q^{(n)} - m_n^q \, \bar{q}^{(n)} q^{(n)} \right\} \tag{2.54}$$

requires the following orthonormality condition to hold

$$\int_{-\pi}^{\pi} d\phi \, e^{\sigma(\phi)} \left\{ a_m^{(Q,q)} C_m^{(Q,q)} C_n^{(Q,q)} b_n^{(Q,q)} + b_m^{(q,Q)} S_m^{(q,Q)} S_n^{(q,Q)} a_n^{(q,Q)} \right\} = \delta_{mn} \tag{2.55}$$

and constrains the a- and b-vectors by

$$a_n^{(Q,q)} = b_n^{(Q,q)} \qquad \text{and} \qquad a_n^{(Q)\dagger} a_n^{(Q)} + a_n^{(q)\dagger} a_n^{(q)} = 1 \; . \tag{2.56}$$

Before proceeding, we will switch to t-notation and define more compact expressions for the profiles [37],

$$\chi_m^{(Q)}(t) = \sqrt{\frac{2\pi}{L\epsilon}} \begin{pmatrix} C_n^{(Q)}(t) a_n^{(Q)} \\ S_n^{(q)}(t) a_n^{(q)} \end{pmatrix}, \qquad \chi_m^{(q)}(t) = \sqrt{\frac{2\pi}{L\epsilon}} \begin{pmatrix} S_n^{(Q)}(t) a_n^{(Q)} \\ C_n^{(q)}(t) a_n^{(q)} \end{pmatrix}, \tag{2.57}$$

such that the orthonormality condition in (2.55), by making use of (2.56), can be rewritten as

$$\int_{\epsilon}^{1} dt \, \chi_m^{(Q,q)\dagger}(t) \chi_n^{(Q,q)}(t) = \delta_{mn} \; . \tag{2.58}$$

With respect to the expressions in (2.57), the equations of motion take the form

$$t\partial_t \chi_n^{(Q)}(t) = -x_n t \chi_n^{(q)}(t) + \mathcal{M}_q(t) \chi_n^{(Q)}(t),$$
$$t\partial_t \chi_n^{(q)}(t) = x_n t \chi_n^{(Q)}(t) - \mathcal{M}_q(t) \chi_n^{(q)}(t), \tag{2.59}$$

where we defined

$$\mathcal{M}_q(t) = \begin{pmatrix} c_Q & 0 \\ 0 & -c_q \end{pmatrix} + \frac{vt\delta(t - 1^-)}{\sqrt{2}M_{\text{KK}}} \begin{pmatrix} 0 & Y_q \\ Y_q^\dagger & 0 \end{pmatrix} \; . \tag{2.60}$$

We introduced the dimensionless c-parameters, given by $c_{Q_i} \equiv +M_{Q,i}/k$ and $c_{q_i} \equiv -M_{q,i}/k$. Integrating (2.59) along small intervals around the fixed point ϵ, one can derive the UV BC $\boldsymbol{S}_n^{(Q,q)}(\epsilon^+) = 0$. In case of the IR boundary condition, the calculation is not straight forward since one needs a finite-width regularization of the appearing δ-function [37] in (2.60). Thus, one finds

$$\boldsymbol{S}_n^{(Q)}(1^-)a_n^{(Q)} = \frac{v}{\sqrt{2}M_{\text{KK}}}\tilde{\boldsymbol{Y}}_q\boldsymbol{C}_n^{(q)}(1^-)a_n^{(q)},$$

$$\boldsymbol{S}_n^{(q)}(1^-)a_n^{(q)} = -\frac{v}{\sqrt{2}M_{\text{KK}}}\tilde{\boldsymbol{Y}}_q^\dagger\boldsymbol{C}_n^{(Q)}(1^-)a_n^{(Q)}, \tag{2.61}$$

with rescaled Yukawa matrices

$$\tilde{\boldsymbol{Y}}_q = \boldsymbol{f}\left(\frac{v}{\sqrt{2}M_{\text{KK}}}\sqrt{\boldsymbol{Y}_q\boldsymbol{Y}_q^\dagger}\right)\boldsymbol{Y}_q, \qquad \boldsymbol{f}(\boldsymbol{A}) = \tanh(\boldsymbol{A})\boldsymbol{A}^{-1}. \tag{2.62}$$

When we expand the tanh-function around small arguments, both Yukawa matrices coincide at leading order in v^2/M_{KK}^2.

Since the profile matrices are regular, we can reformulate the IR boundary condition into two eigenvalue equations for $a_n^{(Q,q)}$, whose eigenvalues can be determined from

$$\det\left(\mathbb{1} + \frac{v^2}{2M_{\text{KK}}^2}\tilde{\boldsymbol{Y}}_q^\dagger\boldsymbol{C}_n^{(q)}(1^-)\left[\boldsymbol{S}_n^{(q)}(1^-)\right]^{-1}\tilde{\boldsymbol{Y}}_q\boldsymbol{C}_n^{(Q)}(1^-)\left[\boldsymbol{S}_n^{(Q)}(1^-)\right]^{-1}\right) = 0. \tag{2.63}$$

This can be done numerically and yields the physical masses of the SM modes and its KK excitations.

Fermionic bulk profiles

The set of EOMs in (2.59) for the profiles $\boldsymbol{C}_n^{(Q,q)}$ and $\boldsymbol{S}_n^{(Q,q)}$ simplifies, when we consider only the homogeneous part, since the mass and profile matrices are both in diagonal form, yielding

$$(t\partial_t - c_{Q_i,q_i})f_{n,i}^L = -x_n t f_{n,i}^R, \qquad (t\partial_t + c_{Q_i,q_i})f_{n,i}^R = x_n t f_{n,i}^L, \tag{2.64}$$

with $f_{n,i}^L = \boldsymbol{C}_{n,i}^{(Q)}(t), \boldsymbol{S}_{n,i}^{(q)}(t)$ and corresponding $f_{n,i}^R = \boldsymbol{S}_{n,i}^{(Q)}(t), \boldsymbol{C}_{n,i}^{(q)}(t)$. Taking into account the boundary conditions, induced by the Yukawa terms, one arrives at the following explicit solutions

$$\boldsymbol{C}_n^{(Q,q)}(\phi) = N_n(\boldsymbol{c}_{Q,q})\sqrt{\frac{L\epsilon t}{\pi}}f_n^+(t,\boldsymbol{c}_{Q,q}),$$

$$\boldsymbol{S}_n^{(Q,q)}(\phi) = \pm\text{sgn}(\phi)N_n(\boldsymbol{c}_{Q,q})\sqrt{\frac{L\epsilon t}{\pi}}f_n^-(t,\boldsymbol{c}_{Q,q}), \tag{2.65}$$

where we returned to the argument ϕ to stress the orbifold symmetry properties of the profiles[18]. On the r.h.s. of (2.65), we further used special combinations of Bessel functions,

$$f_n^\pm(t,c) = J_{-1/2-c}(x_n\epsilon)\,J_{\mp1/2+c}(x_nt) \pm J_{1/2+c}(x_n\epsilon)\,J_{\pm1/2-c}(x_nt) \ . \tag{2.66}$$

As in the bosonic case, the orthonormality condition (2.55) determines the normalization constant to

$$N_n^{-2}(c) = [f_n^+(1,c)]^2 + [f_n^-(1,c)]^2 - \frac{2c}{x_n}f_n^+(1,c)f_n^-(1,c) - \epsilon^2[f_n^+(\epsilon,c)]^2 \ . \tag{2.67}$$

Note that for the special case of $(c+1/2) \in \mathbb{N}$, the correct solutions have to be obtained by a limiting procedure.

Zero-Mode Approximation (ZMA)

In low energy processes external fermions always correspond to zero-modes ($n = 1,2,3$), therefore it is useful for the physical interpretation to have an analytic expression of the profile functions. These can be achieved by expanding the exact solutions (2.65) in the limit $x_n \ll 1$, since all SM fermion masses are much lighter than the KK scale. One finds,

$$\boldsymbol{C}_n^{(Q,q)}(\phi) \approx \sqrt{\frac{L\epsilon}{\pi}}\frac{F(\boldsymbol{c}_{Q,q})}{\sqrt{1+\delta_n(\boldsymbol{c}_{Q,q})}}\left[t^{\boldsymbol{c}_{Q,q}} - \delta_n(\boldsymbol{c}_{Q,q})t^{1-\boldsymbol{c}_{Q,q}}\right] + \mathcal{O}(x_n^2)$$

$$\boldsymbol{S}_n^{(Q,f)}(\phi) \approx \pm\mathrm{sgn}(\phi)\sqrt{\frac{L\epsilon}{\pi}}\frac{x_nF(\boldsymbol{c}_{Q,q})}{\sqrt{1+\delta_n(\boldsymbol{c}_{Q,q})}}\left[\frac{t^{1+\boldsymbol{c}_{Q,q}} - \epsilon^{1+2\boldsymbol{c}_{Q,q}}t^{-\boldsymbol{c}_{Q,q}}}{1+2\boldsymbol{c}_{Q,q}}\right] + \mathcal{O}(x_n^3),$$

$$\tag{2.68}$$

making use of the "zero-mode profile"

$$F(c) \equiv \mathrm{sgn}[\cos(\pi c)]\sqrt{\frac{1+2c}{1-\epsilon^{1+2c}}}, \tag{2.69}$$

and the parameter (valid for $c^2 \neq 1/4$)

$$\delta_n(c) \equiv \frac{x_n^2}{4c^2-1}\epsilon^{1+2c} \ . \tag{2.70}$$

As expressed in (2.53), each profile function is always multiplied with its corresponding $a_n^{(Q,q)}$ vectors. When considering the complete profiles $\boldsymbol{C}_n^{(Q,q)}(\phi)a_n^{(Q,q)}$ and

---

[18]In t-notation, the even and odd $\mathbb{Z}_2$ parity behavior of the profiles is not directly visible. For clarity, we use expressions in dependence of ϕ.

$S_n^{(Q,q)}(\phi)a_n^{(Q,q)}$, it turns out that the parameter function $\delta_n(c)$ gives only a small contribution and can be neglected. The relevant function is then the zero-mode profile, which behaves like

$$F(c) \approx \begin{cases} \sqrt{1+2c} & , \; -1/2 < c < 1/2 \\ -\sqrt{-1-2c}\,\epsilon^{-c-1/2} & , \; -3/2 < c < -1/2 \end{cases} . \qquad (2.71)$$

In this thesis, typical bulk mass parameters, except for the top, lie in the range $[-3/2, -1/2]$, where $F(c)$ is exponentially suppressed ($\epsilon \approx 10^{-16}$). This suppression effect over several orders of magnitude, generated by small $\mathcal{O}(1)$ variations in the c-parameters, allows for an explanation of the flavor hierarchy, discussed in the next section.

Note, that when we speak of ZMA profiles, we refer only to the leading order expressions,

$$\boldsymbol{C}_n^{(Q,q)}(\phi)\hat{a}_n^{(Q,q)} \approx \sqrt{\frac{L\epsilon}{2\pi}}F(\boldsymbol{c}_{Q,q})t^{\boldsymbol{c}_{Q,q}}\,\hat{a}^{(Q,q)}, \qquad \boldsymbol{S}_n^{(Q,q)}(\phi)\hat{a}^{(Q,q)} \approx 0, \qquad (2.72)$$

where $\hat{a}_n^{(Q,q)}$ are the eigenvectors to the mass equation (2.74), discussed in the following.

2.2.4. Flavor Structure and Hierarchy

For a better understanding of the relations between the input parameters and the fermion mass spectrum and mixing, it is adequate to work with the leading terms of the $\boldsymbol{C}$ and $\boldsymbol{S}$ profiles. Evaluating (2.68) on the IR brane and neglecting the $\delta_n(c)$ functions, yields

$$\boldsymbol{C}_n^{(Q,q)}(\pi^-) \approx \sqrt{\frac{L\epsilon}{\pi}}F(\boldsymbol{c}_{Q,q}), \qquad \boldsymbol{S}_n^{(Q,q)}(\pi^-) \approx \pm\sqrt{\frac{L\epsilon}{\pi}}\frac{x_n}{F(\boldsymbol{c}_{Q,q})} \; . \qquad (2.73)$$

Here we can directly infer the meaning of the zero-mode function as determining the value of a quark profile at the IR brane. Another common way to state this is to say that $F(c)$ gives the wavefunction overlap of a quark profile with the Higgs profile. Inserting the expressions (2.73) into the fermionic boundary conditions on the IR brane in (2.61), one can derive the eigenvalue equations

$$\left(m_n^2 \mathbb{1} - \frac{v^2}{2}\boldsymbol{Y}_q^{\mathrm{eff}}(\boldsymbol{Y}_q^{\mathrm{eff}})^\dagger\right)\hat{a}_n^{(Q)} = 0, \qquad \left(m_n^2 \mathbb{1} - \frac{v^2}{2}(\boldsymbol{Y}_q^{\mathrm{eff}})^\dagger\boldsymbol{Y}_q^{\mathrm{eff}}\right)\hat{a}_n^{(q)} = 0, \qquad (2.74)$$

with orthonormalized vectors $\hat{a}_n^{(Q,q)} \equiv \sqrt{2}a_n^{(Q,q)}$ and effective Yukawa matrices

$$\left(Y_q^{\mathrm{eff}}\right)_{ij} \equiv F(c_{Q_i})(Y_q)_{ij}F(c_{q_j}) \; . \qquad (2.75)$$

The eigenvectors $\hat{a}_n^{(Q)}$ and $\hat{a}_n^{(q)}$ form the columns of unitary matrices

$$\boldsymbol{U}_q = \left(a_1^{(Q)}, a_2^{(Q)}, a_3^{(Q)}\right), \qquad \boldsymbol{W}_q = \left(a_1^{(q)}, a_2^{(q)}, a_3^{(q)}\right), \qquad (2.76)$$

which can be used to diagonalize the effective Yukawa matrix, yielding

$$\boldsymbol{\lambda}_q = \boldsymbol{U}_q^\dagger \, \boldsymbol{Y}_q^{\text{eff}} \, \boldsymbol{W}_q = \begin{cases} \frac{\sqrt{2}}{v} \operatorname{diag}(m_u, m_c, m_t), & \text{for } q = u \\ \frac{\sqrt{2}}{v} \operatorname{diag}(m_d, m_s, m_b), & \text{for } q = d \end{cases} . \qquad (2.77)$$

As comprehensively shown in [28], the elements of the matrices $\boldsymbol{U}_q$ and $\boldsymbol{W}_q$ are given to leading order in hierarchies by

$$(U_q)_{ij} = (u_q)_{ij} \begin{cases} \frac{F(c_{Q_i})}{F(c_{Q_j})}, & i \le j \\ \frac{F(c_{Q_j})}{F(c_{Q_i})}, & i > j \end{cases} , \quad (W_q)_{ij} = (w_q)_{ij} \, e^{i\phi_j} \begin{cases} \frac{F(c_{q_i})}{F(c_{q_j})}, & i \le j \\ \frac{F(c_{q_j})}{F(c_{q_i})}, & i > j \end{cases} , \quad (2.78)$$

with coefficient matrices

$$\boldsymbol{u}_q = \begin{pmatrix} 1 & \frac{(M_q)_{21}}{(M_q)_{11}} & \frac{(Y_q)_{13}}{(Y_q)_{33}} \\ -\frac{(M_q)_{21}^\star}{(M_q)_{11}^\star} & 1 & \frac{(Y_q)_{23}}{(Y_q)_{33}} \\ \frac{(M_q)_{31}^\star}{(M_q)_{11}^\star} & -\frac{(Y_q)_{23}^\star}{(Y_q)_{33}^\star} & 1 \end{pmatrix}, \quad \boldsymbol{w}_q = \begin{pmatrix} 1 & \frac{(M_q)_{12}^\star}{(M_q)_{11}^\star} & \frac{(Y_q)_{31}^\star}{(Y_q)_{33}^\star} \\ -\frac{(M_q)_{12}}{(M_q)_{11}} & 1 & \frac{(Y_q)_{32}^\star}{(Y_q)_{33}^\star} \\ \frac{(M_q)_{13}^\star}{(M_q)_{11}} & -\frac{(Y_q)_{32}}{(Y_q)_{33}} & 1 \end{pmatrix} . \quad (2.79)$$

The minor $(M_q)_{ij}$ denotes the determinant of a q-type Yukawa submatrix, where the i-th row and j-th column has been removed. Moving along, one can express all SM masses in dependence of Yukawa components and zero-mode profile functions [28],

$$\begin{aligned} m_u &= \frac{v}{\sqrt{2}} \frac{|\det(\boldsymbol{Y}_u)|}{(M_u)_{11}} |F(c_{Q_1})F(c_{u_1})|, & m_d &= \frac{v}{\sqrt{2}} \frac{|\det(\boldsymbol{Y}_d)|}{(M_d)_{11}} |F(c_{Q_1})F(c_{d_1})|, \\ m_c &= \frac{v}{\sqrt{2}} \frac{(M_u)_{11}}{(\boldsymbol{Y}_u)_{33}} |F(c_{Q_2})F(c_{u_2})|, & m_s &= \frac{v}{\sqrt{2}} \frac{(M_d)_{11}}{(\boldsymbol{Y}_d)_{33}} |F(c_{Q_2})F(c_{d_2})|, \\ m_t &= \frac{v}{\sqrt{2}} |(\boldsymbol{Y}_u)_{33}||F(c_{Q_3})F(c_{u_3})|, & m_b &= \frac{v}{\sqrt{2}} |(\boldsymbol{Y}_d)_{33}||F(c_{Q_3})F(c_{d_3})| . \end{aligned} \qquad (2.80)$$

The experimental mass hierarchies in the up- and down-sector can be realized through the functions $F(\boldsymbol{c}_{Q,u,d})$, which is in analogy to a mechanism named after Froggatt and Nielsen [38]. In other words, the localization of the quark profiles in the bulk allows for a geometrical explanation of the mass splittings, while the Yukawa matrices $\boldsymbol{Y}_u$, $\boldsymbol{Y}_d$ can have anarchic and $\mathcal{O}(1)$ entries solving the Yukawa HP in section 1.4. The implication for the possible values of the c-parameters is discussed in part 5.2.1 of chapter 5.

For the later numerical analysis, we will need to calculate the Wolfenstein parameters for a given set of 4D Yukawa matrices and bulk mass entries, the formulas can

be found in [27] and read

$$\lambda = \frac{|F(c_{Q_1})|}{|F(c_{Q_2})|}\left|\frac{(M_d)_{21}}{(M_d)_{11}} - \frac{(M_u)_{21}}{(M_u)_{11}}\right|, \quad A = \frac{|F(c_{Q_2})|^3}{|F(c_{Q_1})|^2|F(c_{Q_3})|}\left|\frac{\frac{(Y_d)_{23}}{(Y_d)_{33}} - \frac{(Y_u)_{23}}{(Y_u)_{33}}}{\left[\frac{(M_d)_{21}}{(M_d)_{11}} - \frac{(M_u)_{21}}{(M_u)_{11}}\right]^2}\right|,$$

$$\bar{\rho} - i\bar{\eta} = \frac{(Y_d)_{33}(M_u)_{31} - (Y_d)_{23}(M_u)_{21} + (Y_d)_{13}(M_u)_{11}}{(Y_d)_{33}(M_u)_{11}\left[\frac{(Y_d)_{23}}{(Y_d)_{33}} - \frac{(Y_u)_{23}}{(Y_u)_{33}}\right]\left[\frac{(M_d)_{21}}{(M_d)_{11}} - \frac{(M_u)_{21}}{(M_u)_{11}}\right]} \ . \tag{2.81}$$

Note that the expression for $\bar{\rho}$ and $\bar{\eta}$ does not involve any zero-mode profile, therefore we automatically obtain values of order one in agreement with their experimental values in table B.1. On the basis of (2.80) and (2.81), we can express eight of the zero-mode profile functions in terms of the quark masses, Yukawa entries and the c_{u3} profile function. The necessary relations are given by

$$|F(c_{Q_1})| = \frac{\lambda}{\left|\frac{(M_d)_{21}}{(M_d)_{11}} - \frac{(M_u)_{21}}{(M_u)_{11}}\right|}|F(c_{Q_2})|, \qquad |F(c_{Q_3})| = \frac{\left|\frac{(Y_d)_{23}}{(Y_d)_{33}} - \frac{(Y_u)_{23}}{(Y_u)_{33}}\right|}{A\lambda^2}|F(c_{Q_2})|$$

$$|F(c_{q_1})| = \frac{\sqrt{2}m_{q_1}}{v}\frac{|(M_u)_{11}|\left|\frac{(M_d)_{21}}{(M_d)_{11}} - \frac{(M_u)_{21}}{(M_u)_{11}}\right|}{\lambda|\det(\boldsymbol{Y}_u)|}\frac{1}{|F(c_{Q_2})|}$$

$$|F(c_{q_2})| = \frac{\sqrt{2}m_{q_2}}{v}\frac{|(Y_u)_{33}|}{|(M_u)_{11}|}\frac{1}{|F(c_{Q_2})|},$$

$$|F(c_{q_3})| = \frac{\sqrt{2}m_{q_3}}{v}\frac{A\lambda^2}{|(Y_d)_{33}|\left|\frac{(Y_d)_{23}}{(Y_d)_{33}} - \frac{(Y_u)_{23}}{(Y_u)_{33}}\right|}\frac{1}{|F(c_{Q_2})|} \ . \tag{2.82}$$

Parameter Counting

Additional fundamental parameters in the RS model, compared to the SM, are the hermitian 3×3 bulk mass matrices $\boldsymbol{M}_{Q,u,d}$. They introduce $N_c = (18, 9)$ parameters[19], that are supplemented with the $N_Y = (18, 18)$ parameters from the quark Yukawa matrices. As in the SM, when restricting to the quark sector, see (1.72), the global symmetry group $G_Y = U(3)_Q \times U(3)_u \times U(3)_d$ with $N_{G_Y} = (9, 18)$ generators is broken by the Yukawa terms to the abelian subgroup $H_Y = U(1)_B$ with $N_{H_Y} = (0, 1)$, resulting in[20]

$$N_{\text{phys}} = N_Y + N_c - (N_{G_Y} - N_{H_Y}) = (27, 10) \tag{2.83}$$

physical parameters [39]. We end up with 27 moduli and ten phases. The moduli can be identified in the ZMA with the six quark masses, the twelve mixing angles appearing in $\boldsymbol{U}_{u,d}$, $\boldsymbol{W}_{u,d}$ and the nine zero-mode profiles $F(\boldsymbol{c}_{Q,u,d})$. One of the ten phases can be traced to the CKM phase.

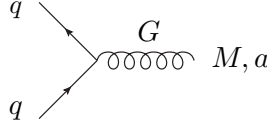[19] A general $N \times N$ hermitian matrix has $N(N+1)/2$ real parameters and $N(N-1)/2$ complex phases.

[20] The generalized formula for N_f fermion generations reads, $N_{\text{phys}} = \left(N_f(2N_f+3), (N_f-1)(2N_f-1)\right)$. A detailed discussion can be found in [28].

2.2.5. Quarks Coupling to Gluons and KK Excitations

This subsection introduces the techniques and Feynman rules to calculate tree-level diagrams of quarks exchanging a tower of gluon particles, since this will be relevant in subsequent chapters. We start with the general 5D Lagrangian for quarks where D_M represents the covariant derivative in (2.27). For our purpose, the coupling of the 5D gluon to quarks is of relevance and the corresponding Lagrangian is given by
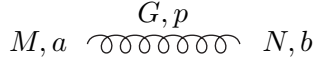
$$\mathcal{L}_{Gqq} = \sqrt{|G|}g_{s5}\Big(\bar{Q}\Gamma^m E_m^M T^a G_M^a Q + \sum_{q=u,d} \bar{q}^c \Gamma^m E_m^M T^a G_M^a q^c\Big)$$

$$= g_{s5}\, e^{-3\sigma(\phi)} \sum_{q=u,d} \Big\{ \bar{q}(\gamma^\mu G_\mu^a + i\gamma^5 G_5^a e^{-\sigma(\phi)})T^a q$$

$$+ \bar{q}^c(\gamma^\mu G_\mu^a + i\gamma^5 G_5^a e^{-\sigma(\phi)})T^a q^c\Big\} \qquad (2.84)$$

where we inserted the RS vielbein and used $Q = (u,d)^\top$ in the second step. Based on (2.84), we can read off the vertex rule expressed in 4D momentum space-time and in position space for the fifth coordinate, yielding

$$iV_{(5),M}^{G,a} = ig_{s5}\, e^{-3\sigma(\phi)}(\gamma_\mu \delta_M^\mu + i\gamma^5 \delta_M^5 e^{-\sigma(\phi)})T^a, \qquad (2.85)$$

where the same rule also applies in case of the singlet quarks q^c. In order to describe the exchange of a 5D gluon, we need the corresponding propagator $D_{\xi_G,ab}^{G,MN}(p,\phi,\phi')$, which will be derived as part of a more general solution within the next section. We just state the Feynman rule,

$$iD_{\xi_G,ab}^{G,MN}(p,\phi,\phi')\,. \qquad (2.86)$$

In the following, we want to consider tree-level diagrams with two incoming and two outgoing quarks, exchanging a SM gluon and its KK excitations. Such a diagram can be extracted from a 5D amplitude with external 5D quark fields q, q^c, q' and q'^c as shown on the left-hand side of fig. 2.2. When we assign incoming and outgoing momenta p_1, p_2 and $-p_3$, $-p_4$ respectively, we can write the total amplitude as

$$-i\mathcal{M}_G = \int_{-\pi}^{\pi} d\phi \int_{-\pi}^{\pi} d\phi'\, r^2 \Big\{ \Big[\bar{q}(p_1,\phi)iV_{(5),M}^{G,a}(\phi)q(p_2,\phi) + \bar{q}^c(p_1,\phi)iV_{(5),M}^{G,a}(\phi)q^c(p_2,\phi)\Big]$$

$$D_{\xi_G,ab}^{G,MN}(p,\phi,\phi')\Big[\bar{q}'(p_3,\phi')iV_{(5),N}^{G,b}(\phi')q'(p_4,\phi') + \bar{q}'^c(p_3,\phi')iV_{(5),N}^{G,b}(\phi')q'^c(p_4,\phi')\Big] \Big\},$$

$$(2.87)$$

where $p = p_1 + p_2 = -(p_3 + p_4)$. For instance, let us extract the 4D diagram, shown on the right-hand side of fig. 2.2, where KK gluons are exchanged between the 4D
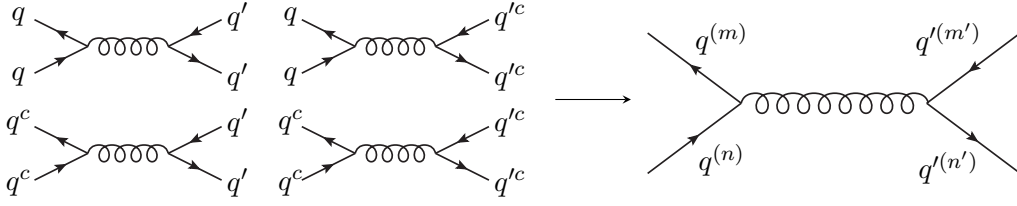
Figure 2.2.: From the four 5D diagrams on the left-hand side, exchanging a boson (e.g. a gluon) between doublet and singlet quarks, we can extract the desired diagram with external 4D modes.

quark modes $q^{(m)}$, $q^{(n)}$, $q'^{(m')}$ and $q'^{(n')}$. Therefore we decompose the quark fields in (2.87) by using the 4D Fourier-transformed version of (2.53). Keeping only the relevant contributions that belong to the desired 4D diagram, we finally obtain in t-notation

$$
\begin{aligned}
-i\mathcal{M}_G = i2\pi r\, g_s^2 \int_\epsilon^1 dt \int_\epsilon^1 dt' \bigg\{ & D^{G,\mu\nu}_{\xi_G,ab}(p,t,t') \\
& \times \left[\chi_m^{(Q)\dagger}(t)\chi_n^{(Q)}(t)\, \bar{q}_L^{(m)}\gamma_\mu T^a q_L^{(n)} + \chi_m^{(q)\dagger}(t)\chi_n^{(q)}(t)\, \bar{q}_R^{(m)}\gamma_\mu T^a q_R^{(n)} \right] \\
& \times \left[\chi_{m'}^{(Q')\dagger}(t')\chi_{n'}^{(Q')}(t')\, \bar{q}_L'^{(m')}\gamma_\nu T^b q_L'^{(n')} + \chi_{m'}^{(q')\dagger}(t')\chi_{n'}^{(q')}(t')\, \bar{q}_R'^{(m')}\gamma_\nu T^b q_R'^{(n')} \right] \\
& + \left(\frac{M_{\mathrm{KK}}^2}{tt'k^2} \right) D^{G,55}_{\xi_G,ab}(p,t,t') \\
& \times \left[\chi_m^{(Q)\dagger}(t)\chi_n^{(q)}(t)\, \bar{q}_L^{(m)}\gamma_5 T^a q_R^{(n)} + \chi_m^{(q)\dagger}(t)\chi_n^{(Q)}(t)\, \bar{q}_R^{(m)}\gamma_5 T^a q_L^{(n)} \right] \\
& \times \left[\chi_{m'}^{(Q')\dagger}(t')\chi_{n'}^{(q')}(t')\, \bar{q}_L'^{(m')}\gamma_5 T^b q_R'^{(n')} + \chi_{m'}^{(q')\dagger}(t')\chi_{n'}^{(Q')}(t')\, \bar{q}_R'^{(m')}\gamma_5 T^b q_L'^{(n')} \right] \bigg\},
\end{aligned}
$$

$$(2.88)$$

where we used the expressions $\chi_n^{(Q,q)}$ in (2.57), that contain the quark profiles. Contributions from the mixed vector-scalar $\mu 5$-component of the 5D propagator have been neglected in (2.88), since the gauge-fixing terms in (2.33) are chosen such, that the scalar and vector components of a gauge boson do not mix with each other, independently of the value for ξ. This can be seen explicitly from the differential equation in (3.6) of the subsequent chapter.

Alternatively, one can directly work with four dimensional Feynman rules, which are comprehensively listed in [40] and [41]. Concerning the gluon case, we have to insert the Kaluza-Klein decompositions directly into the Lagrangian (2.84), integrate over the fifth dimension and read off the rules, yielding

$$q^{(k)} \quad \overset{G^{(m)}}{\text{(gluon)}} \quad \mu, a \qquad ig_s T^a \gamma^\mu \Big[(V_q^G)_{nmk} P_L + (\tilde{V}_q^G)_{nmk} P_R \Big], \qquad (2.89)$$

$$q^{(k)} \quad \overset{G^{(m)}}{\text{- - - -}} \quad 5, a \qquad -g_s T^a \Big[(S_q^G)_{nmk} P_L - (\tilde{S}_q^G)_{nmk} P_R \Big], \qquad (2.90)$$

where

$$(V_q^G)_{nmk} = \sqrt{2\pi} \int_\epsilon^1 dt\, \chi_m^G \chi_n^{(Q)\dagger} \chi_k^{(Q)}, \qquad (\tilde{V}_q^G)_{nmk} = \sqrt{2\pi} \int_\epsilon^1 dt\, \chi_m^G \chi_n^{(q)\dagger} \chi_n^{(q)}, \tag{2.91}$$

$$(S_q^G)_{nmk} = \frac{\sqrt{2\pi}}{x_m^G} \int_\epsilon^1 dt\, (\partial_t \chi_m^G) \chi_n^{(q)\dagger} \chi_k^{(Q)}, \quad (\tilde{S}_q^G)_{nmk} = \frac{\sqrt{2\pi}}{x_m^G} \int_\epsilon^1 dt\, (\partial_t \chi_m^G) \chi_n^{(Q)\dagger} \chi_k^{(q)}, \tag{2.92}$$

and $x_m^G \equiv m_m^G / M_{\text{KK}}$. These overlap integrals determine if different quark flavors can couple to the vertex. Inserting the flat SM gluon profile $\chi_0^G = 1/\sqrt{2\pi}$ into (2.91), we encounter the orthonormality condition for fermions (2.58), which requires $m = n$. Thus, a flavor changing process through a SM gluon is not allowed at tree-level. But once the profile is not a constant, which is the case for the gluon KK excitations $\chi_{n\geq 1}^G$, the integral does not vanish for $m \neq n$.

Concerning the propagators for the 4D modes $G_\mu^{(n)}$ and $\varphi_G^{(n)}$, they are just given by analogous expressions as in the SM, i.e.

$$\mu, a \quad \overset{G^{(n)}, p}{\text{(gluon)}} \quad \nu, b \qquad i\delta_{ab} \frac{-g^{\mu\nu} + (1 - \frac{1}{\xi_G}) p^\mu p^\nu / p^2}{p^2 - (m_n^G)^2 + i\epsilon}, \qquad (2.93)$$

$$a \quad \overset{\varphi_G^{(n)}, p}{\text{- - - - -}} \quad b \qquad i \frac{\delta_{ab}}{p^2 - \xi_G (m_n^G)^2 + i\epsilon} . \qquad (2.94)$$

Using the vertex rules (2.91), (2.92) as well as (2.93), (2.94) for the propagators, we can work out the right diagram in fig. 2.2 and compare it to the five-dimensional result in (2.88). We encounter sums over gluon profiles, referred to as the KK towers, which correspond to the 5D propagators, whose derivation is the subject of the following chapter.

3. 5D Gauge Boson Propagator

In this chapter we calculate a general formula for the Feynman propagator of a five-dimensional (spin one) boson, without restriction to specific boundary conditions. The result is needed in chapter 5, when we extend the Minimal RS model by a new gauge boson particle.

We begin the calculation for the case of a gluon field, but we will obtain a general result that is also valid for the remaining gauge bosons. In quantum field theory, the propagator is given by the two-point Green's function. Since we already know the 4D momentum propagator, it is convenient to perform a Fourier integration to momentum space for the non-compactified four dimensional space-time, yielding the propagator in mixed momentum/position space

$$iD_{\xi_G,ab}^{G,MN}(p,t,t') = \int d^4x\, e^{-ipx} \langle 0|T\left\{G_a^M(x,t)\,G_b^N(0,t')\right\}|0\rangle, \tag{3.1}$$

where we used translation invariance in the x^μ directions. Inserting the decomposition (2.34) of the gluon field into (3.1) and using the momentum representation of the 4D Feynman propagators in (2.93) and (2.94), we arrive at

$$D_{\xi_G,ab}^{G,\mu\nu}(p,t,t') = \delta_{ab}\,\frac{1}{r}\sum_{n=0}^{\infty}\chi_n^G(t)\chi_n^G(t')\frac{-g^{\mu\nu}+(1-\frac{1}{\xi_G})p^\mu p^\nu/p^2}{p^2-(m_n^G)^2+i\epsilon} \tag{3.2}$$

for the vector components and at

$$D_{\xi_G,ab}^{G,55}(p,t,t') = \delta_{ab}\,\frac{1}{r}\sum_{n=0}^{\infty}\frac{k^2 tt'}{(m_n^G)^2}\frac{\partial_t\chi_n^G(t)\,\partial_{t'}\chi_n^G(t')}{p^2-\xi_G(m_n^G)^2+i\epsilon} \tag{3.3}$$

for the scalar part of the 5D propagator. Mixed components do not appear, which will be explained below. In principle, the 5D propagator represents a weighted sum over KK profiles, evaluated at t and t'. The factor $1/r$ on the r.h.s. of (3.2) and (3.3) ensures the correct mass dimension of -1 for the 5D propagator in mixed momentum/position space. The derivation starts with the action for G_M^a, containing the kinetic part (without self-interactions) and the gauge fixing part,

$$S_{\rm BS}^{(5)} \ni \int d^4x \int_{-r\pi}^{r\pi} dx_5 \left\{-\frac{\sqrt{|G|}}{4}G^{KM}G^{LN}\partial_{[K}G_{L]}^a\partial_{[M}G_{N]}^a - \frac{1}{2\xi_G}\left[\partial^\mu G_\mu^a - \xi_G\partial_5(e^{-2\sigma}G_5^a)\right]^2\right\}, \tag{3.4}$$

with $|G| \equiv |\det(G)| = e^{-8\sigma}$ and the gauge-fixing parameter ξ_G. Now we perform several partial integrations to get rid of terms mixing G_μ^a and G_5^a. Appearing boundary terms can be set to zero, when using the fact that G_5^a with G_μ^a have opposite

orbifold symmetries, leading to

$$S_{\text{BS}}^{(5)} \ni \frac{1}{2} \int d^4x \int_{-r\pi}^{r\pi} dx_5 \, G_M^a K_{\xi_G,ab}^{G,MN} G_N^b, \tag{3.5}$$

with

$$K_{\xi_G,ab}^{G,MN} = \delta_{ab} \begin{pmatrix} \partial_\alpha \partial^\alpha \eta^{\mu\nu} - (1 - \frac{1}{\xi_G})\partial^\mu \partial^\nu - \partial_5 e^{-2\sigma} \partial_5 \eta^{\mu\nu} & 0 \\ 0 & -e^{-2\sigma}\partial_\mu \partial^\mu + \xi_G \, e^{-2\sigma}\partial_5 \partial_5 e^{-2\sigma} \end{pmatrix}, \tag{3.6}$$

being the differential operator standing in between the gluon fields. The Feynman propagator $D_{\xi_G,\nu\rho}^{G,ab}$ is the inverse of $K_{\xi_G,ab}^{G,MN}$, fulfilling

$$\int d^4y \int_{-r\pi}^{r\pi} dy_5 \, \tilde{K}_{\xi_G,ab}^{MN}(x,y) D_{\xi_G,NR}^{G,bc}(y,z) = \delta_{ac}\delta_R^M \delta^{(5)}(x-z), \tag{3.7}$$

where we introduced $\tilde{K}_{\xi_G,ab}^{G,MN}(x,y) \equiv \delta(x-y)K_{\xi_G,ab}^{G,MN}$. Since the differential operator (3.6) is diagonal in the mixed vector-scalar components, we can split the derivation of the propagator from (3.7) into two sections 3.1 and 3.2. From this point on, we can drop the color indices as well as the label G and generalize the calculation.

3.1. Vector Components

Starting with the vector components of (3.7), we can transform the non-compact dimensions of the equation to momentum space, such that

$$\left[\left(p^2 + \partial_5^x e^{-2\sigma(\phi_x)} \partial_5^x \right) \eta^{\mu\nu} - (1 - \frac{1}{\xi})p^\mu p^\nu \right] D_{\xi,\nu\rho}(p,\phi_x,\phi_z) = -\frac{1}{2r}\delta_\rho^\mu \delta(\phi_x - \phi_z), \tag{3.8}$$

where $\partial_5^x \equiv \frac{1}{r}\partial_{\phi_x}$. The factor $1/2$ on the r.h.s. appears, since we now restrict our coordinate ϕ to the range $[0,\pi]$ (instead of $[-\pi,\pi]$), which leads to the mentioned normalisation factor for the delta-function $\delta(\phi_x - \phi_z)$. Transforming to t-notation, see appendix A.2, we obtain

$$\left[\left(p^2 + M_{\text{KK}}^2 t\partial_t \frac{1}{t}\partial_t \right) \eta^{\mu\nu} - (1 - \frac{1}{\xi})p^\mu p^\nu \right] D_{\xi,\nu\rho}(p,t,t') = -\frac{Lt'}{2\pi r}\delta_\rho^\mu \delta(t-t'), \tag{3.9}$$

where we have further introduced $t \equiv t_x$ and $t' \equiv t_z$. In order to solve this equation, we try the following ansatz [42]

$$D_{\xi,\nu\rho}(p,t,t') = A_\xi(p,t,t')\frac{p_\nu p_\rho}{p^2} + B(p,t,t')(\eta_{\nu\rho} - \frac{p_\nu p_\rho}{p^2}), \tag{3.10}$$

where we anticipatingly assume that only A_ξ depends on the choice of gauge. Plugging this ansatz into into (3.9), we encounter

$$p^\mu p_\rho \left[\left(\frac{p^2}{\xi} + D_t \right) A_\xi - \left(p^2 + D_t \right) B \right] + \delta_\rho^\mu p^2 \left[(p^2 + D_t)B + \frac{Lt'}{2\pi r}\delta(t-t') \right] = 0, \tag{3.11}$$

while using the short notation $D_t \equiv M_{\mathrm{KK}}^2 t \partial_t \frac{1}{t} \partial_t$ for the differential operator. Since each bracket has to vanish by itself, we only need to solve the following differential equation for B,

$$\left(p^2 + D_t\right) B(p, t, t') = -\frac{Lt'}{2\pi r}\delta(t - t'), \tag{3.12}$$

while obtaining A_ξ through the relation $A_\xi(p, t, t') = B(p/\sqrt{\xi}, t, t')$. We can rewrite (3.12) as

$$\left(t^2\partial_t^2 + t\partial_t + t^2p^2 - 1\right)\frac{B(p, t, t')}{t} = -\frac{Ltt'}{2\pi r M_{\mathrm{KK}}^2}\delta(t - t'), \tag{3.13}$$

whose homogeneous part is a Bessel differential equation of order one. The two independent solutions, for $t \neq t'$, are given by

$$B^>(p, t, t') = t\left[\tilde{C}_J^>(p, t')J_1(pt/M_{\mathrm{KK}}) + \tilde{C}_Y^>(p, t')Y_1(pt/M_{\mathrm{KK}})\right] \quad \text{for} \quad t > t',$$

$$B^<(p, t, t') = t\left[\tilde{C}_J^<(p, t')J_1(pt/M_{\mathrm{KK}}) + \tilde{C}_Y^<(p, t')Y_1(pt/M_{\mathrm{KK}})\right] \quad \text{for} \quad t < t', \tag{3.14}$$

with Bessel functions of the first and second kind, J_1 and Y_1 respectively, and coefficients $\tilde{C}_{J,Y}^>$, $\tilde{C}_{J,Y}^<$ depending in general on t' and on the momentum $p \equiv \sqrt{p_\mu p^\mu}$. Since the propagator $D_\xi^{\mu\nu}(p, t, t')$ must be symmetric in t and t', we may write the homogeneous solution of (3.12) as

$$B(p, t, t') = N(\tilde{p})\, t_> t_< \left[C_J^>(\tilde{p})\, J_1(\tilde{p}t_>) + C_Y^>(\tilde{p})\, Y_1(\tilde{p}t_>)\right]$$
$$\times \left[C_J^<(\tilde{p})\, J_1(\tilde{p}t_<) + C_Y^<(\tilde{p})\, Y_1(\tilde{p}t_<)\right], \tag{3.15}$$

where $t_> \equiv \mathrm{Max}[t, t']$, $t_< \equiv \mathrm{Min}[t, t']$ and $\tilde{p} \equiv p/M_{\mathrm{KK}}$. The new coefficients $C_{J,Y}^>$ and $C_{J,Y}^<$ do not depend on t' any more. We further introduced an additional normalisation constant N, dependent on $\tilde{p}$, that can be fixed by integrating (3.12) along a small ϵ-interval around t' with respect to t (inside the bulk), yielding

$$\int_{t'-\epsilon}^{t'+\epsilon} dt \left(p^2 + D_t\right) B(p, t, t') = -\frac{Lt'}{2\pi r}\,. \tag{3.16}$$

Evaluating both sides, we find for the normalization

$$N(\tilde{p}) = \frac{L}{4r M_{\mathrm{KK}}^2}\frac{1}{C_J^>(\tilde{p})C_Y^<(\tilde{p}) - C_J^<(\tilde{p})C_Y^>(\tilde{p})}, \tag{3.17}$$

which completes the solution for $B(p, t, t')$. Finally, (3.9) together with (3.15) and (3.17), represents a fundamental solution for the propagator $D_\xi^{\mu\nu}(p, t, t')$, whose coefficients can be fixed by imposing boundary conditions at the UV and IR branes. Such BCs are the same as the ones imposed for the profiles, since the propagator is just the sum over profiles, see (3.2).

Note further that the 5D propagators for A, W and Z bosons read analogously to (3.2) when striking off the color indices and inserting the corresponding modes and masses. In a similar manner, we can perform the above mentioned steps, that will lead to the same fundamental solution. The boundary conditions in (2.37) then determine the special solution.

To be more general, let us assume a gauge boson having a similar decomposition as in (2.34) with profiles χ_n, fulfilling the following BCs

$$\partial_t \chi_n(t)\big|_{t=\epsilon^+} = b_\epsilon\, \chi_n(\epsilon^+), \qquad\qquad \partial_t \chi_n(t)\big|_{t=1^-} = -b_1\, \chi_n(1^-)\,, \qquad (3.18)$$

with the boundary parameters b_ϵ and b_1 for the UV ($t = \epsilon$) and IR ($t = 1$) brane respectively. Consequently the 5D vector propagator, being the sum of profiles, admits the same conditions

$$\partial_t D_\xi^{\mu\nu}(p,t,t')\big|_{t=\epsilon^+} = b_\epsilon\, D_\xi^{\mu\nu}(p,\epsilon^+,t'), \quad \partial_t D_\xi^{\mu\nu}(p,t,t')\big|_{t=1^-} = -b_1\, D_\xi^{\mu\nu}(p,1^-,t'),$$
$$(3.19)$$

where analogous expression hold for the variable t', due to the symmetry properties. Evaluating (3.19), we obtain the following solutions for the coefficients

$$C_Y^<(\tilde p) = \tilde p J_0(\tilde p\epsilon) - b_\epsilon J_1(\tilde p\epsilon), \qquad\qquad C_Y^>(\tilde p) = \tilde p J_0(\tilde p) + b_1 J_1(\tilde p),$$
$$C_J^<(\tilde p) = -\tilde p Y_0(\tilde p\epsilon) + b_\epsilon Y_1(\tilde p\epsilon), \qquad\qquad C_J^>(\tilde p) = -\tilde p Y_0(\tilde p) - b_1 Y_1(\tilde p), \qquad (3.20)$$

which depend on the boundary parameters b_ϵ and b_1. Note that they are not unique by themselves, but they are sufficient to completely specify the propagator solution, due to the symmetry in t and t'. We distinguish three types of boundary conditions, that can occur at each of the two branes,

$$\textbf{Dirichlet (D):} \qquad\qquad \chi(t)\big|_{\text{brane}} = 0, \qquad (3.21)$$

$$\textbf{Neumann (N):} \qquad\qquad \partial_t \chi(t)\big|_{\text{brane}} = 0, \qquad (3.22)$$

$$\textbf{Mixed (M):} \qquad\qquad \partial_t \chi(t)\big|_{\text{brane}} \neq 0\,. \qquad (3.23)$$

In this notation, the photon and gluon have profiles with (NN) boundary conditions, while the massive Z and W bosons have profiles of type (NM), see (2.37).

Since we will need to calculate low energy tree-level processes in the subsequent chapters, we are especially interested in the limit $p \to 0$. Starting with the (NN) case, meaning $a = b = 0$, we expand the full solution around $p = 0$, yielding

$$D_\xi^{\mu\nu}(p,t,t') = \frac{-g^{\mu\nu} + (1 - \frac{1}{\xi})p^\mu p^\nu / p^2}{2\pi r p^2}$$
$$+ \frac{-g^{\mu\nu}}{4\pi r M_{\text{KK}}^2}\left[\frac{1-\epsilon^2}{2L} + Lt_<^2 - t^2\left(\frac{1}{2} - \ln t\right) - t'^2\left(\frac{1}{2} - \ln t'\right)\right] + \mathcal{O}(p^2)\,.$$
$$(3.24)$$

The first term is just the addend $n = 0$ of (3.2), when inserting the zero mode profile of a massless particle, $\chi_0 = 1/\sqrt{2\pi}$. The second term in (3.24) is a finite expression for the summation of massive KK particles in the limit $p \to 0$ and is in agreement with [27] (dropping the $\mathcal{O}(\epsilon^2)$ term), where the calculation was performed by using the EOMs. Note that this term does not depend on the gauge parameter ξ. In the RS model, each gauge boson (4D) mode for $n \geq 1$ "eats" the corresponding scalar excitation, which provides the longitudinal degree of freedom. We will see below, that the 55-component of the propagator contains the gauge dependence.

For the remaining cases, assuming that at least one of the BCs is not of Neumann type ($a \neq 0$ or $b \neq 0$), the limit $p \to 0$ can be performed at once and yields the solution

$$D_\xi^{\mu\nu}(p, t, t') = -g^{\mu\nu} \frac{L}{4\pi r M_{\mathrm{KK}}^2} \left[c_0 + t_<^2 + c_1(t^2 + t'^2) + c_2\, t^2 t'^2 \right] + \mathcal{O}(p^2), \quad (3.25)$$

where c_0, c_1 and c_2 are functions of the boundary parameters b_ϵ and b_1. They are given by

$$c_0(b_\epsilon, b_1) = \frac{\epsilon(2 + b_1)(2 - b_\epsilon \epsilon)}{2(b_\epsilon + b_1 \epsilon) - b_\epsilon b_1(\epsilon^2 - 1)}, \qquad c_1(b_\epsilon, b_1) = -\frac{b_1 \epsilon(2 - b_\epsilon \epsilon)}{2(b_\epsilon + b_1 \epsilon) - b_\epsilon b_1(\epsilon^2 - 1)},$$

$$c_2(b_\epsilon, b_1) = -\frac{b_\epsilon b_1}{2(b_\epsilon + b_1 \epsilon) - b_\epsilon b_1(\epsilon^2 - 1)}, \tag{3.26}$$

and will play an important role in the analysis of chapter 5.

As an example, let us consider the W or Z boson. Their BCs, see (2.37), can be expressed in t-notation as

$$b_\epsilon = 0, \qquad\qquad b_1 = \frac{r\pi M_{W,Z}^2}{2L\epsilon^2} = \frac{L m_{W,Z}^2}{M_{\mathrm{KK}}^2}, \qquad (3.27)$$

where we used (2.32) for $M_{W,Z}^2$ and $m_W^2 = v^2 g^2/4$ as well as $m_Z^2 = v^2(g^2 + g'^2)/4$ to rewrite the IR boundary condition. Based on this notation, the propagator (3.25) takes the following form

$$D_\xi^{\mu\nu}(p, t, t') = -g^{\mu\nu} \left(\frac{1}{2\pi\, m_{W,Z}^2} + \frac{L}{4\pi M_{\mathrm{KK}}^2} \left[1 - t_>^2 \right] \right) + \mathcal{O}(p^2), \qquad (3.28)$$

which is the exact expression, compared with the approximate result in [27].

3.2. Scalar Components

The scalar 5D propagator is the solution to the 55-component of the differential equation in (3.7),

$$\left(p^2 e^{-2\sigma(\phi_x)} + \xi e^{-2\sigma(\phi_x)} \partial_5^x \partial_5^x e^{-2\sigma(\phi_x)} \right) D_\xi^{55}(p, \phi_x, \phi_z) = \frac{1}{2r}\delta(\phi_x - \phi_z). \qquad (3.29)$$

Performing the same steps leading from (3.8) to (3.9), we can stick to the t-notation and find

$$\left[p^2 + \xi M_{\mathrm{KK}}^2 t \partial_t t \partial_t \frac{1}{t^2} \right] D_\xi^{55}(p, t, t') = \frac{L t'^3}{2\pi r \epsilon^2} \delta(t - t') \tag{3.30}$$

After some simple manipulations, this equation can be rewritten as

$$\left[t^2 \partial_t^2 + t \partial_t + \frac{p^2 t^2}{\xi M_{\mathrm{KK}}^2} \right] \frac{\xi D_\xi^{55}(p, t, t')}{t^2} = \frac{L t'^3}{2\pi r M_{\mathrm{KK}}^2 \epsilon^2} \delta(t - t'), \tag{3.31}$$

where the left bracket contains a Bessel differential operator of order zero. Solutions contain superpositions of the Bessel functions J_0 and Y_0. Considering the symmetry under exchange of t and t', the homogeneous solution to (3.31) can be expressed as

$$D_\xi^{55}(p, t, t') = N(\hat{p}) \frac{t_>^2 t_<^2}{\xi} \left[C_J^>(\hat{p}) J_0(\hat{p} t_>) + C_Y^>(\hat{p}) Y_0(\hat{p} t_>) \right]$$
$$\times \left[C_J^<(\hat{p}) J_0(\hat{p} t_<) + C_Y^<(\hat{p}) Y_0(\hat{p} t_<) \right], \tag{3.32}$$

with the normalization constant $N(\hat{p})$ and $\hat{p} \equiv p/(\sqrt{\xi} M_{\mathrm{KK}})$. In analogy to the vector case, matching to the δ-function in (3.31) yields

$$N(\hat{p}) = -\frac{L k^2}{4\pi r M_{\mathrm{KK}}^4} \frac{1}{C_J^>(\hat{p}) C_Y^<(\hat{p}) - C_J^<(\hat{p}) C_Y^>(\hat{p})} \,. \tag{3.33}$$

This completes the fundamental solution, which is also valid for gauge bosons like the A, W and Z. The scalar propagator is the sum of profile derivatives. Thus, in the gluon case, the (NN) conditions translate into Dirichlet-Dirichlet (DD) BCs at both branes

$$\partial_t D_\xi^{55}(p, t, t') \big|_{t = \epsilon^+, 1^-} = 0, \tag{3.34}$$

and analogously for t', which can be evaluated on (3.32), thus fixing the coefficients to

$$
\begin{aligned}
C_Y^<(\hat{p}) &= J_0(\hat{p}\epsilon), & C_Y^>(\hat{p}) &= J_0(\hat{p}), \\
C_J^<(\hat{p}) &= -Y_0(\hat{p}\epsilon), & C_J^>(\hat{p}) &= -Y_0(\hat{p}) \,.
\end{aligned} \tag{3.35}
$$

Inserting these into (3.32) and expanding around small momenta $p = 0$ gives the following solution for the scalar propagator

$$D_\xi^{55}(p, t, t') = -\frac{1}{\xi} \frac{k^2 t_>^2 t_<^2}{2\pi r M_{\mathrm{KK}}^4} \ln(t_>) \left[L + \ln(t_<) \right] + \mathcal{O}(p^2), \tag{3.36}$$

which inherits the gauge dependence. When performing tree-level calculations, we will work in unitary gauge $\xi \to \infty$, allowing us to discard the exchanging scalar contributions in (2.88).

4. RS Flavor Problem

The Minimal Randall-Sundrum model admits explanations for the Gauge and Yukawa Hierarchy Problems, which makes it, from the theoretical viewpoint, more preferable than the Standard Model. Still, in order to measure New Physics effects at collider experiments, the RS model must make predictions at (currently) reachable energy ranges. This depends on the energy scale M_{KK}, which sets the mass scale for the lowest modes of the KK particles, for instance $m_1^G = 2.448\, M_{\text{KK}}$ in case of the first gluon mode. To obtain observable effects, we need to allow for M_{KK} values in the few TeV range, $M_{\text{KK}} \sim 1\text{-}2\,\text{TeV}$. At the same time, one has to reproduce all previous measurements that are in good agreement with the SM predictions. Concerning the flavor sector, strong tensions arise only for a few CP violating observables ("little CP problem") that push the M_{KK} scale up to higher values, making the RS model phenomenologically less attractive. On the one hand, there are the flavor changing observables ϵ_K and ϵ'/ϵ_K [43], while on the other hand there is the flavor diagonal electric dipole moment of the neutron (nEDM) [44]. In the following, we will concentrate on the flavor-changing ϵ_K observable[1] and on its impact on the M_{KK} scale within the Minimal RS model, which we will refer to as the RS flavor problem. This will give us the necessary background knowledge for the chapters 5 and 6.

We begin this chapter by defining the CP violating observable ϵ_K and by relating it to a calculable matrix element (section 4.1). In order to parametrize NP contributions, we introduce a general effective Hamiltonian in section 4.2. Within the SM, we explain the GIM mechanism (section 4.3.1), which effectively suppresses flavor-changing processes, and then perform the leading order calculation for K^0-$\bar{K}^0$ mixing (section 4.3.2). It is remarkable that the RS model does also admit an intrinsic suppression mechanism, referred to as the RS GIM mechanism (section 4.4.2), that works well for all remaining observables, see for instance [27] and [45]. Still the suppression is not sufficient in case of ϵ_K and we will give the main reason in section 4.4.3, augmented by a short comment on existing proposals to deal with the RS flavor problem.

4.1. Indirect CP Violation in the Kaon Sector

We consider the neutral Kaon sector consisting of the flavor eigenstates $K^0 = \bar{s}d$ and $\bar{K}^0 = \bar{d}s$. They transform under a CP transformation as

$$\boldsymbol{CP}|K^0\rangle = |\bar{K}^0\rangle, \qquad\qquad \boldsymbol{CP}|\bar{K}^0\rangle = |K^0\rangle, \qquad\qquad (4.1)$$

---

[1]We deal with the obervable ϵ_K, since it is more restrictive than ϵ'/ϵ_K.

where we have chosen the unphysical CP phase $\eta_{CP} = 1$. Both states can mix with each other and we can express their mass eigenstates by the linear combinations[2]

$$|K_l\rangle = p|K^0\rangle + q|\bar{K}^0\rangle, \qquad\qquad |K_h\rangle = p|K^0\rangle - q|\bar{K}^0\rangle, \qquad (4.2)$$

where K_h denotes the heavier and K_l the lighter state. Possible CP violation can be inferred from experiments, when measuring amplitudes of decaying physical Kaons into two-pion states $\pi^0\pi^0$ and $\pi^+\pi^-$. For the definition of ϵ_K, it is convenient to switch to the isospin basis[3], in which the decay amplitudes read

$$A_I = \langle(\pi\pi)_I|\mathcal{H}|K^0\rangle = a_I\,e^{i\delta_I}, \quad \bar{A}_I = \langle(\pi\pi)_I|\mathcal{H}|\bar{K}^0\rangle = a_I^*\,e^{i\delta_I}, \quad a_I = |a_I|e^{i\phi_I}, \quad (4.3)$$

where $I = 0, 2$. There appear two types of complex phases. The phase coming from the interaction term in the Lagrangian is often called "weak" phase and is denoted here as ϕ_I. Another phase can emerge from intermediate on-shell states in the decay process, which is usually dominated by strong interactions and therefore called "strong" phase δ_I. Important is that A_I and $\bar{A}_I$ are related by a CP transformation on the external states, which conjugates the weak but not the strong phase. Experimentally, one finds for the magnitudes $|A_2/A_0| \approx 1/20$, so one is allowed to neglect decays into the $I = 2$ states. With this in mind, one can define the ϵ_K-observable by

$$\epsilon_K \equiv \frac{\langle(\pi\pi)_{I=0}|\mathcal{H}|K_{\text{long}}\rangle}{\langle(\pi\pi)_{I=0}|\mathcal{H}|K_{\text{short}}\rangle}, \qquad (4.4)$$

with the experimentally motivated notation $K_{\text{long}} = K_h$ and $K_{\text{short}} = K_l$. The fraction is chosen such that if CP is a good symmetry, then ϵ_K would vanish. To analyze deviations of ϵ_K from zero, it is convenient to replace in (4.4) the mass eigenstates with the flavor eigenstates by (4.2) and to use (4.3), yielding

$$\epsilon_K = \frac{1-\lambda}{1+\lambda} \qquad \text{with} \qquad \lambda = \frac{q}{p}\frac{\bar{A}_0}{A_0}, \qquad (4.5)$$

where we have introduced the complex quantity λ. On the basis of λ, one can distinguish three types of CP violation [46]:

$|q/p| \neq 1$: This results from mass eigenstates being different from CP eigenstates and one speaks therefore of CP violation in mixing. Otherwise, supposing $|q| = |p|$ leads, with the exact eigenstates (4.9) in mind, to a further constraint, which relates their phases by $q = p^*$. Knowing that a CP transformation conjugates complex numbers q and p, we then find that the mass eigenstates are also CP eigenstates, fulfilling $\boldsymbol{CP}|K_h\rangle = -|K_h\rangle$ and $\boldsymbol{CP}|K_l\rangle = +|K_l\rangle$.

---

[2]The exact form of the eigenstates is given in (4.9).

[3]Since a pion has isospin $I = 1$, a two pion system can have isospin 0 and 2 with the Clebsch-Gordan decompositions $|\pi^0\pi^0\rangle = \sqrt{\frac{1}{3}}|(\pi\pi)_{I=0}\rangle - \sqrt{\frac{2}{3}}|(\pi\pi)_{I=2}\rangle$ and $|\pi^+\pi^-\rangle = \sqrt{\frac{2}{3}}|(\pi\pi)_{I=0}\rangle + \sqrt{\frac{1}{3}}|(\pi\pi)_{I=2}\rangle$.

$|\bar{A}_0/A_0| \neq 1$: In our case, both amplitudes A_0 and $\bar{A}_0$ can have a relative phase, but are of equal magnitude. So, ϵ_K as defined in (4.4) is not sensitive on direct CP violation.

$\text{Im}\,\lambda \neq 0$: This quantity relates the mixing phase from q/p to the weak phase of the decay amplitude, $\text{Im}\,\lambda = \text{Im}\left(e^{-2\phi_I}q/p\right)$. It measures CP violation in the interference between decays with and without mixing.

After having introduced ϵ_K, we have to link the definition of ϵ_K to a matrix element, that allows us to calculate the contributions from theory [29]. Therefore, we start with the time-evolution of the two flavor states K^0 and $\bar{K}^0$, which is given by a Schrödinger-like equation[4]

$$i\frac{d}{dt}\begin{pmatrix}|K^0(t)\rangle \\ |\bar{K}^0(t)\rangle\end{pmatrix} = \boldsymbol{H}\begin{pmatrix}|K^0(t)\rangle \\ |\bar{K}^0(t)\rangle\end{pmatrix}, \tag{4.6}$$

where $\boldsymbol{H}$ is a time-independent 2×2 complex matrix, which can always be decomposed in a hermitian and anti-hermitian part

$$\boldsymbol{H} = \boldsymbol{M} - \frac{i}{2}\boldsymbol{\Gamma} = \begin{pmatrix} M_{11} - \frac{i}{2}\Gamma_{11} & M_{12} - \frac{i}{2}\Gamma_{12} \\ M_{12}^* - \frac{i}{2}\Gamma_{12}^* & M_{22} - \frac{i}{2}\Gamma_{22} \end{pmatrix}, \tag{4.7}$$

with the mass matrix $\boldsymbol{M} = \boldsymbol{M}^\dagger$ and the decay matrix $\boldsymbol{\Gamma} = \boldsymbol{\Gamma}^\dagger$. Employing CPT invariance further leads to the relations

$$M_{11} = M_{22}, \qquad\qquad \Gamma_{11} = \Gamma_{22}\,. \tag{4.8}$$

We are interested in the physical states, so we diagonalize (4.7) including (4.8) and find for the eigenvalues and corresponding mass eigenstates [48]

$$\lambda_h = (M_{11} + \text{Re}\,Q) - \frac{i}{2}(\Gamma_{11} - 2\,\text{Im}\,Q), \quad |K_h\rangle = N_{\bar{\epsilon}}[(1+\bar{\epsilon})|K^0\rangle - (1-\bar{\epsilon})|\bar{K}^0\rangle],$$

$$\lambda_l = (M_{11} - \text{Re}\,Q) - \frac{i}{2}(\Gamma_{11} + 2\,\text{Im}\,Q), \quad |K_l\rangle = N_{\bar{\epsilon}}[(1+\bar{\epsilon})|K^0\rangle + (1-\bar{\epsilon})|\bar{K}^0\rangle],$$
$$\tag{4.9}$$

with $Q = [(M_{12} - i\Gamma_{12}/2)(M_{12}^* - i\Gamma_{12}^*/2)]^{1/2}$ and normalization $N_{\bar{\epsilon}} = [2(1+|\bar{\epsilon}|^2)]^{-1/2}$. Comparing (4.9) with the eigenstates in (4.2), we can identify $p = N_{\bar{\epsilon}}(1 + \bar{\epsilon})$ and $q = N_{\bar{\epsilon}}(1 - \bar{\epsilon})$. The complex quantity $\bar{\epsilon}$ can be calculated from one of the eigenvalue equations, for instance

$$(\boldsymbol{H} - \lambda_h \mathbb{1})\begin{pmatrix}1+\bar{\epsilon} \\ 1-\bar{\epsilon}\end{pmatrix} = 0 \quad \Rightarrow \quad \frac{1-\bar{\epsilon}}{1+\bar{\epsilon}} = \frac{\Delta M_K - i\Delta\Gamma_K/2}{2M_{12} - i\Gamma_{12}} = \frac{2M_{12}^* - i\Gamma_{12}^*}{\Delta M_K - i\Delta\Gamma_K/2}, \tag{4.10}$$

---

[4]This formula is based on the Weisskopf-Wigner approximation in [47].

where we introduced the Kaon mass and decay-width differences

$$\Delta M_K \equiv 2\operatorname{Re}Q, \qquad\qquad \Delta\Gamma_K \equiv -4\operatorname{Im}Q. \qquad (4.11)$$

Solving (4.10) for $\bar{\epsilon}$, we find

$$\bar{\epsilon} = \frac{2M_{12} - i\Gamma_{12} - \Delta M_K + i\Delta\Gamma_K/2}{2M_{12} - i\Gamma_{12} + \Delta M_K - i\Delta\Gamma_K/2}. \qquad (4.12)$$

Before further simplifying this expression, we will relate $\bar{\epsilon}$ to ϵ_K. Inserting the mass eigenstates (4.9) into the definition (4.4), we obtain

$$\epsilon_K = \frac{(1+\bar{\epsilon})a_0 - (1-\bar{\epsilon})a_0^*}{(1+\bar{\epsilon})a_0 + (1-\bar{\epsilon})a_0^*} = \frac{\bar{\epsilon}\operatorname{Re}a_0 + i\operatorname{Im}a_0}{\operatorname{Re}a_0 + i\bar{\epsilon}\operatorname{Im}a_0} = \frac{\bar{\epsilon} + i\xi}{1 + i\bar{\epsilon}\xi} \approx \bar{\epsilon} + i\xi, \qquad (4.13)$$

with $\xi \equiv \operatorname{Im}a_0 / \operatorname{Re}a_0$ and where we used the experimental value of $\epsilon_K = \mathcal{O}(10^{-3})$ to deduce that $\bar{\epsilon}\xi \ll 1$ in the last step. Proceeding with $\bar{\epsilon}$, it is convenient to derive the following approximations:

$\operatorname{Im}M_{12} \ll \operatorname{Re}M_{12}$ & $\operatorname{Im}\Gamma_{12} \ll \operatorname{Re}\Gamma_{12}$:
Using the equalities in (4.10), we can deduce from

$$\left(\frac{1-\bar{\epsilon}}{1+\bar{\epsilon}}\right)^2 = \frac{2M_{12}^* - i\Gamma_{12}^*}{2M_{12} - i\Gamma_{12}}, \qquad (4.14)$$

knowing $\bar{\epsilon} \ll 1$, that the imaginary parts of M_{12} and Γ_{12} are small compared to the real parts.

$\Delta M_K \approx 2\operatorname{Re}M_{12}$ & $\Delta\Gamma \approx 2\operatorname{Re}\Gamma_{12}$:
Both relations can be obtained from (4.11), when we use the above approximation for the imaginary parts in Q, since

$$Q \approx \left[\left(\operatorname{Re}M_{12} - \frac{i}{2}\operatorname{Re}\Gamma_{12}\right)\left(\operatorname{Re}M_{12}^* - \frac{i}{2}\operatorname{Re}\Gamma_{12}^*\right)\right]^{1/2} = \operatorname{Re}M_{12} - \frac{i}{2}\operatorname{Re}\Gamma_{12}. \qquad (4.15)$$

$\Delta\Gamma_K \approx -2\Delta M$:
This approximation can be justified when comparing the experimental values for the mass and decay differences

$$\Delta M_K = 3.4833\,10^{-15}\,\text{GeV [11]}, \quad \Delta\Gamma_K = -7.4\,10^{-15}\,\text{GeV [49]}. \qquad (4.16)$$

$(\operatorname{Im}\Gamma_{12}/\operatorname{Re}\Gamma_{12}) \approx -2\xi$:
The off-diagonal element of the decay matrix involves decays into intermediate on-shell states. In our case with one possible state $(\pi\pi)_0$, we have

$$\Gamma_{12} \propto \langle K^0|\mathcal{H}|(\pi\pi)_0\rangle\,\langle(\pi\pi)_0|\mathcal{H}|\bar{K}^0\rangle = (a_0^*)^2, \qquad (4.17)$$

where we used (4.3) in the second step. Therefore we can write

$$\frac{\operatorname{Im}\Gamma_{12}}{\operatorname{Re}\Gamma_{12}} = \frac{\operatorname{Im}(a_0^*)^2}{\operatorname{Re}(a_0^*)^2} = \frac{-2\xi}{1-\xi^2} \approx -2\xi, \tag{4.18}$$

since $\xi \ll 1$.

With these approximations at hand, we can proceed with $\bar{\epsilon}$ in (4.12), yielding

$$\begin{aligned}
\bar{\epsilon} &\approx \frac{2i\operatorname{Im}M_{12} + \operatorname{Im}\Gamma_{12}}{2\operatorname{Re}M_{12} - i\operatorname{Re}\Gamma_{12} + \Delta M_K - i\Delta\Gamma_K/2} \\
&\approx \frac{1}{1+i}\left(\frac{i\operatorname{Im}M_{12}}{\Delta M_K} + \frac{\operatorname{Im}\Gamma_{12}}{-2\operatorname{Re}\Gamma_{12}}\right) \approx \frac{1}{1+i}\left(\frac{i\operatorname{Im}M_{12}}{\Delta M_K} + \xi\right),
\end{aligned} \tag{4.19}$$

which can be inserted into (4.13) to obtain

$$\begin{aligned}
\epsilon_K &\approx \frac{1}{1+i}\left(\frac{i\operatorname{Im}M_{12}}{\Delta M_K} + \xi\right) + i\xi = \frac{i}{1+i}\left(\frac{\operatorname{Im}M_{12}}{\Delta M_K} + \xi\right) \\
&\approx \frac{e^{i\pi/4}}{\sqrt{2}\Delta M_K}\left(\operatorname{Im}M_{12} + 2\xi\operatorname{Re}M_{12}\right) .
\end{aligned} \tag{4.20}$$

The term $\operatorname{Re}M_{12}$ is suppressed by ξ and can be shifted into the prefactor, including the replacement of the approximate phase $\pi/4$ with its experimental phase ϕ_ϵ, see [50]. We also replace the Kaon mass-difference ΔM_K by its experimental value, yielding the final form

$$\epsilon_K = \frac{\kappa_\epsilon e^{i\phi_\epsilon}}{\sqrt{2}(\Delta M_K)_{\text{exp}}} \operatorname{Im}\langle K^0|\mathcal{H}|\bar{K}^0\rangle, \tag{4.21}$$

with $\kappa_\epsilon = 0.92 \pm 0.02$ and $\phi_\epsilon = (43.51 \pm 0.05)^\circ$ [50]. The matrix element on the r.h.s. of (4.21) is the quantity, which we have to calculate.

4.2. Effective Hamiltonian for K^0-$\bar{K}^0$ mixing

In order to calculate matrix elements with K^0 and $\bar{K}^0$ as external states, we make use of the effective field theory concept, see section 1.3. We can expand our effective Hamiltonian describing K^0-$\bar{K}^0$ mixing, into the product of Wilson coefficients with four quark operators. A general parametrization [5] is given by [27]

$$\mathcal{H}_{\text{eff}}^{\Delta S=2} = \sum_{i=1}^{5} C_i(\mu)Q_i(\mu) + \sum_{i=1}^{3} \tilde{C}_i(\mu)\tilde{Q}_i(\mu) + \text{h.c.}, \tag{4.22}$$

---

[5]The operators $Q_i, \tilde{Q}_i$ form a basis, chosen such as to describe the process $\bar{K}^0 \to K^0$.

with the operator basis

$$
\begin{aligned}
Q_1 &= (\bar{d}_L \gamma^\mu s_L)(\bar{d}_L \gamma_\mu s_L), & \tilde{Q}_1 &= (\bar{d}_R \gamma^\mu s_R)(\bar{d}_R \gamma_\mu s_R), \\
Q_2 &= (\bar{d}_R s_L)(\bar{d}_R s_L), & \tilde{Q}_2 &= (\bar{d}_L s_R)(\bar{d}_L s_R), \\
Q_3 &= (\bar{d}_R^\alpha s_L^\beta)(\bar{d}_R^\beta s_L^\alpha), & \tilde{Q}_3 &= (\bar{d}_L^\alpha s_R^\beta)(\bar{d}_L^\beta s_R^\alpha), \\
Q_4 &= (\bar{d}_R s_L)(\bar{d}_L s_R), \\
Q_5 &= (\bar{d}_R^\alpha s_L^\beta)(\bar{d}_L^\beta s_R^\alpha), & &(4.23)
\end{aligned}
$$

where a summation over color indices α and β is implied. In case they are omitted, a contraction within the Dirac bilinears is understood.

Concerning the Randall-Sundrum Model, the strategy is to calculate the relevant leading order amplitudes that contribute to K^0-$\bar{K}^0$ mixing. We match these to the general operator basis above and read off the Wilson coefficients, evaluated at the New Physics scale in the RS model, which is M_{KK}. In order to perform the renormalization group (RG) running from the high scale M_{KK} to the low hadronic scale of 2 GeV, we fall upon the work done in [51]. Their running formula is based on calculations of the anomalous dimension matrix (ADM), which can be extracted from the effective diagrams including QCD corrections, for instance the three diagrams in fig 4.1 at leading order. Actually the formula includes next-to-leading order ADMs from
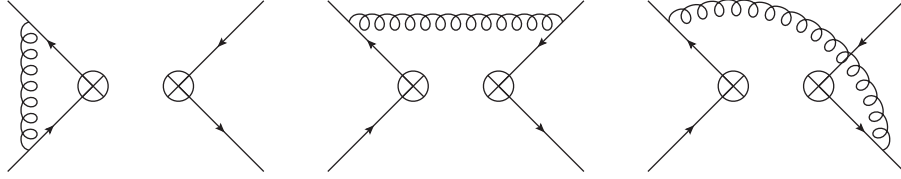

Figure 4.1.: One loop QCD corrections to an effective four-quark vertex.

[52]. After the RG running, we multiply the coefficients with the hadronic matrix elements $\langle K^0|Q_i|\bar{K}^0\rangle$ and $\langle K^0|\tilde{Q}_i|\bar{K}^0\rangle$, which can be obtained from lattice calculations. The concrete implementation of these steps is explained in the numerical part 5.2.2 of the subsequent chapter.

4.3. Observable ϵ_K in the SM

4.3.1. GIM Mechanism

The GIM mechanism, going back to Glashow, Iliopolous and Maiani [53], can efficiently suppress flavor-changing neutral current processes. Such a process involves in the SM at least two W boson vertices that are accommodated by the CKM factors $\lambda_i^{(kl)} \equiv V_{il}^* V_{ik}$, where $i \in \{u, c, t\}$ and $k, l \in \{d, s, b\}$ with $k \neq l$ (considering here
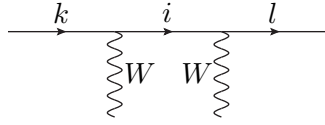
external down-type quarks). Corresponding Feynman amplitudes are then proportional to the sum

$$\sum_{i=u,c,t} \lambda_i^{(kl)} F(m_i) \tag{4.24}$$

where the function F depends on the mass of the internal quark propagator. In case of

- an unitary CKM matrix: $\lambda_u^{(kl)} + \lambda_c^{(kl)} + \lambda_t^{(kl)} = \delta_{kl}$,

- degenerate up-type quark masses,

the sum in (4.24) vanishes and FCNC processes are completely forbidden to all orders. So, the size of breaking is mainly given by the disparity of the quark masses, which is more distinctive in the up-quark sector. This is the reason why K^0-$\bar{K}^0$ mixing plays an important role in the investigation of flavor-changing neutral processes.

4.3.2. Leading Order Calculation

In the Standard Model, FCNC processes can only occur at loop-level via the interchange of $W^\pm$ bosons. For K^0-$\bar{K}^0$ mixing, the eight box diagrams in figure 4.2 contribute to the mixing of neutral Kaons and Antikaons, where $\phi^\pm$ are the charged scalars, that represent the longitudinal components of $W^\pm$. All amplitudes can be
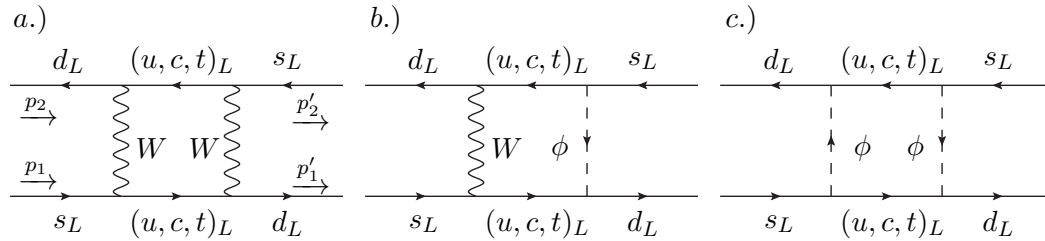
Figure 4.2.: Displayed are three types of box diagrams, contributing at leading order to K^0-$\bar{K}^0$ mixing. For the diagrams a.) and c.), there exist further ones with the inner box rotated by 90°. In case b.), there are four possibilities that give topologically different diagrams. The four-momenta shall be spaced everywhere as in diagram a.).

matched to the four-point interaction operator $Q_1 = \frac{1}{4}\bar{d}\gamma^\mu(1 - \gamma_5)s\,\bar{d}\gamma_\mu(1 - \gamma_5)s$

of the effective Hamiltonian in (4.23). It is convenient to parametrize the Wilson coefficient ($C_1 = C_1^{\text{SM}}$) by

$$C_1^{\text{SM}} = \frac{1}{4} \frac{G_F^2}{\pi^2} M_W^2 \sum_{i,j=u,c,t} V_{id}^* V_{is} V_{jd}^* V_{js} F_0(x_i, x_j), \tag{4.25}$$

where the function $F_0(x_i, x_j)$ corresponds to a given box diagram with i and j quark exchanges and depends on the squared mass ratios of the fermions running through the loop, $x_{i,j} \equiv m_{i,j}^2 / M_W^2$. The subscript "0" indicates that QCD corrections are not included. Since all calculations can be performed in a similar way, it is sufficient to restrict the explicit calculation to one of the diagrams. We choose diagram b.) in figure 4.2, involving an unphysical charged scalar and a W boson. When drawing upon the Feynman rules in 't Hooft-Feynman gauge, as summarised in [5], the corresponding amplitude in its full form reads

$$-i\mathcal{M}^{b.)} = \frac{1}{4} \int \frac{d^4 k}{(2\pi)^4} \bar{u}_d(p_1') \left(\frac{-ig}{2\sqrt{2} M_W} [m_d(1 - \gamma_5) - m_i(1 + \gamma_5)] V_{id}^* \right)$$

$$\frac{i(\not{p}_1' - \not{k} + m_i)}{(p_1 - k)^2 - m_i^2 + i\epsilon} \left(\frac{ig}{2\sqrt{2}} \gamma_\mu (1 - \gamma_5) V_{is} \right) v_s(p_2')$$

$$\frac{i}{k^2 - M_W^2 + i\epsilon} \frac{-i}{(p_1 + p_2 - k)^2 - M_W^2 + i\epsilon}$$

$$\bar{v}_d(p_2) \left(\frac{ig}{2\sqrt{2}} \gamma^\mu (1 - \gamma_5) V_{jd}^* \right) \frac{i(\not{p}_1 - \not{k} + m_j)}{(p_1 - k)^2 - m_j^2 + i\epsilon}$$

$$\left(\frac{-ig}{2\sqrt{2} M_W} [m_s(1 + \gamma_5) - m_j(1 - \gamma_5)] V_{js} \right) u_s(p_1), \tag{4.26}$$

where u_d, u_s and v_d, v_s are the Dirac spinors describing particles and antiparticles respectively. The amplitude (4.26) can be further simplified in the approximation of taking all external momenta to be zero, as they are small compared to M_W and heavy quark masses. Then for (4.26), as well as for the remaining diagrams, the extracted integral part reads

$$I_{qrst} = \int \frac{d^4 k}{(2\pi)^4} \frac{\not{k}_{qr} \not{k}_{st} + (m_i)_{qr} (m_j)_{st}}{[k^2 - M_W^2 + i\epsilon]^2 [k^2 - m_i^2 + i\epsilon][k^2 - m_j^2 + i\epsilon]}, \tag{4.27}$$

with the Dirac indices q, r, s and t. Introducing Feynman parameters to combine the denominators and using four-dimensional master integrals, which can be found for instance in [19], (4.27) can be evaluated to

$$I_{qrst} = \frac{i}{(4\pi)^2 M_W^2} \left[-\frac{1}{2} (\gamma^\alpha)_{qr} (\gamma_\alpha)_{st} I_1(x_i, x_j) + \frac{m_i m_j}{M_W^2} I_2(x_i, x_j) \right], \tag{4.28}$$

where I_1 and I_2 are analytic functions in the mass ratios $x_i \equiv \frac{m_i^2}{M_W^2}$,

$$I_1(x_i, x_j) = \frac{1}{2} \left[\frac{1}{(1-x_i)(1-x_j)} + \frac{1}{(x_i - x_j)} \left(\frac{x_i^2 \ln x_i}{(1-x_i)^2} - \frac{x_j^2 \ln x_j}{(1-x_j)^2} \right) \right], \quad (4.29)$$

$$I_2(x_i, x_j) = - \left[\frac{1}{(1-x_i)(1-x_j)} + \frac{1}{(x_i - x_j)} \left(\frac{x_i \ln x_i}{(1-x_i)^2} - \frac{x_j \ln x_j}{(1-x_j)^2} \right) \right]. \quad (4.30)$$

For the considered amplitude (4.26), the term involving I_1 vanishes due to zero d- and s-quark masses, leaving us with the result

$$-i\mathcal{M}^{b.)} = -i \frac{G_F^2}{(4\pi)^2} M_W^2 \lambda_i^{(ds)} \lambda_j^{(ds)} \left[2x_i x_j I_2(x_i, x_j) \right] \bar{u}_d \gamma_\mu (1 - \gamma_5) v_s \, \bar{v}_d \gamma^\mu (1 - \gamma_5) u_s, \quad (4.31)$$

were $\lambda_i^{(ds)} \equiv V_{id}^* V_{is}$ for $i = u, c, t$. While comparing (4.31) with $\mathcal{H}_{\text{eff}} = C_1 Q_1$, one must account for the Wick contraction factors 2!2!, when expressing the spinor products on the r.h.s of (4.31) in terms of corresponding operators. This explains the factor $1/4$ in front of (4.25). Extending the calculation and matching procedure to all diagrams leads finally to

$$F_0(x_i, x_j) = (2 + x_i x_j) I_1(x_i, x_j) + 2x_i x_j I_2(x_i, x_j), \quad (4.32)$$

where the evaluated integrals I_1 and I_2 refer to (4.29) and (4.30) respectively. Now we can use the unitarity condition $\lambda_u^{(ds)} + \lambda_c^{(ds)} + \lambda_t^{(ds)} = 0$ to eliminate the up-quark CKM entries, yielding

$$C_1^{\text{SM}} = \frac{G_F^2}{4\pi^2} M_W^2 \left(\lambda_t^2 S_0(x_t, x_t) + \lambda_c^2 S_0(x_c, x_c) + 2\lambda_c \lambda_t S_0(x_c, x_t) \right), \quad (4.33)$$

while introducing the basic Inami-Lim function [54]

$$S_0(x_i, x_j) = F_0(x_i, x_j) + F_0(x_u, x_u) - F_0(x_u, x_i) - F_0(x_u, x_j), \quad (4.34)$$

for $i, j = c, t$. Keeping only linear terms in $x_c \ll 1$ and setting x_u to zero, leads to the same expressions as given in [49],

$$S_0(x_t) \equiv S_0(x_t, x_t) \approx \frac{4x_t - 11x_t^2 + x_t^3}{4(1-x_t)^2} - \frac{3x_t^3 \ln x_t}{4(1-x_t)^3},$$

$$S_0(x_c) \approx x_c, \qquad S_0(x_c, x_t) \approx x_c \left[\ln \frac{x_t}{x_c} - \frac{3x_t}{4(1-x_t)} - \frac{3x_t^2 \ln x_t}{4(1-x_t)^2} \right]. \quad (4.35)$$

At this stage, the GIM mechanism may be explored. The breakdown occurs at the one loop level, due to the disparity of the up-type quark masses. The size of this breakdown depends on the behavior of the basic functions in (4.35). For small $x_i \ll 1$, relevant for $(i \neq t)$, $S_0(x_i)$ is proportional to x_i which implies a quadratic

suppression for light quarks. In the limit of large x_i, $S_0(x_i) \propto x_i$, sizeable contributions can occur for heavy quarks like the top. But in (4.33), the top part is accommodated by the small CKM factor $V_{td}^* V_{ts}$, which mitigates the effect. Thus the main contributions to ϵ_K arise from the exchange of two tops together with a charm and a top.

The next step is to include QCD corrections for the diagrams, which can be looked up for instance in [55] and [56]. At next-to-leading order, the ϵ_K parameter may then be expressed as [49]

$$\epsilon_K = C_\epsilon \hat{B}_K \operatorname{Im} \lambda_t^* \left\{ \operatorname{Re} \lambda_c^* \left[\eta_1 S_0(x_c) - \eta_3 S_0(x_c, x_t) \right] - \operatorname{Re} \lambda_t^* \eta_2 S_0(x_t) \right\} \exp(i\pi/4), \tag{4.36}$$

with correction factors η_i, a numerical constant C_ϵ and the non-perturbative paramter $\hat{B}_K$, that can be obtained from lattice calculations. Based on this formula one can infer, from indirect constraints of a global unitarity triangle fit, a SM value of

$$|\epsilon_K^{\text{SM}}| = (1.9 \pm 0.4) \, 10^{-3} \, [57], \tag{4.37}$$

where the dominant theoretical uncertainties arise from the lattice QCD parameter $\hat{B}_K$. Within the errors, this value agrees with the experimental one

$$|\epsilon_K^{\text{exp}}| = (2.229 \pm 0.010) \, 10^{-3} \, [11] \, . \tag{4.38}$$

Thus, the smallness of ϵ_K in the SM is based on the GIM mechanism in relation with small CKM elements for the top quark contributions.

4.4. Observable ϵ_K in the Minimal RS Model

Contributions to the ϵ_K observable arise already at tree level in the RS model, from s- and t-channel diagrams exchanging heavy modes of the gluon, photon, Z boson and the Higgs particle, see fig. (4.3). These contributions make up $\Delta\epsilon_K^{\text{RS}}$, hence we can write

$$\epsilon_K^{\text{RS}} = \epsilon_K^{\text{RS,Box}} + \Delta\epsilon_K^{\text{RS}}, \tag{4.39}$$

where $\epsilon_K^{\text{RS,Box}}$ stems from box diagrams extending the SM diagrams in fig. 4.2, by involving various 4D modes of quarks $u^{(n)}$, $d^{(n)}$ and bosons $W^{(n)}$, $G^{(n)}$, $A^{(n)}$, $Z^{(n)}$, $h^{(n)}$. A complete calculation would be desirable, but is behind the scope of this thesis. Instead we assume that the additional box diagrams are sufficiently suppressed for two reasons[6]:

---

[6] Another question concerns the convergence of the tower sums within each box, which can only be settled by an explicit calculation.
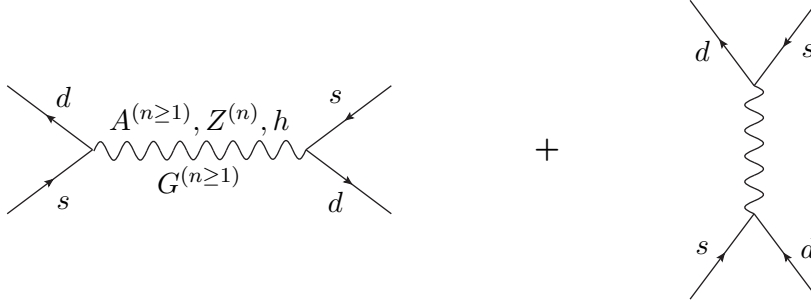
Figure 4.3.: Both, s- and t-channel diagrams contribute to ϵ_K. The exchange of the massive gluon tower gives the dominant part, as explained in section 4.4.3.

- Each box including at least one neutral gauge boson is suppressed by the RS GIM mechanism, which is the analog to the SM GIM needed to suppress FCNC processes. More details on the RS GIM mechanism will be given in section 4.4.2.

- For each higher non-SM mode in the loop, its propagator contributes with a factor $1/m_n^2$, resulting in a m_W^2/m_n^2 suppression compared to the SM box diagrams.

Still we need to translate the remaining Standard Model box diagrams in fig. 4.2 into the RS framework by replacing the Fermi constant of the SM with the expression within the RS model [27],

$$\frac{G_F^{\text{RS}}}{\sqrt{2}} = \frac{G_F^{\text{SM}}}{\sqrt{2}} \left(\frac{m_{\text{exp}}^W}{m_0^W}\right)^2 \left[1 + \frac{(m_0^W)^2}{2M_{\text{KK}}^2}\left(1 - \frac{1}{2L}\right) + \mathcal{O}\left(\frac{(m_0^W)^4}{M_{\text{KK}}^4}\right)\right] \tag{4.40}$$

where m_{exp}^W is the experimental W boson mass obtained from direct measurements and m_0^W denotes its mass within the RS model. Note that m_0^W can be calculated by solving the boundary conditions in (2.46).

Finally, for our purpose it should be viable to replace $\epsilon_K^{\text{RS,Box}}$ by the theoretical value of the SM in (4.37), when corrected for the Fermi constant. Then, we can proceed with the contributions to $\Delta\epsilon_K^{\text{RS}}$.

4.4.1. Wilson Coefficients

It is convenient to split the coefficients of the operator basis in (4.23) into

$$C_i = C_i^{\text{RS,Box}} + C_i^{\text{RS}}, \tag{4.41}$$

and analogously for $\tilde{C}_i$. As explained above, we replace $C_i^{\text{RS,Box}}$ by the coefficients in the SM, where there is only C_1^{SM} non-vanishing. The additional tree level contributions are incorporated in C_i^{RS} and $\tilde{C}_i^{\text{RS}}$, which are evaluated at the scale M_{KK}.

Let us sketch the calculation of the effective Hamiltonian for the diagram, that exchanges a complete gluon tower. We start with equation (2.88) in section (2.2.5) and take the limit of vanishing momenta[7]. When working in unitarity gauge $\xi_G \to \infty$, the scalar propagator vanishes according to (3.36) and we find

$$
\mathcal{H}_{\text{eff}}^G = \frac{2\pi L \, \alpha_s}{M_{\text{KK}}^2} \int_\epsilon^1 dt \int_\epsilon^1 dt' \left[\frac{1 - \epsilon^2}{2L^2} + t_<^2 - t^2 \frac{1}{L} \left(\frac{1}{2} - \ln t \right) - t'^2 \frac{1}{L} \left(\frac{1}{2} - \ln t' \right) \right]
$$
$$
\times \left[\chi_1^{(D)\dagger}(t) \chi_2^{(D)}(t) \, \bar{d}_L \gamma_\mu T^a s_L + \chi_1^{(d)\dagger}(t) \chi_2^{(d)}(t) \, \bar{d}_R \gamma_\mu T^a s_R \right]
$$
$$
\times \left[\chi_1^{(D)\dagger}(t') \chi_2^{(D)}(t') \, \bar{d}_L \gamma^\mu T^a s_L + \chi_1^{(d)\dagger}(t') \chi_2^{(d)}(t') \, \bar{d}_R \gamma^\mu T^a s_R \right] . \qquad (4.42)
$$

Here we directly see, which terms in the propagator can give rise to flavor-changing transitions. The constant term, that is independent of t and t', can be pulled out of the integral and we can use twice the orthonormality condition for the quark profiles in (2.58), giving no contribution for our $\Delta S = 2$ process. Similarly, the terms depending either on t or t' can lead maximally to $\Delta S = 1$ processes. So, only the $t_<^2$ term allows for nonzero Wilson coefficients. To obtain them, we have to transform the four quark operators in (2.58) into the basis (4.23) by using the relation [19]

$$
T_{\alpha\beta}^a \otimes T_{\gamma\delta}^a = \frac{1}{2} \left(\delta_{\alpha\delta}\delta_{\beta\gamma} - \frac{1}{N_c}\delta_{\alpha\beta}\delta_{\gamma\delta} \right) \qquad \text{with} \qquad N_c = \# \, \text{colors}, \qquad (4.43)
$$

and the following Fierz identities for operators (appendix A in [5]),

$$
(\bar{q}_L^i \gamma_\mu q_L^j)(\bar{q}_L^k \gamma^\mu q_L^l) = (\bar{q}_L^i \gamma_\mu q_L^l)(\bar{q}_L^k \gamma^\mu q_L^j), \qquad (4.44)
$$
$$
(\bar{q}_R^i \gamma_\mu q_R^j)(\bar{q}_R^k \gamma^\mu q_R^l) = (\bar{q}_R^i \gamma_\mu q_R^l)(\bar{q}_R^k \gamma^\mu q_R^j), \qquad (4.45)
$$
$$
(\bar{q}_L^i \gamma_\mu q_L^j)(\bar{q}_R^k \gamma^\mu q_R^l) = -2 \, (\bar{q}_L^i q_R^l)(\bar{q}_R^k q_L^j) . \qquad (4.46)
$$

Note, that the labels i, j, k, l are only used to distinguish the field operators and that one has to keep track of the color indices, when performing the transformations. We receive contributions for C_1^{RS}, $\tilde{C}_1^{\text{RS}}$, C_4^{RS} and C_5^{RS}. In a similar manner, one can proceed with the remaining diagrams in fig. 4.3 and determine the Wilson coefficients, yielding [45]

$$
C_1^{\text{RS}} = \frac{4\pi L}{M_{\text{KK}}^2} (\tilde{\Delta}_D)_{12} \otimes (\tilde{\Delta}_D)_{12} \left[\frac{\alpha_s}{2} \left(1 - \frac{1}{N_c} \right) + (Q_e^d)^2 \alpha_e + \frac{(T_3^d - s_W^2 Q_e^d)^2 \alpha_e}{s_W^2 c_W^2} \right],
$$
$$
\tilde{C}_1^{\text{RS}} = \frac{4\pi L}{M_{\text{KK}}^2} (\tilde{\Delta}_d)_{12} \otimes (\tilde{\Delta}_d)_{12} \left[\frac{\alpha_s}{2} \left(1 - \frac{1}{N_c} \right) + (Q_e^d)^2 \alpha_e + \frac{(s_W^2 Q_e^d)^2 \alpha_e}{s_W^2 c_W^2} \right],
$$
$$
C_4^{\text{RS}} = \frac{4\pi L}{M_{\text{KK}}^2} (\tilde{\Delta}_D)_{12} \otimes (\tilde{\Delta}_d)_{12} \left[-2\alpha_s \right],
$$

---

[7]In this limit, the s- and t- channel diagrams yield the same contributions. Note that the resulting factor of two, as well as the Wick contraction factor of $1/4$ is already accommodated for in the definition of the hadronic matrix elements. Otherwise (4.42) would have to be multiplied by $1/2$.

$$C_5^{\text{RS}} = \frac{4\pi L}{M_{\text{KK}}^2} (\tilde{\Delta}_D)_{12} \otimes (\tilde{\Delta}_d)_{12} \left[\frac{2\alpha_s}{N_c} - 4(Q_e^d)^2 \alpha_e + \frac{4 s_W^2 Q_e^d (T_3^d - s_W^2 Q_e^d) \alpha_e}{s_W^2 c_W^2} \right],$$

$$(4.47)$$

where $Q_e^d = -1/3$, $T_3^d = -1/2$ and $s_W \equiv \sin\theta_W$ as well as $c_W \equiv \cos\theta_W$. The expressions in brackets refer to the contributions from KK gluons, KK photons and from the Z^0 boson and its KK excitations. A possible Higgs boson exchange is suppressed additionally by $\mathcal{O}(v^2/M_{\text{KK}}^2)$ compared to (4.47) and therefore neglected.

The tensor structures appearing in (4.47) represent double integrals over the profile functions of exchanged KK modes m, n and m', n' at each vertex. They are part of a more general class of double integrals, which can be defined by

$$\tilde{O}_1 \otimes \tilde{O}_2 \equiv \frac{2\pi^2}{L^2 \epsilon^2} \int_\epsilon^1 dt \int_\epsilon^1 dt' \, t_<^2 \, \tilde{O}_1(t) \, \tilde{O}_2(t'),$$

$$(4.48)$$

where $\tilde{O}_1$ and $\tilde{O}_2$ can be replaced by one of the following terms

$$(\tilde{\Delta}_{Q,q})_{mn} = a_m^{(Q,q)\dagger} \boldsymbol{C}_m^{(Q,q)} \boldsymbol{C}_n^{(Q,q)} a_n^{(Q,q)} + a_m^{(q,Q)\dagger} \boldsymbol{S}_m^{(q,Q)} \boldsymbol{S}_n^{(q,Q)} a_n^{(q,Q)},$$

$$(4.49)$$

$$(\tilde{\epsilon}_{Q,q})_{mn} = a_m^{(q,Q)\dagger} \boldsymbol{S}_m^{(q,Q)} \boldsymbol{S}_n^{(q,Q)} a_n^{(q,Q)},$$

$$(4.50)$$

$$(\tilde{\delta}_{Q,q})_{mn} = a_m^{(q,Q)\dagger} \boldsymbol{S}_m^{(q,Q)} \boldsymbol{S}_n^{(q,Q)} a_n^{(q,Q)},$$

$$(4.51)$$

with $Q \in \{U, D\}$ and $q \in \{u, d\}$. For instance, in case of the tensor structure appearing in C_4^{RS}, we can use (4.48) with (4.49) and obtain the expression

$$\begin{aligned} (\tilde{\Delta}_D)_{12} \otimes (\tilde{\Delta}_d)_{12} = & \frac{2\pi^2}{L^2 \epsilon^2} \int_\epsilon^1 dt \int_\epsilon^1 dt' t_<^2 \\ & \times \left[a_1^{(D)\dagger} \boldsymbol{C}_1^{(D)}(t) \boldsymbol{C}_2^{(D)}(t) a_2^{(D)} + a_m^{(d)\dagger} \boldsymbol{S}_1^{(d)}(t) \boldsymbol{S}_2^{(d)}(t) a_2^{(d)} \right] \\ & \times \left[a_1^{(d)\dagger} \boldsymbol{C}_1^{(d)}(t') \boldsymbol{C}_2^{(d)}(t') a_2^{(d)} + a_1^{(D)\dagger} \boldsymbol{S}_1^{(D)}(t') \boldsymbol{S}_2^{(D)}(t') a_2^{(D)} \right] . \end{aligned}$$

$$(4.52)$$

Since we will encounter further overlap integrals in the subsequent chapter, consisting of a single integration over t, we quote them here as well,

$$(\Delta_{Q,q})_{mn} = \frac{2\pi}{L\epsilon} \int_\epsilon^1 dt \, t^2 \left[a_m^{(Q,q)\dagger} \boldsymbol{C}_m^{(Q,q)} \boldsymbol{C}_n^{(Q,q)} a_n^{(Q,q)} + a_m^{(q,Q)\dagger} \boldsymbol{S}_m^{(q,Q)} \boldsymbol{S}_n^{(q,Q)} a_n^{(q,Q)} \right],$$

$$(4.53)$$

$$(\epsilon_{Q,q})_{mn} = \frac{2\pi}{L\epsilon} \int_\epsilon^1 dt \, t^2 \, a_m^{(q,Q)\dagger} \boldsymbol{S}_m^{(q,Q)} \boldsymbol{S}_n^{(q,Q)} a_n^{(q,Q)},$$

$$(4.54)$$

$$(\delta_{Q,q})_{mn} = \frac{2\pi}{L\epsilon} \int_\epsilon^1 dt \, a_m^{(q,Q)\dagger} \boldsymbol{S}_m^{(q,Q)} \boldsymbol{S}_n^{(q,Q)} a_n^{(q,Q)} .$$

$$(4.55)$$

4.4.2. RS GIM Mechanism

In general, FCNC processes involve overlap integrals like the ones in (4.48) - (4.55). Their size depends strongly on the bulk parameters c_{Q_i, q_i}. In the numerical analysis

of chapter 5.2, we will encounter typical parameter values fulfilling

$$c_{Q_3,u_3} > -1/2, \qquad\qquad -3/2 < c_{Q_1,Q_2,u_1,u_2,d_1,d_2,d_3} < -1/2, \qquad (4.56)$$

which lead by solving equation (2.63) to the correct SM masses. To obtain approximations for the Δ-integrals, we insert the ZMA profiles into (4.53), perform the integrations and assume $c_{Q_i,u_i,d_i} < -1/2$ (not valid for the top), yielding

$$(\Delta_A)_{mn} \sim (\Delta'_A)_{mn} \sim F(c_{A_m})F(c_{A_n}), \qquad (4.57)$$

for $A, B \in \{U, D, u, d\}$. Since the δ- and ϵ-integrals involve the $\boldsymbol{S}$ profiles, which vanish in the ZMA, we use (2.68) and perform the same steps as above, yielding

$$(\delta_A)_{mn} \sim (\epsilon_A)_{mn} \sim (\epsilon'_A)_{mn} \sim \frac{v^2 Y_\star^2}{M_{\text{KK}}^2} F(c_{A_m})F(c_{A_n}), \qquad (4.58)$$

where $Y_\star$ just represents a typical 4D Yukawa entry of $\mathcal{O}(1)$. If additionally $c_{A_i} + c_{B_j} > -2$ for all $i, j \in \{1, 2, 3\}$ holds, one can approximate the tensor structures by

$$(\tilde{\Delta}_A)_{mn} \otimes (\tilde{\Delta}_B)_{m'n'} \sim F(c_{A_m})F(c_{A_n})F(c_{B_{m'}})F(c_{B_{n'}}), \qquad (4.59)$$

More details can be found in [58]. As can be seen, all integrals are proportional to several products of zero-mode profiles. Using (2.71) and $\epsilon \equiv e^{-kr\pi} = e^{-L}$, these products are exponentially suppressed for the assumed parameter range, yielding

$$F(c_{A_m})F(c_{B_n}) \sim e^{-L|1+c_{A_m}+c_{B_n}|}, \qquad (4.60)$$

$$F(c_{A_m})F(c_{A_n})F(c_{B_{m'}})F(c_{B_{n'}}) \sim e^{-L\left|2+c_{A_m}+c_{A_n}+c_{B_{m'}}+c_{B_{n'}}\right|}. \qquad (4.61)$$

which is referred to as the RS GIM mechanism.

4.4.3. Origin of the $\epsilon_K^{\mathbf{RS}}$ Problem

Now we can come back to the ϵ_K observable in the Minimal RS model. As we have mentioned in the introduction of this chapter, the flavor problem means that when we calculate ϵ_K^{RS} via the coefficients in (4.47), we encounter values that are disfavored by experiment, unless one raises the M_{KK} scale up to energies, which are phenomenologically undesirable. More details including plots will be given in the numerical section of chapter 5.

In the following, we will estimate ϵ_K and highlight the origin of the flavor problem. Therefore, we start with the Wilson coefficients C_1^{RS}, $\tilde{C}_1^{\text{RS}}$, C_4^{RS} and C_5^{RS} in (4.47), which receive the main contributions from Feynman diagrams exchanging KK gluon modes. Electroweak contributions are suppressed by $\alpha_e(M_{\text{KK}})/\alpha_s(M_{\text{KK}}) \sim \mathcal{O}(0.1)$, since the Wilson coefficients are evaluated at the scale M_{KK}. To estimate the down quark tensor structures, we can use (4.59) and replace the zero-mode functions by

their expressions in (2.82). Approximating the 4D Yukawa matrix entries with $Y_\star$, we can derive the relations

$$(\tilde{\Delta}_D)_{12} \otimes (\tilde{\Delta}_D)_{12} \sim \frac{\lambda^2}{Y_\star^4} F(c_{Q_2})^4, \qquad (\tilde{\Delta}_D)_{12} \otimes (\tilde{\Delta}_d)_{12} \sim \frac{2m_d m_s}{Y_\star^2 v^2},$$

$$(\tilde{\Delta}_d)_{12} \otimes (\tilde{\Delta}_d)_{12} \sim \left(\frac{2m_d m_s}{\lambda v^2}\right)^2 \frac{1}{F(c_{Q_2})^4} . \tag{4.62}$$

Applying them to the tensor structures in the Wilson coefficients (4.47) and neglecting electroweak contributions, we obtain

$$C_1^{\mathrm{RS}}(\mu) \sim \frac{4\pi L}{M_{\mathrm{KK}}^2} \frac{\alpha_s(\mu)}{2} \left(1 - \frac{1}{N_c}\right) \frac{\lambda^2}{Y_\star^2} F(c_{Q_2})^4,$$

$$\tilde{C}_1^{\mathrm{RS}}(\mu) \sim \frac{4\pi L}{M_{\mathrm{KK}}^2} \frac{\alpha_s(\mu)}{2} \left(1 - \frac{1}{N_c}\right) \left(\frac{2m_d m_s}{\lambda v^2}\right)^2 \frac{1}{F(c_{Q_2})^4}$$

$$C_4^{\mathrm{RS}}(\mu) \sim -N_c\, C_5^{\mathrm{RS}}(\mu) \sim \frac{4\pi L}{M_{\mathrm{KK}}^2} 2\alpha_s(\mu) \left(\frac{2m_d m_s}{Y_\star^2 v^2}\right) . \tag{4.63}$$

Using the median value $\overline{F(c_{Q_2})} = -0.023$ of our dataset in the numerical section together with the values λ, m_d, m_s at $\mu \approx 1.5\,\mathrm{TeV}$ (see appendix B.1) and $\mathcal{O}(1)$ Yukawa entries, we can estimate the ratios of the coefficients to

$$C_1^{\mathrm{RS}} : \tilde{C}_1^{\mathrm{RS}} : C_4^{\mathrm{RS}} : C_5^{\mathrm{RS}} \sim 1 : 1/10 : 1 : 1 . \tag{4.64}$$

They are of similar size, except for the coefficient $\tilde{C}_1^{\mathrm{RS}}$, which is relatively suppressed by a factor of $\mathcal{O}(10)$. In order to calculate the matrix element $\langle K^0 | \mathcal{H}_{\mathrm{eff}}^{\mathrm{RS}} | \bar{K}^0 \rangle$, one evolves the coefficients determined at the high scale of M_{KK} down to $2\,\mathrm{GeV}$ and multplies them with the hadronic matrix elements, see section 5.2.2 for more details. This will lead to a relative weighting between the coefficients, such that

$$\langle K^0 | \mathcal{H}_{\mathrm{eff}}^{\mathrm{RS}} | \bar{K}^0 \rangle \propto C_1^{\mathrm{RS}} + \tilde{C}_1^{\mathrm{RS}} + 117\,(C_4^{\mathrm{RS}} + \frac{1}{N_c} C_5^{\mathrm{RS}}), \tag{4.65}$$

which demonstrates the relevance of the Wilson coefficients C_4^{RS} and C_5^{RS}. The large enhancement factor of roughly 117 is the real reason for the ϵ_K problem. With (4.65) in mind, the main contribution to $\Delta\epsilon_K^{\mathrm{RS}}$ within the ZMA and for anarchic Yukawa entries can be expressed by

$$|\Delta\epsilon_K^{\mathrm{RS}}| \sim \frac{\kappa_\epsilon}{\sqrt{2}(\Delta M_K)} C_{\mathrm{f}} \left(N_c + \frac{1}{N_c}\right) \left(\frac{8\pi L \alpha_s(M_{\mathrm{KK}})}{M_{\mathrm{KK}}^2}\right) \left(\frac{2m_d m_s}{Y_\star^2 v^2}\right), \tag{4.66}$$

where C_{f} denotes the explicit RG and matrix element factor. The question is how one can minimize the contributions in (4.66). At first glance, one may see two adjusting screws:

Yukawa $Y_\star$: A significant raise of the Yukawa matrix entries would shift the bulk profiles in the direction of the UV brane, yielding smaller overlap integrals and thus a suppression of $\Delta\epsilon_K^{\mathrm{RS}}$. But one usually requires natural and perturbative[8] Yukawa entries, meaning that they are of $\mathcal{O}(1)$. Furthermore, increasing $Y_\star$ leads to a tension with the ϵ_K'/ϵ_K observable, where the contributing coefficients are proportional to the square of the Yukawa entries, see [43] for details. Thus, the RS flavor problem remains.

Volume L: Another idea, proposed in [59], might be to lower the UV cutoff Λ_{UV} of the RS model to a value significantly below the Planck scale, allowing for a smaller volume $L = \ln(\Lambda_{\mathrm{UV}}/M_{\mathrm{EW}})$. But this will shift the bulk mass parameters to smaller values, since they must still produce the correct SM masses in (2.80). Once the condition $c_{Q_2} + c_{d_2} < -2$ is fulfilled, the approximation for the tensor structures in (4.59) does not hold anymore and the $\Delta\epsilon_K^{\mathrm{RS}}$ estimation (4.66) expires its validity. It turns out, see [58], that for smaller values than $L \approx 8.2$, the ϵ_K contribution even starts to increase exponentially.

Besides these obvious attempts, there is a further proposal to deal with the problem.

Aligned c_{d_i} parameters: A different proposal by Santiago [60] is to align all c_{d_i} parameters, $c_{d_1} = c_{d_2} = c_{d_3}$, in order to eliminate the flavor non-diagonal overlap integrals at leading order in v^2/M_{KK}^2. This can be seen from the following term

$$a_m^{(d)\dagger} C_m^{(d)} C_n^{(d)} a_n^{(d)}, \tag{4.67}$$

which appears in the integrand of the C_4^{RS}, C_5^{RS} tensor structure in (4.52) (with $m = 1$ and $n = 2$). Using the ZMA relations, we can rewrite the $a^{(d)}$ vectors as the columns, see (2.76), of the unitary matrix W_d, yielding

$$a_m^{(d)\dagger} C_m^{(d)} C_n^{(d)} a_n^{(d)} \approx \frac{1}{2} \sum_{l=1}^{3} (W_d^\dagger)_{ml} (\underbrace{C_m^{(d)} C_n^{(d)}}_{\propto \mathbb{1}})_{ll} (W_d)_{ln}, \tag{4.68}$$

where a summation over the components is shown for clarity. Note that with aligned parameters, the $C^{(d)}$ profiles are diagonal matrices with equal components. We can use the unitarity of W_d yielding a final result proportional to the Kronecker delta δ_{mn}, which renders the tensor structure flavor diagonal and therefore eliminates the C_4^{RS} and C_5^{RS} coefficients within the ZMA. Remaining terms are of order v^2/M_{KK}^2 and can suppress sufficiently the $\Delta\epsilon_K^{\mathrm{RS}}$ contribution, see [27]. The problem with Santiago's approach is that the mechanism is very sensitive to small deviations from aligned masses c_{d_i}. For instance, small variations may be induced due to the renormalization group running of the quark masses.

---

[8]Yukawa interactions receive one loop corrections, which can be estimated via naive dimensional analysis. A discussion is given in [27], where some arguments are presented to mitigate the usually adopted upper bound of $|Y_\star| < \pi$ to $|Y_\star| < 4\pi$.

In fact, there is no satisfactory proposal how to effectively suppress the dangerous coefficients C_4^{RS} and C_5^{RS} of $\Delta\epsilon_K^{\mathrm{RS}}$. A new idea, that extends the Minimal Randall-Sundrum Model, will be the topic of the following chapter.

5. Solving the RS Flavor Problem

This chapter presents a solution to mitigate the ϵ_K problem. The underlying idea has been proposed by Martin Bauer, and together with Matthias Neubert we worked out the final form [61]. After discussing this proposal in the beginning section 5.1, we perform a numerical analysis in 5.2 and compare the new results with the original fine-tuning issue.

5.1. Theoretical Approach

As mentioned in the previous chapter, we want to minimize/cancel the contributions to the Wilson coefficients C_4^{RS} and C_5^{RS}, which belong to the operators (see (4.23))

$$Q_4 = (\bar{d}_R^\alpha s_L^\alpha)(\bar{d}_L^\beta s_R^\beta) = -\frac{1}{2}(\bar{d}_L^\beta \gamma_\mu s_L^\alpha)(\bar{d}_R^\alpha \gamma^\mu s_R^\beta), \tag{5.1}$$

$$Q_5 = (\bar{d}_R^\alpha s_L^\beta)(\bar{d}_L^\beta s_R^\alpha) = -\frac{1}{2}(\bar{d}_L^\beta \gamma_\mu s_L^\beta)(\bar{d}_R^\alpha \gamma^\mu s_R^\alpha) . \tag{5.2}$$

In the second step we made use of the Fierz transformation in (4.46). Both operators appear, when we calculate diagrams with oppposite quark chiralities on both vertices (see figures below). To eliminate those gluon contributions, we may think of a new

color mediating gauge boson $G_\mu'^a$ (only used in this passage), having an axial coupling between the down and strange quark,

$$\bar{d}\gamma_\mu \gamma_5 T^a G'^{a\mu} s = -\bar{d}_L \gamma^\mu T^a G'^{a\mu} s_L + \bar{d}_R \gamma_\mu T^a G'^{a\mu} s_R, \tag{5.3}$$

where we used $\gamma_5 P_{L/R} = \mp P_{L/R}$ with chirality projectors $P_{L/R} = (1 \mp \gamma_5)/2$. In the effective theory[1], the above diagrams then give rise to the following four-quark operator

$$(\bar{d}_L \gamma_\mu \gamma_5 s_L)(\bar{d}_R \gamma^\mu \gamma_5 s_R) = -(\bar{d}_L \gamma_\mu s_L)(\bar{d}_R \gamma^\mu s_R), \tag{5.4}$$

which comes with the opposite sign to the gluon contribution. As a result the contributions from the gluon and G' cancel, when we consider the coefficients C_4^{RS}

---

[1]The field $G_\mu'^a$ is assumed to be heavy and hence can be integrated out.

and C_5^{RS}. So, the important feature is the axial coupling of a newly introduced color mediating gauge boson. In the following, we will deal with a likewise extension within the Minimal Randall-Sundrum model.

Extending the Color Group

We replace the bulk $SU(3)_c$ by the gauge group $G_c \equiv SU(3)_D \times SU(3)_S$, leading to the enlarged symmetry group (before SSB[2])

$$G \equiv SU(3)_D \times SU(3)_S \times SU(2)_L \times U(1)_Y, \tag{5.5}$$

of our model. The $SU(2)_L$ doublet fields[3] $Q^n \equiv (u^n, d^n)$ transform as triplets under $SU(3)_D$ and as singlets under $SU(3)_S$. Reversely, the $SU(2)_L$ singlet fields $u^{c,n}$, $d^{c,n}$ transform as triplets under $SU(3)_S$ but are invariant under $SU(3)_D$. So, the transformation behavior under G_c can be stated as

$$Q^n \sim (\mathbf{3}, \mathbf{1}) \quad \text{and} \quad q^{c,n} \sim (\mathbf{1}, \mathbf{3}) \quad \text{for } q = u, d \,. \tag{5.6}$$

The transformation properties under the complete group G is summarized in table 6.1. Furthermore, G_c is gauged by the mediating octets G_D and G_S respectively, changing the covariant derivative in 2.27 for the 5D quark fields to[4]

$$D_M \, Q = (\partial_M - ig_5 W_M^i \tau^i - ig_5' B_M Y_Q - ig_{D5}(G_D)_M^a T^a) \, Q, \tag{5.7}$$

$$D_M \, q^c = (\partial_M - ig_5' B_M Y_{q^c} - ig_{S5}(G_S)_M^a T^a) \, q^c, \tag{5.8}$$

with new five-dimensional gauge couplings g_{D5} and g_{S5}.

Pseudo-Axial Gluon $\mathcal{A}$

We are interested in the interactions between the quarks and the newly introduced color octets. Replacing the covariant derivatives appearing in (2.52) with the ones in (5.7) and (5.8), the relevant action takes the following form (compared with (2.84))

$$S_{Gqq} = \int dx_5 \, e^{-3\sigma} \sum_{q=u,d} \left[g_{D5} \, \bar{q}(G_D)_M^a \gamma^M T^a q + g_{S5} \, \bar{q}^c(G_S)_M^a \gamma^M T^a q^c \right] \,. \tag{5.9}$$

The 5D gluon G must be a linear combination of G_D and G_S. So, we perform a rotation to another basis $\{G, \mathcal{A}\}$ via

$$\begin{pmatrix} G_D \\ G_S \end{pmatrix} = \begin{pmatrix} \cos\vartheta & -\sin\vartheta \\ \sin\vartheta & \cos\vartheta \end{pmatrix} \begin{pmatrix} G \\ \mathcal{A} \end{pmatrix}, \tag{5.10}$$

---

[2]The group G_c has to be broken down to the color group. It is not of relevance here, but will be discussed in chapter 6.

[3]with generation index $n = 1, 2, 3$.

[4]In the following, we suppress the generation index n.

with the mixing angle ϑ. Inserting (5.10) into (5.9), we obtain

$$S_{Gqq} = \int dx_5\, e^{-3\sigma} \sum_{q=u,d} \left\{ g_{D5}\, \bar{q} \left(\slashed{G}^a \cos\vartheta - \slashed{A}^a \sin\vartheta \right) T^a q \right.$$
$$\left. + g_{S5}\, \bar{q}^c \left(\slashed{G}^a \sin\vartheta + \slashed{A}^a \cos\vartheta \right) T^a q^c \right\}, \qquad (5.11)$$

with abbreviations $\slashed{G} \equiv G_M \gamma^M$ and $\slashed{A} \equiv A_M \gamma^M$. To implement the gluon field, that couples with equal strength g_{s5} to both fields q and q^c, we demand

$$g_{s5} = g_{D5} \cos\vartheta = g_{S5} \sin\vartheta, \qquad (5.12)$$

and (5.11) finally becomes

$$S_{Gqq} = \int dx_5\, e^{-3\sigma} \sum_{q=u,d} \left\{ g_{s5} \left(\bar{q}\slashed{G}^a T^a q + \bar{q}^c \slashed{G}^a T^a q^c \right) \right.$$
$$\left. + g_{s5} \left(-\tan\vartheta\, \bar{q}\slashed{A}^a T^a q + \cot\vartheta\, \bar{q}^c \slashed{A}^a T^a q^c \right) \right\}. \qquad (5.13)$$

The additional field A has an opposite sign coupling between the doublet and singlet quarks, with a magnitude depending on the angle ϑ. We refer to this gauge boson as the pseudo-axial gluon.

KK Decomposition

In a similar manner as for the other gauge bosons in (2.34), we decompose this field into 4D modes and profiles, such that

$$A_\mu^a(x,\phi) = \frac{1}{\sqrt{r}} \sum_{n=0}^\infty A_\mu^{(n)a}(x)\chi_n^A(\phi), \quad A_\phi^a(x,\phi) = \frac{1}{\sqrt{r}} \sum_n a_n^A \varphi_A^{(n)a}(x)\partial_\phi\chi_n^A(\phi), \quad (5.14)$$
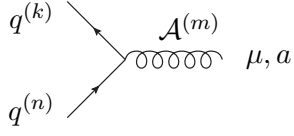
where $a = 1, ..., 8$. The coefficient $a_n^A = -1/m_n^A$ can be determined by matching the 5D action to the 4D one, which is performed in section 6.1. The profile functions $\chi_n^A(\phi)$ fulfill the homogeneous equation (2.41) with boundary conditions, that we will not specify at this stage. Assuming therefore general BCs, we set (in t-notation)

$$\left. \partial_t \chi_n^A(t) \right|_{t=\epsilon^+} = b_\epsilon\, \chi_n^A(\epsilon^+), \qquad \left. \partial_t \chi_n^A(t) \right|_{t=1^-} = -b_1\, \chi_n^A(1^-), \qquad (5.15)$$
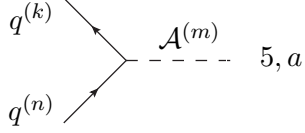
with boundary parameters b_ϵ and b_1. Note that when $b_\epsilon, b_1 \neq 0$, the profile derivative $\partial_\phi \chi(\phi)$ has now kinks not only at $\phi = -\pi, \pi$ but also at $\phi = 0$.

4D Feynman Rules

Since we want to calculate the axial-gluon contributions to the Wilson coefficients, we need its Feynman rules. Therefore we insert the decomposition (5.14), in tandem with (2.53) for the quark fields, into (5.13) and extract the following 4D rules

$$ig_s T^a \gamma^\mu \Big[(V_q^\mathcal{A})_{nmk} P_L + (\tilde{V}_q^\mathcal{A})_{nmk} P_R \Big], \qquad (5.16)$$

$$-g_s T^a \Big[(S_q^\mathcal{A})_{nmk} P_L - (\tilde{S}_q^\mathcal{A})_{nmk} P_R \Big], \qquad (5.17)$$

where

$$(V_q^\mathcal{A})_{nmk} = \frac{(2\pi)^{3/2}}{L\epsilon} \int_\epsilon^1 dt\, \chi_m^\mathcal{A} \Big[-\tan\vartheta\, a_n^{(Q)\dagger} \boldsymbol{C}_n^Q \boldsymbol{C}_k^Q a_k^{(Q)\dagger} + \cot\vartheta\, a_n^{(q)\dagger} \boldsymbol{S}_n^q \boldsymbol{S}_k^q a_k^{(q)\dagger} \Big],$$

$$(\tilde{V}_q^\mathcal{A})_{nmk} = \frac{(2\pi)^{3/2}}{L\epsilon} \int_\epsilon^1 dt\, \chi_m^\mathcal{A} \Big[-\tan\vartheta\, a_n^{(Q)\dagger} \boldsymbol{S}_n^Q \boldsymbol{S}_k^Q a_k^{(Q)\dagger} + \cot\vartheta\, a_n^{(q)\dagger} \boldsymbol{C}_n^q \boldsymbol{C}_k^q a_k^{(q)\dagger} \Big],$$

$$(5.18)$$

$$(S_q^\mathcal{A})_{nmk} = \frac{(2\pi)^{3/2}}{L\epsilon\, x_m^\mathcal{A}} \int_\epsilon^1 dt (\partial_t \chi_m^\mathcal{A}) \Big[-\tan\vartheta\, a_n^{(Q)\dagger} \boldsymbol{S}_n^Q \boldsymbol{C}_k^Q a_k^{(Q)\dagger} + \cot\vartheta\, a_n^{(q)\dagger} \boldsymbol{C}_n^q \boldsymbol{S}_k^q a_k^{(q)\dagger} \Big],$$

$$(\tilde{S}_q^\mathcal{A})_{nmk} = \frac{(2\pi)^{3/2}}{L\epsilon\, x_m^\mathcal{A}} \int_\epsilon^1 dt (\partial_t \chi_m^\mathcal{A}) \Big[-\tan\vartheta\, a_n^{(Q)\dagger} \boldsymbol{C}_n^Q \boldsymbol{S}_k^Q a_k^{(Q)\dagger} + \cot\vartheta\, a_n^{(q)\dagger} \boldsymbol{S}_n^q \boldsymbol{C}_k^q a_k^{(q)\dagger} \Big],$$

$$(5.19)$$

and $x_m^\mathcal{A} \equiv m_m^\mathcal{A}/M_{\rm KK}$. Suppose that two SM quarks and the zero-mode $\mathcal{A}_\mu^{(0)}$ attach at the vector vertex (5.16). For $\vartheta = 45°$, we find to leading order in $\mathcal{O}(v^2/M_{\rm KK}^2)$, that $\mathcal{A}_\mu^{(0)}$ couples with equal strength g_s but opposite sign to left- and right-chiral quarks. This would make $\mathcal{A}_\mu^{(0)}$ a canonical axial gluon. But, since the coupling depends on the angle ϑ and on the profile overlap, we will refer to $\mathcal{A}_\mu^{(0)}$ or $\mathcal{A}_M$ as the pseudo-axial gluon in four or five dimensions.

Effective Hamiltonian

Let us now understand how the pseudo-axial gluon might suppress the contributions, that result from mixed chirality diagrams. Working in unitary gauge ($\xi \to \infty$), we can compare the effective 5D Hamiltonian for the gluon

$$\mathcal{H}_{\rm eff}^G = \frac{2\pi L \alpha_s}{M_{\rm KK}} \sum_{q,q'} \left(\frac{2\pi}{L\epsilon}\right)^2 \int_\epsilon^1 dt \int_\epsilon^1 dt' \Big[\frac{1-\epsilon^2}{2L^2} + t_<^2 - \frac{t^2}{L}\left(\frac{1}{2} - \ln t\right) - \frac{t'^2}{L}\left(\frac{1}{2} - \ln t'\right) \Big]$$

$$\times \big[\bar{q}_L \gamma_\mu T^a q_L + \bar{q}_R \gamma_\mu T^a q_R + \bar{q}_L^c \gamma_\mu T^a q_L^c + \bar{q}_R^c \gamma_\mu T^a q_R^c \big]$$

$$\times \big[\bar{q}'_L \gamma_\mu T^a q'_L + \bar{q}'_R \gamma_\mu T^a q'_R + \bar{q}'^c_L \gamma_\mu T^a q'^c_L + \bar{q}'^c_R \gamma_\mu T^a q'^c_R \big], \qquad (5.20)$$

with the one for the pseudo-axial gluon

$$
\begin{aligned}
\mathcal{H}_{\text{eff}}^{\mathcal{A}} =& \frac{2\pi L \alpha_s}{M_{\text{KK}}} \sum_{q,q'} \left(\frac{2\pi}{L\epsilon}\right)^2 \int_\epsilon^1 dt \int_\epsilon^1 dt' \left[c_0 + t_<^2 + c_1(t^2 + t'^2) + c_2\, t^2 t'^2 \right] \\
&\times \left[-\tan\vartheta\, (\bar{q}_L \gamma_\mu T^a q_L + \bar{q}_R \gamma_\mu T^a q_R) + \cot\vartheta\, (\bar{q}_L^c \gamma_\mu T^a q_L^c + \bar{q}_R^c \gamma_\mu T^a q_R^c) \right] \\
&\times \left[-\tan\vartheta\, (\bar{q}_L' \gamma_\mu T^a q_L' + \bar{q}_R' \gamma_\mu T^a q_R') + \cot\vartheta\, (\bar{q}_L'^c \gamma_\mu T^a q_L'^c + \bar{q}_R'^c \gamma_\mu T^a q_R'^c) \right],
\end{aligned}
\tag{5.21}
$$

where we made use of the general propagator in (3.25). This expression is valid for arbitrary BCs except for the (NN) case, but which is already excluded since we demand a priori that the new gauge boson is massive. The choice of possible boundary conditions will be examined later in this section. Relevant for C_4^{RS} and C_5^{RS} are the integrands involving mixed left/right-chiral four-quark operators multiplied by $t_<^2$ in (5.20). Here, the dominant contributions come from the left-chiral doublet paired with right-chiral singlet operators. Such combinations can be eliminated by adding the corresponding pseudo-axigluon expressions in (5.21), since they come with an opposite sign. This cancellation works independently of the boundary parameters b_ϵ, b_1 as well as the mixing angle ϑ. But, we have to ensure that the new contribution from $t^2 t'^2$ will not spoil this suppression mechanism.

Decomposing the quark fields in (5.21) and using the abbreviations for the overlap integrals (4.52), (4.53), (4.54) and (4.55), we find after some steps the exact result

$$
\begin{aligned}
\mathcal{H}_{\text{eff}}^{\mathcal{A}} =& \frac{2\pi L \alpha_s}{M_{\text{KK}}^2} \frac{T^a \otimes T^a}{\sin^2\vartheta \cos^2\vartheta} \sum_{q,q'=\{u,d\}} \sum_{m,m'} \sum_{n,n'} \\
& \left\{ c_0 \left[\bar{q}_L^{(m)} \gamma_\mu (\mathbb{1}\sin^2\vartheta - \delta_Q)_{mn} q_L^{(n)} - \bar{q}_R^{(m)} \gamma_\mu (\mathbb{1}\cos^2\vartheta - \delta_q)_{mn} q_R^{(n)} \right] \right. \\
& \qquad \times \left[\bar{q}_L'^{(m')} \gamma^\mu (\mathbb{1}\sin^2\vartheta - \delta_{Q'})_{m'n'} q_L'^{(n')} - \bar{q}_R'^{(m')} \gamma^\mu (\mathbb{1}\cos^2\vartheta - \delta_{q'})_{m'n'} q_R'^{(n')} \right] \\
& + c_1 \left[\bar{q}_L^{(m)} \gamma_\mu (\Delta_Q \sin^2\vartheta - \epsilon_Q)_{mn} q_L^{(n)} - \bar{q}_R^{(m)} \gamma_\mu (\Delta_q \cos^2\vartheta - \epsilon_q)_{mn} q_R^{(n)} \right] \\
& \qquad \times \left[\bar{q}_L'^{(m')} \gamma^\mu (\mathbb{1}\sin^2\vartheta - \delta_{Q'})_{m'n'} q_L'^{(n')} - \bar{q}_R'^{(m')} \gamma^\mu (\mathbb{1}\cos^2\vartheta - \delta_{q'})_{m'n'} q_R'^{(n')} \right] \\
& + c_1 \left[\bar{q}_L^{(m)} \gamma_\mu (\mathbb{1}\sin^2\vartheta - \delta_Q)_{mn} q_L^{(n)} - \bar{q}_R^{(m)} \gamma_\mu (\mathbb{1}\cos^2\vartheta - \delta_q)_{mn} q_R^{(n)} \right] \\
& \qquad \times \left[\bar{q}_L'^{(m')} \gamma^\mu (\Delta_{Q'} \sin^2\vartheta - \epsilon_{Q'})_{m'n'} q_L'^{(n')} - \bar{q}_R'^{(m')} \gamma^\mu (\Delta_{q'} \cos^2\vartheta - \epsilon_{q'})_{m'n'} q_R'^{(n')} \right] \\
& + c_2 \left[\bar{q}_L^{(m)} \gamma_\mu (\Delta_Q \sin^2\vartheta - \epsilon_Q)_{mn} q_L^{(n)} - \bar{q}_R^{(m)} \gamma_\mu (\Delta_q \cos^2\vartheta - \epsilon_q)_{mn} q_R^{(n)} \right] \\
& \qquad \times \left[\bar{q}_L'^{(m')} \gamma^\mu (\Delta_{Q'} \sin^2\vartheta - \epsilon_{Q'})_{m'n'} q_L'^{(n')} - \bar{q}_R'^{(m')} \gamma^\mu (\Delta_{q'} \cos^2\vartheta - \epsilon_{q'})_{m'n'} q_R'^{(n')} \right] \\
& + \left[\bar{q}_L^{(m)} \gamma_\mu (\tilde{\Delta}_Q \sin^2\vartheta - \epsilon_Q)_{mn} q_L^{(n)} - \bar{q}_R^{(m)} \gamma_\mu (\tilde{\Delta}_q \cos^2\vartheta - \epsilon_q)_{mn} q_R^{(n)} \right] \\
& \qquad \left. \otimes \left[\bar{q}_L'^{(m')} \gamma^\mu (\tilde{\Delta}_{Q'} \sin^2\vartheta - \epsilon_{Q'})_{m'n'} q_L'^{(n')} - \bar{q}_R'^{(m')} \gamma^\mu (\tilde{\Delta}_{q'} \cos^2\vartheta - \epsilon_{q'})_{m'n'} q_R'^{(n')} \right] \right\},
\end{aligned}
\tag{5.22}
$$

where $q = u\,(d)$ implies $Q = U\,(D)$ and analogously for q', Q'. It is further understood, that the color generators T^a are inserted within each operator bilinear. Note that the terms in the last two lines of (5.22) represent tensor integrals, that can be expressed as double integrals via relations (4.48) - (4.51).

Wilson Coefficients

Formula (5.22) is the starting point from which we derive the contribution to the Wilson coefficients in (4.47), stemming from the tree level diagram in fig. 5.1. We set $q = q' = d$, $m = m' = 1$ and $n = n' = 2$ and use (4.43) and (4.44) to transform into the operator basis (4.23). Then we can read off the coefficients $C_{1,\mathcal{A}}^{\mathrm{RS}}$, $\tilde{C}_{1,\mathcal{A}}^{\mathrm{RS}}$, $C_{4,\mathcal{A}}^{\mathrm{RS}}$ and $C_{5,\mathcal{A}}^{\mathrm{RS}}$. Adding also the gluon contributions, the combined and exact coefficients finally read
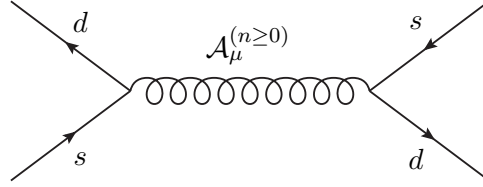

Figure 5.1.: Tree-level diagram, contributing to K^0-$\bar{K}^0$ mixing, by exchanging all (massive) 4D modes of the pseudo-axial gluon.

$$
\begin{aligned}
C_{1,G+\mathcal{A}}^{\mathrm{RS}} =& \frac{4\pi L}{M_{\mathrm{KK}}^2} \left[\frac{\alpha_s}{2} \left(1 - \frac{1}{N_c} \right) \right] \left\{ \frac{1}{c_\vartheta^2} (\tilde{\Delta}_D)_{12} \otimes (\tilde{\Delta}_D)_{12} - \frac{2}{c_\vartheta^2} (\tilde{\Delta}_D)_{12} \otimes (\tilde{\epsilon}_D)_{12} \right. \\
&+ \frac{1}{s_\vartheta^2 c_\vartheta^2} (\tilde{\epsilon}_D)_{12} \otimes (\tilde{\epsilon}_D)_{12} + \frac{c_0}{2 s_\vartheta^2 c_\vartheta^2} (\delta_D)_{12}^2 - \frac{c_1}{c_\vartheta^2} \left[(\Delta_D)_{12} - \frac{1}{s_\vartheta^2} (\epsilon_D)_{12} \right] (\delta_D)_{12} \\
&\left. + \frac{c_2}{2 c_\vartheta^2} \left[s_\vartheta^2 (\Delta_D)_{12}^2 - 2 (\Delta_D)_{12} (\epsilon_D)_{12} + \frac{1}{s_\vartheta^2} (\epsilon_D)_{12}^2 \right] \right\},
\end{aligned}
\tag{5.23}
$$

$$
\begin{aligned}
\tilde{C}_{1,G+\mathcal{A}}^{\mathrm{RS}} =& \frac{4\pi L}{M_{\mathrm{KK}}^2} \left[\frac{\alpha_s}{2} \left(1 - \frac{1}{N_c} \right) \right] \left\{ \frac{1}{s_\vartheta^2} (\tilde{\Delta}_d)_{12} \otimes (\tilde{\Delta}_d)_{12} - \frac{2}{s_\vartheta^2} (\tilde{\Delta}_d)_{12} \otimes (\tilde{\epsilon}_d)_{12} \right. \\
&+ \frac{1}{s_\vartheta^2 c_\vartheta^2} (\tilde{\epsilon}_d)_{12} \otimes (\tilde{\epsilon}_d)_{12} + \frac{c_0}{2 s_\vartheta^2 c_\vartheta^2} (\delta_d)_{12}^2 - \frac{c_1}{s_\vartheta^2} \left[(\Delta_d)_{12} - \frac{1}{c_\vartheta^2} (\epsilon_d)_{12} \right] (\delta_d)_{12} \\
&\left. + \frac{c_2}{2 s_\vartheta^2} \left[c_\vartheta^2 (\Delta_d)_{12}^2 - 2 (\Delta_d)_{12} (\epsilon_d)_{12} + \frac{1}{c_\vartheta^2} (\epsilon_d)_{12}^2 \right] \right\},
\end{aligned}
\tag{5.24}
$$

$$
\begin{aligned}
C_{4,G+\mathcal{A}}^{\mathrm{RS}} = \frac{4\pi L}{M_{\mathrm{KK}}^2} \left[2\alpha_s\right] \Bigg\{ &- \frac{1}{c_\vartheta^2} (\tilde{\Delta}_D)_{12} \otimes (\tilde{\epsilon}_d)_{12} - \frac{1}{s_\vartheta^2} (\tilde{\Delta}_d)_{12} \otimes (\tilde{\epsilon}_D)_{12} \\
&+ \frac{1}{s_\vartheta^2 c_\vartheta^2} (\tilde{\epsilon}_D)_{12} \otimes (\tilde{\epsilon}_d)_{12} + \frac{c_0}{2 s_\vartheta^2 c_\vartheta^2} (\delta_D)_{12} (\delta_d)_{12} - \frac{c_1}{2} \Big[\frac{1}{c_\vartheta^2} (\Delta_D)_{12} (\delta_d)_{12} \\
&+ \frac{1}{s_\vartheta^2} (\Delta_d)_{12} (\delta_D)_{12} - \frac{1}{s_\vartheta^2 c_\vartheta^2} \Big\{ (\epsilon_D)_{12} (\delta_d)_{12} + (\epsilon_d)_{12} (\delta_D)_{12} \Big\} \Big] \\
&+ \frac{c_2}{2} \Big[(\Delta_D)_{12} (\Delta_d)_{12} - \frac{1}{c_\vartheta^2} (\Delta_D)_{12} (\epsilon_d)_{12} - \frac{1}{s_\vartheta^2} (\Delta_d)_{12} (\epsilon_D)_{12} \Big] \Bigg\},
\end{aligned}
\tag{5.25}
$$

$$
C_{5,G+\mathcal{A}}^{\mathrm{RS}} = - \frac{1}{N_c} C_{4,G+\mathcal{A}}^{\mathrm{RS}},
\tag{5.26}
$$

with the abbreviations $c_\vartheta \equiv \cos\vartheta$ and $s_\vartheta \equiv \sin\vartheta$. The single integrals and the tensor structures are defined in (4.48) - (4.55). At leading order in v^2/M_{KK}^2, we can neglect all terms involving an $\epsilon_{D,d}$, $\tilde{\epsilon}_{D,d}$ or $\delta_{D,d}$ quantity, see (4.58), yielding the simpler expressions

$$
C_{1,G+\mathcal{A}}^{\mathrm{RS}} = \frac{4\pi L}{M_{\mathrm{KK}}^2} \left[\frac{\alpha_s}{2} \left(1 - \frac{1}{N_c} \right) \right] \frac{1}{\cos^2\vartheta} (\tilde{\Delta}_D)_{12} \otimes (\tilde{\Delta}_D)_{12} + \mathcal{O}(v^2/M_{\mathrm{KK}}^4),
\tag{5.27}
$$

$$
\tilde{C}_{1,G+\mathcal{A}}^{\mathrm{RS}} = \frac{4\pi L}{M_{\mathrm{KK}}^2} \left[\frac{\alpha_s}{2} \left(1 - \frac{1}{N_c} \right) \right] \frac{1}{\sin^2\vartheta} (\tilde{\Delta}_d)_{12} \otimes (\tilde{\Delta}_d)_{12} + \mathcal{O}(v^2/M_{\mathrm{KK}}^4),
\tag{5.28}
$$

$$
C_{4,G+\mathcal{A}}^{\mathrm{RS}} = \frac{4\pi L}{M_{\mathrm{KK}}^2} \left[2\alpha_s\right] \frac{c_2}{2} (\Delta_D)_{12} (\Delta_d)_{12} + \mathcal{O}(v^2/M_{\mathrm{KK}}^4) = - \frac{1}{N_c} C_{5,G+\mathcal{A}}^{\mathrm{RS}}.
\tag{5.29}
$$

The tensor structures of $C_{1,G+\mathcal{A}}^{\mathrm{RS}}$ and $\tilde{C}_{1,G+\mathcal{A}}^{\mathrm{RS}}$ receive a ϑ-dependent enhancement, compared to the previous coefficients in (4.47), e.g. by a factor of two for $\vartheta = 45°$. On the other hand, they completely vanish in case of the dangerous coefficients $C_{4,G+\mathcal{A}}^{\mathrm{RS}}$ and $C_{5,G+\mathcal{A}}^{\mathrm{RS}}$. Instead, a new contribution from the $t^2 t'^2$ term of the pseudo-axial gluon propagator appears, that is independent of the angle ϑ but depends on $c_2(b_\epsilon, b_1)$. Within the ZMA, we can see from (4.57) and (4.59), that the product $(\Delta_D)_{12} (\Delta_d)_{12}$ is of the same size as the tensor product before,

$$
(\tilde{\Delta}_D)_{12} \otimes (\tilde{\Delta}_d)_{12} \sim (\Delta_D)_{12} (\Delta_d)_{12}.
\tag{5.30}
$$

So, in order to solve the RS flavor problem, we have to suppress the coefficient c_2, which depends on the boundary parameters b_ϵ and b_1, see (3.26), through

$$
c_2(b_\epsilon, b_1) = - \frac{b_\epsilon b_1}{2(b_\epsilon + b_1\epsilon) - b_\epsilon b_1(\epsilon^2 - 1)}.
\tag{5.31}
$$

Still, these parameters can not be chosen freely, since they are related to the mass of the pseudo axial gluon and they have to be generated by a realistic implementation of the scalar sector. The latter point, the extension of the Higgs sector, will be covered in chapter 6. For our purpose here, we just assume that the $SU(3)_D \times SU(3)_S$ group

gets spontaneously broken down to the color gauge group $SU(3)_c$ at the UV and IR brane, leading to two vacuum expectation values v_{UV} and v_{IR}. A natural size of the UV VEV is the Planck scale, $v_{\text{UV}} \sim M_{\text{Pl}}$, while the IR VEV is warped down to a value near the electroweak scale, $v_{\text{IR}} \sim v$. Their specific values depend on the concrete scalar implementation, therefore we use a parametrization by ζ_ϵ, ζ_1 and set[5]

$$v_{\text{UV}} = \zeta_\epsilon \frac{M_{\text{KK}}}{\epsilon}, \qquad\qquad v_{\text{IR}} = \zeta_1 v \ . \qquad (5.32)$$

For realistic setups, these parameters are postive numbers of $\mathcal{O}(1)$. As we will show in section 6.1, both expectation values are related to the boundary conditions of the pseudo-axial gluon. In our case, with the parametrization in (5.32), this yields

$$b_\epsilon = \frac{\zeta_\epsilon^2}{\epsilon} \frac{Lg_s^2}{2N_c \sin^2 \vartheta \cos^2 \vartheta}, \qquad b_1 = -\frac{\zeta_1^2 v^2}{M_{\text{KK}}^2} \frac{Lg_s^2}{2N_c \sin^2 \vartheta \cos^2 \vartheta}, \qquad (5.33)$$

with the mixing angle ϑ and the number of colors $N_c \equiv 3$. Based on this parametrization, we can calculate the physical masses $m_n^{\mathcal{A}}$ for each 4D mode by imposing the BCs on the homogeneous profile solution in (2.42), which leads to the exact equation

$$\begin{aligned}
&[b_\epsilon J_1(x_n \epsilon) - x_n J_0(x_n \epsilon)] [x_n Y_0(x_n) + b_1 Y_1(x_n)] \\
&\qquad = -[b_1 J_1(x_n) + x_n J_0(x_n)] [x_n Y_0(x_n \epsilon) - b_\epsilon Y_1(x_n \epsilon)], \qquad (5.34)
\end{aligned}$$

whose eigenvalues $x_n = m_n^{\mathcal{A}}/M_{\text{KK}}$ provide the masses. We are interested in the smallest solution of (5.34), since $m_0^{\mathcal{A}}$ might be constrained by current exclusion bounds from collider experiments. An alternative way for obtaining the mass eigenvalues would be to use the 5D solution of the vector propagator in (3.10) and calculate numerically the momentum zeros of its reciprocal.

Discussion of the Boundary Conditions

Now, we can start to examine different BC types. The (NN) case with $b_\epsilon = b_1 = 0$ would imply no breaking of $SU(3)_D \times SU(3)_S$, leading to massless pseudo-axial gluons, which is experimentally excluded. Remaining are therefore three distinct scenarios:

(NM) $\boldsymbol{b_\epsilon = 0}$ **&** $\boldsymbol{b_1 \neq 0}$ **:** This case appears to be a common choice, since the other massive gauge bosons Z, W and A have boundary conditions of this type. From (5.31), we also see that the $t^2 t'^2$ contribution vanishes, since $c_2(0, b_1) = 0$. For completeness, we quote the other coefficients,

$$c_0(0, b_1) = 1 + \frac{2}{b_1} \qquad \text{and} \qquad c_1(0, b_1) = -1 \ . \qquad (5.35)$$

Concerning the zero-mode mass $m_0^{\mathcal{A}}$, we can solve (5.34) numerically in dependence of b_1, which is depicted in the left figure of (5.2). The physical mass is

---

[5]Note, $M_{\text{Pl}} \sim M_{\text{KK}}/\epsilon$.

bounded from below by $m_0^{\mathcal{A}} = 0$ for $b_1 = 0$, which represents the (NN) case, and also from above by $m_0^{\mathcal{A}} = 0.235\, M_{\mathrm{KK}}$ in the limit $b_1 \to \infty$. For low M_{KK} values of 1-2 TeV, such a pseudo-axial gluon would have been seen in the LHC dijet measurements [62],[63].

Note, that we don't need to consider negative values for b_1, since they correspond to an imaginary VEV in (5.32) and lead to tachyonic particles with negative squared masses. This can be seen by directly calculating the eigenvalues of (5.34) or by looking at the 5D vector propagator in (3.25), when we insert our coefficient values c_0, c_1 and c_2. Focusing only on the sum of profiles, we find

$$\sum_{n=0}^{\infty} \frac{\chi_n^{\mathcal{A}}(t)\chi_n^{\mathcal{A}}(t')}{(m_n^{\mathcal{A}})^2} = \frac{L}{4\pi M_{\mathrm{KK}}^2} \left[t_<^2 - t^2 - t'^2 + 1 + \frac{2}{b_1} \right] \,. \tag{5.36}$$

For specific values like $t = t' = 1$, the right-hand side gets negative for $b_1 < 0$. The square of profiles on the left hand side is positive, so an imaginary mass value has to account for the sign.

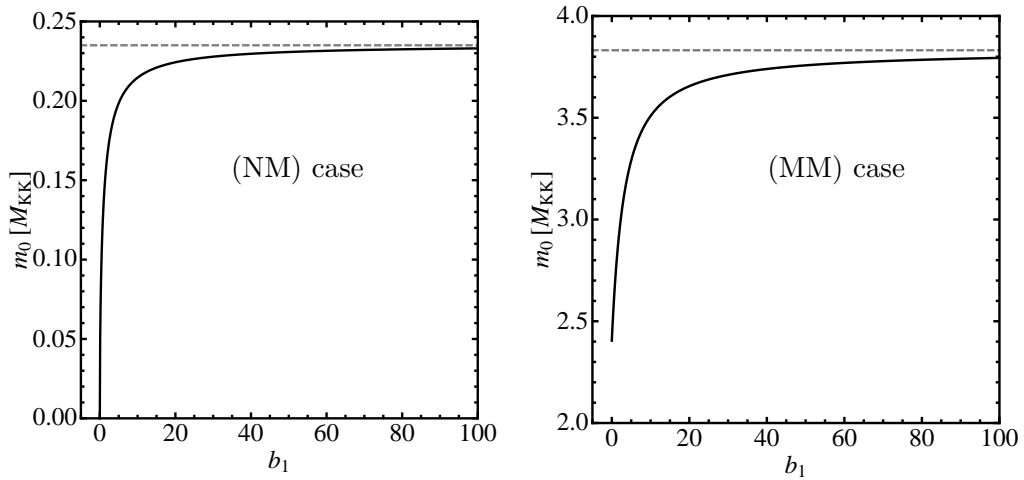As a consequence, the (NM) type is experimentally excluded.

Figure 5.2.: Plots of pseudo-axial gluon masses $m_0^{\mathcal{A}}$, in dependence of the IR boundary parameter b_1. Left is depicted the (NM) case with $b_\epsilon = 0$ and on the right the (MM) type with $b_\epsilon = 1/\epsilon$. In both cases, the horizontal dashed line represents the asymptotic curve for $b_1 \to \infty$.

(MN) $b_\epsilon \neq 0$ & $b_1 = 0$: In this scenario, the sum over profiles strongly simplifies to

$$\sum_{n=0}^{\infty} \frac{\chi_n^{\mathcal{A}}(t)\chi_n^{\mathcal{A}}(t')}{(m_n^{\mathcal{A}})^2} = \frac{L}{4\pi M_{\mathrm{KK}}^2} \left[\frac{2\epsilon}{b_\epsilon} - \epsilon^2 + t_<^2 \right], \tag{5.37}$$

since c_1 and c_2 vanish. When evaluating equation (5.34), we can have physical masses for $\mathcal{A}_\mu^{(0)}$, ranging from zero to $2.41\,M_{\text{KK}}$ for $b_\epsilon \in [0, \infty)$. A heavy pseudo-axial gluon is possible by suitable values of the UV boundary parameter. Again, negative values of b_ϵ are excluded, because they lead to tachyonic particles. This can be seen from (5.37), by setting $t = t' = \epsilon$ and comparing both sides for $b_\epsilon < 0$.

But, a serious problem of the (MN) boundary condition concerns its implementation by a scalar sector. The vanishing parameter $b_1 = 0$ implies the absence of a scalar field, charged under the $SU(3)_D \times SU(3)_S$, that gets broken at the IR brane. Without such a scalar field, we can't write down Yukawa terms at the infrared brane, since the quark fields q and q^c transform as triplets under the $SU(3)_D$ and $SU(3)_S$ respectively, see (5.6). As a consequence we have to discard the (MN) case, too.

(MM) $b_\epsilon \neq 0$ & $b_1 \neq 0$: For a better handling of c_0, c_1 and c_2, we expand them around ϵ and use that $b_\epsilon \propto 1/\epsilon$ in (5.33), yielding

$$c_0 = 0 + \mathcal{O}(\epsilon^2), \quad c_1 = 0 + \mathcal{O}(\epsilon^2) \quad \text{and} \quad c_2 = -\frac{b_1}{2 + b_1} + \mathcal{O}(\epsilon^2) . \qquad (5.38)$$

The coefficients are independent of b_ϵ as long as its value is not of order ϵ, which would be unnatural due to $v_{\text{UV}} \sim \mathcal{O}(M_{\text{Pl}})$. With (5.38), the tower of profiles takes the form

$$\sum_{n=0}^{\infty} \frac{\chi_n^{\mathcal{A}}(t)\chi_n^{\mathcal{A}}(t')}{(m_n^{\mathcal{A}})^2} = \frac{L}{4\pi M_{\text{KK}}^2} \left[t_<^2 - \frac{b_1}{2 + b_1} t^2 t'^2 + \mathcal{O}(\epsilon^2) \right] . \qquad (5.39)$$

The additional $\Delta F = 2$ contribution from the $t^2 t'^2$ depends on the specific value of b_1 in (5.33), that relies itself on the scalar sector at the IR through ζ_1. Exemplary, for $M_{\text{KK}} = 1.5\,\text{TeV}$ and $\vartheta = 45°$, the relation is given by $b_1 = 0.06\,\zeta_1^2$. Small values for b_1 can suppress sufficiently the c_2 coefficient in (5.38).

Concerning the mass plot of $\mathcal{A}^{(0)}$ on the right side of figure (5.2), we have set the UV BC to $b_\epsilon = 1/\epsilon$. Still the result is largely independent of b_ϵ as long as it is not of $\mathcal{O}(\epsilon)$. The curve starts with $m_0^{\mathcal{A}} = 2.405\,M_{\text{KK}}$ for $b_1 = 0$ and approaches $m_0^{\mathcal{A}} = 3.832\,M_{\text{KK}}$ in the limit $b_1 \to \infty$.

As shown above, we are interested in values b_1 smaller than one. For this purpose, we can expand the eigenvalue equation (5.34) in ϵ and find at leading order $x_0 J_0(x_0) = -b_1 J_1(x_0)$. Further expanding this equation around the first zero of J_0, we can solve the leading order term for the pseudo-axial gluon mass and find

$$m_0^{\mathcal{A}} \approx \left(2.405 + \frac{b_1}{2.405} \right) M_{\text{KK}}, \qquad (5.40)$$

which is accurate to two decimal places for $b_1 < 0.3$. Axial gluons in this mass range are not excluded by collider experiments.

Interim Conclusion

In summary, a pseudo-axial gluon with (MM) boundary conditions can solve the RS flavor problem by suppressing the additional $t^2 t'^2$ contribution via a small value for the IR boundary parameter $b_1 \sim \zeta_1^2 v^2 / M_{\text{KK}}^2$. A concrete value for ζ_1 relies on the scalar extension, which is the topic of chapter 6. Still we can vary this parameter in a sensible range $\zeta_1 \in [0.1, 10]$ and calculate the impact on the ϵ_K observable. It also affects the mass $m_0^{\mathcal{A}}$ via (5.40), which can be compared to the masses of the first KK gluon or photon mode $m_1^{G,A} = 2.448 \, M_{\text{KK}}$. For values b_1 smaller than 0.1, the lightest particle that is predicted in our extended RS model will be the zero-mode of the pseudo-axial gluon.

In the following section, we will perform the numerical calculation of ϵ_K in the Minimal RS Model and in our extended version of it.

5.2. Numerical Analysis

5.2.1. Parameter Sets

In comparison with the SM, the RS setup contains the additional parameters L, M_{KK}, $\boldsymbol{M}_{c_Q}$, $\boldsymbol{M}_{c_u}$ and $\boldsymbol{M}_{c_d}$. While the volume is fixed in our scenario[6] to $L = -\ln \epsilon$ with $\epsilon = 10^{-16}$, see (2.20), we randomize the M_{KK} scale in the range $[1, 10]\,\text{TeV}$ using a flat distribution. As mentioned in section 2.2.3, we can choose the bulk mass matrices diagonal and real, leading to the nine c-parameters c_{Q_i, u_i, d_i}. We can fix eight of them. Therefore, we uniformly randomize the bulk parameter $c_{u3} \in [-0.5, 2]$ and the 36 real and imaginary entries of the Yukawa matrices $\boldsymbol{Y}_u$ and $\boldsymbol{Y}_d$ within the range $[0, 3]$. These generated values, together with the experimental values for the quark masses and for the Wolfenstein parameters A and λ from table B.1, can be inserted into (2.82) to calculate the eight remaining F-profiles and to fix the c-parameters. We obtain a parameter set (or point)

$$\bar{X} = (M_{\text{KK}}, \boldsymbol{Y}_u, \boldsymbol{Y}_d, \boldsymbol{c}_Q, \boldsymbol{c}_u, \boldsymbol{c}_d), \tag{5.41}$$

which is then used to calculate the quark masses and Wolfenstein parameters via (2.80) and (2.81). The results are summarized by the list

$$\bar{Y} \equiv (m_u, m_c, m_t, m_d, m_s, m_b, A, \lambda, \bar{\rho}, \bar{\eta}) \,. \tag{5.42}$$

As a selection criteria, we calculate the quantity

$$\chi^2[\bar{X}] = \sum_{n=1}^{10} \left(\frac{Y_n - Y_{\text{exp},n}}{\sigma_n(\bar{Y}_{\text{exp}})} \right)^2 , \tag{5.43}$$

where $\bar{Y}_{exp}$ and $\sigma(\bar{Y}_{exp})$ represent analogous lists composed of the experimental values and errors (see table B.1). The point $\bar{X}$ is kept when $\chi^2[\bar{X}] < 10$, otherwise

---

[6]A different scenario would be the LRS model with a reduced value for L, see [29] for discussions.

it is rejected. A more detailed description of the algorithm for generating physical parameter sets can be found in [29].

For the upcoming analysis, we use a subset of 10000 points, which have been generated by Sandro Casagrande [45]. Each of these points $\bar{X}_i$ ($i \in [1, 10000]$) is physical in the sense that it fulfills the criterion $\chi^2[\bar{X}_i] < 10$.

Let us look at the c-parameters of our data set. While c_{u3} is randomized in the range $[-0.5, 2]$, the remaining bulk mass parameters are calculated via (2.82), as mentioned above. Their frequency within the data points is qualitatively illustrated in the three diagrams at the end of this section in fig. 5.3, where the c-parameters are binned in 0.01 steps and the number of parameter points, which contain c-values within the corresponding bin, is plotted on the y-axis. Up to c_{u3}, the distributions are distinctively peaked. For example, the maximum of the c_{d1} distribution is located at -0.64 with a full width at half maximum (FWHM) value of circa 0.07.

In general, we can infer from the distributions, that the solution of the Yukawa Hierarchy Problem relies on the restricted range of the c-parameters, in order to reproduce physical parameter sets. Thus, the issue of Yukawa couplings varying over several orders of magnitude in the SM gets replaced by the demand to precisely adjust the $\mathcal{O}(1)$ c-parameters in the RS model.
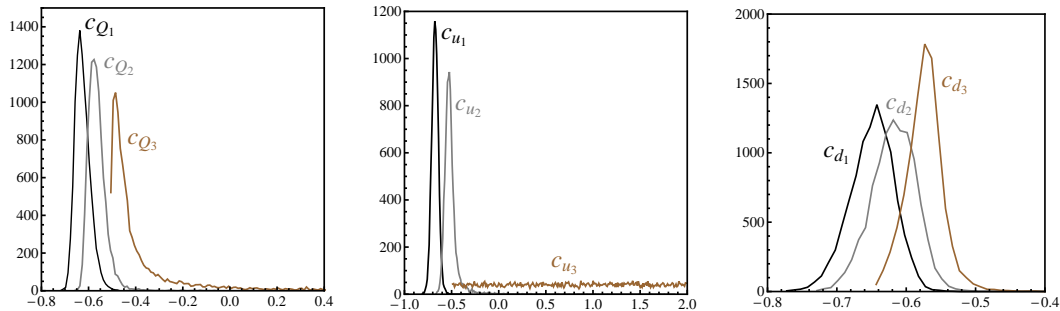

Figure 5.3.: Distributions of the bulk mass parameters in our data set consisting of 10000 points. See the text for more details.

5.2.2. RG Evolution and Hadronic Matrix Elements

We are interested in the effective Hamiltonian matrix element with one incoming $\bar{K}^0$ and one outgoing K^0, which can be decomposed as (see (4.22))

$$\langle K^0 | \mathcal{H}_{\text{eff}} | \bar{K}^0 \rangle = \sum_{i=1}^{5} C_i(\mu) \langle Q_i(\mu) \rangle + \sum_{i=1}^{3} \tilde{C}_i(\mu) \langle \tilde{Q}_i(\mu) \rangle \,. \tag{5.44}$$

We evaluate the coefficients at M_{KK} for each parameter point and then evolve them down to the low scale $\mu = 2\,\text{GeV}$, where the hadronic matrix elements are known. One has to calculate anomalous dimensions, coming from effective diagrams with gluon lines connecting two external quarks. This has been done at NLO in [52], including also two loop diagrams, and is then implemented in [51] to provide an evolution formula. Adopted to our case, the formula reads

$$C_r(2\,\text{GeV}) = \sum_i \sum_s \left(b_i^{(r,s)} + \eta\, c_i^{(r,s)} \right) \eta^{a_i}\, C_s(M_{\text{KK}}), \tag{5.45}$$

with

$$\eta = \frac{\alpha_s(M_{\text{KK}})}{\alpha_s(m_t)} \,. \tag{5.46}$$

The parameters $b_i^{(r,s)}$, $c_i^{(r,s)}$ and a_i are referred to as "magic numbers" and can be found in the appendix B.2. As can be seen from (5.45), the coefficients in general mix with each other. In our case, we encounter a mixing of C_2 with C_3 and C_4 with C_5. This is due to the diagrams in fig. 4.1, when the relation for the generator product $T_{\alpha\beta} T_{\gamma\delta}$ in (4.43) is used. Note that formula (5.45) does also hold for the coefficients $\tilde{C}_1$ - $\tilde{C}_3$.

Now we can numerically calculate all coefficients at $\mu = 2\,\text{GeV}$. What remains are the operator matrix elements, which can not be calculated perturbatively. They can be defined via

$$\langle K^0 | O_1 | \bar{K}^0 \rangle = \frac{1}{3} M_K f_K^2 B_1(\mu), \qquad \langle K^0 | O_2 | \bar{K}^0 \rangle = -\frac{5}{24} \tilde{M}^2 B_2(\mu),$$

$$\langle K^0 | O_3 | \bar{K}^0 \rangle = \frac{1}{24} \tilde{M}^2 B_3(\mu), \qquad \langle K^0 | O_4 | \bar{K}^0 \rangle = \frac{1}{4} \tilde{M}^2 B_4(\mu),$$

$$\langle K^0 | O_5 | \bar{K}^0 \rangle = \frac{1}{12} \tilde{M}^2 B_5(\mu), \qquad \text{with} \quad \tilde{M} \equiv \left(\frac{M_K}{m_s(\mu) + m_d(\mu)} \right), \tag{5.47}$$

where the $B_i(\mu)$ are so called bag parameters, which are calculated on the lattice

$$B_1(\mu) = (0.527 \pm 0.022)\,[64], \quad B_2(\mu) = (0.7 \pm 0.2)\,[65], \quad B_3(\mu) = (1.0 \pm 0.4)\,[65],$$

$$B_4(\mu) = (0.9 \pm 0.2)\,[65], \qquad B_5(\mu) = (0.6 \pm 0.1)\,[65] \,. \tag{5.48}$$

Concerning the kaon decay constant f_K and the masses appearing in (5.47), we use the following values

$$f_K = (156.1 \pm 0.12)\,\text{MeV}\,[11], \qquad m_d(\mu) + m_s(\mu) = (135 \pm 18)\,\text{MeV}\,[65],$$

$$M_K = (497.614 \pm 0.024)\,\text{MeV}\,[11] \,. \tag{5.49}$$

For illustration, we can combine the running and the hadronic matrix elements to express the effective Hamiltonian in terms of the Wilson coefficients evaluated at a fixed scale of $M_{\mathrm{KK}} = 1.5\,\mathrm{TeV}$, yielding

$$\langle K^0 | \mathcal{H}_{\mathrm{eff}} | \bar{K}^0 \rangle = 0.0016 \left[C_1 + \tilde{C}_1 + 117 \left(C_4 + \frac{1}{3.1} C_5 \right) \right] . \tag{5.50}$$

We encounter the previously in (4.65) mentioned enhancement of C_4 and C_5 relative to C_1 and $\tilde{C}_1$, which gets even stronger when we increase the M_{KK} value.

5.2.3. Results

For each parameter point, we calculate the ϵ_K value via

$$\epsilon_K^{\mathrm{RS}} = \epsilon_K^{\mathrm{SM}} + \Delta\epsilon_K^{\mathrm{RS}}, \tag{5.51}$$

where ϵ_K^{SM} is the theoretical SM value in (4.37), including the G_F correction in (4.40). In the Minimal RS model we obtain the scatter plot in fig. 5.4, where the ϵ_K^{RS} values for 10000 points are plotted against the M_{KK} values. The subset of points, that are colored in black do fulfill the following bound

$$|\epsilon_K^{\mathrm{exp}}| - 10^{-3} < |\epsilon_K^{\mathrm{RS}}| < |\epsilon_K^{\mathrm{exp}}| + 10^{-3}, \tag{5.52}$$

with the experimental value $|\epsilon_K^{\mathrm{exp}}| = 2.229\,10^{-3}$ in (4.38). We choose a bound width of $\pm 10^{-3}$ due to the hadronic uncertainties in (5.48). The red line represents the median curve and and reflects the $1/M_{\mathrm{KK}}^2$ behavior of the Wilson coefficients in $\Delta\epsilon_K^{\mathrm{RS}}$. Crossing the above boundary region only in between 8-9 TeV indicates that high values for M_{KK} are generically favored in the Minimal RS model. This introduces the flavor problem.

When we add the pseudo-axial gluon contributions to $\Delta\epsilon_K^{\mathrm{RS}}$, we have to specify the mixing angle ϑ and the UV and IR boundary conditions through ζ_ϵ and ζ_1 in (5.33). Their specific values depend on the implementation of the scalar sector. But in case of the UV BC, it turns out that the results are largely independent as long as ζ_ϵ is not of order ϵ. Therefore we fix its value to $\zeta_\epsilon = 1/\epsilon$ in our numerical evaluations. Setting $\zeta_1 = 1$ and $\vartheta = 45°$, we obtain the scatter plot in fig. 5.5, which shows a clear shifting of the red median curve to lower M_{KK} values compared to fig. 5.4 without the pseudo-axial gluon contributions. Here, the crossing point is reduced to 2.3 TeV.

To be more quantitative, we plot the percentages of points fulfilling the ϵ_K bound for one TeV-wide bins. They can be seen in the histogram 5.6, where blue colored bins refer to the Minimal RS model and the orange ones to our extended version. In the low range of 1-2 TeV, the percentage terms raise from 3% to 12% and for 2-3 TeV from 7% to 30%.

Up to now we have considered the results for $\zeta_1 = 1$ and $\vartheta = 45°$. Keeping the mixing angle fixed, fig. 5.7 shows the effect of varying ζ_1 in the range $[0.1, 10]$.
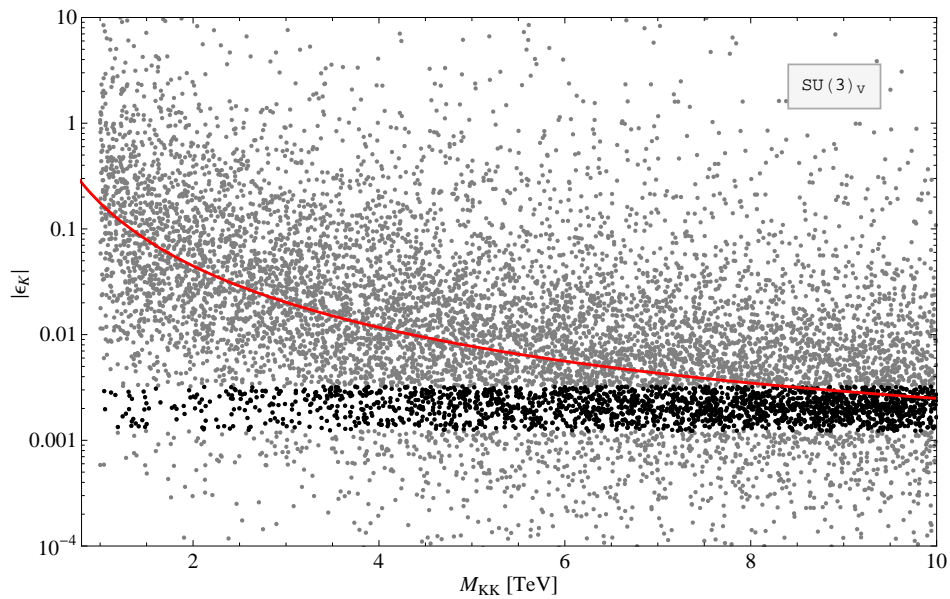
Figure 5.4.: Depicted are 10000 ϵ_K^{RS} values within the Minimal RS model. Points, which lie inside the range of (5.52), are colored in black otherwise in gray. The median curve for all points is the red line.
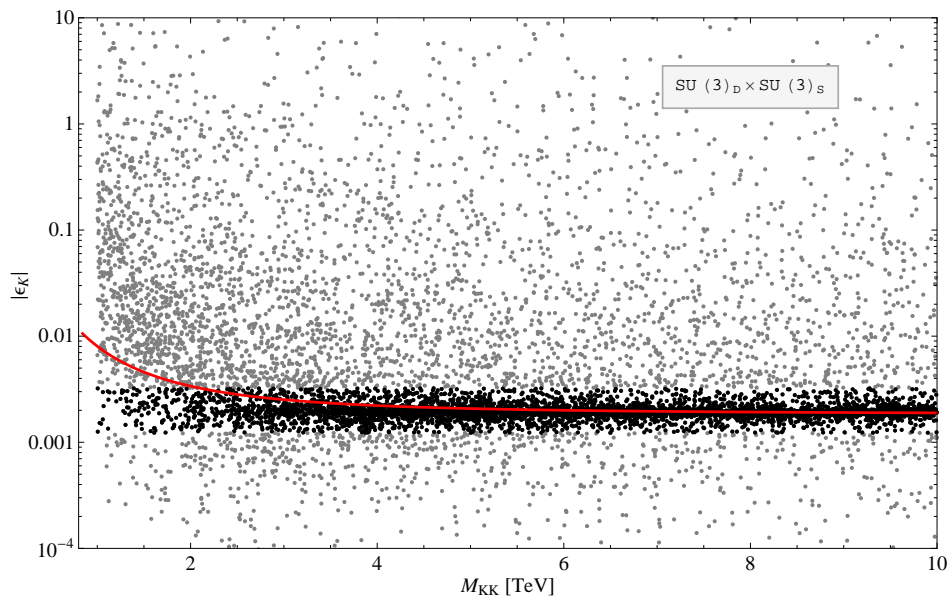

Figure 5.5.: This is the analogous scatter plot to fig. 5.4, including the pseudo-axial contributions for $\zeta_\epsilon = 1/\epsilon$, $\zeta_1 = 1$ and a fixed mixing angle $\vartheta = 45°$.
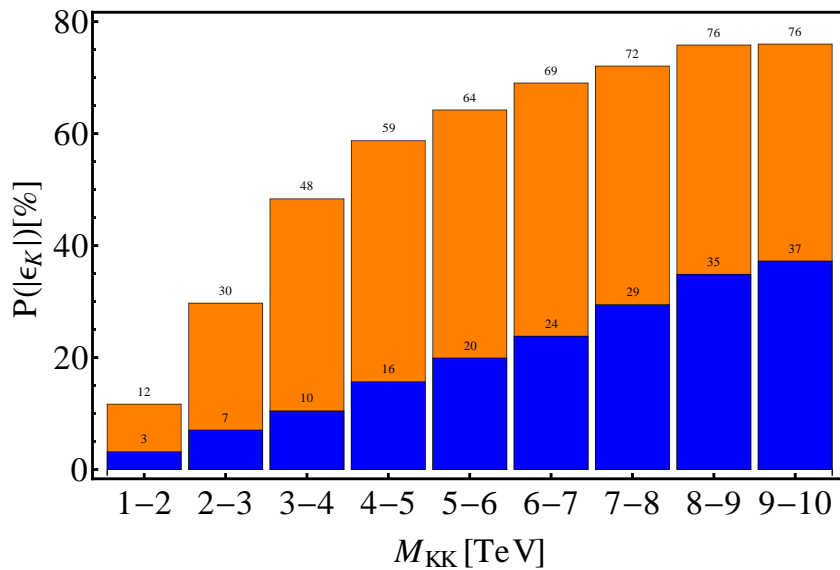
Figure 5.6.: Each bin height represents the percentage of points, that lie within the ϵ_K range (5.52). Blue bins correspond to the Minimal RS model, while the orange bins include the pseudo-axial contributions. Parameter values are fixed to $\zeta_\epsilon = 1/\epsilon$, $\zeta_1 = 1$ and $\vartheta = 45°$.

Plotted are the percentage numbers for the two lowest bins. For low values $\zeta_1 < 1$, the additional contribution from the $t^2 t'^2$-term in the propagator (5.39) is negligible, leading to a plateau and a maximum value of $\sim 12\%$ for the 1-2 TeV bin. On the other hand, increasing $\zeta_1 > 1$ lowers the percentages significantly.

Concerning the mixing angle, we find for deviations from $\vartheta = 45°$ by $\pm 20°$ that our results are not strongly affected. For more extreme values near $0°$ and $90°$, the factors $1/\sin^2 \vartheta$ and $1/\cos^2 \vartheta$ in (5.23) - (5.26) blow up and therefore enhance the ϵ_K values.

Interim Summary

Extending the RS model by a pseudo-axial gluon reduces the ϵ_K^{RS} values for the 10000 parameter points. Of interest is especially the low M_{KK} region of 1-2 TeV, where we find in our numerical calculations ($\zeta_1 = 1$), that 12 points out of 100 are compatible with the ϵ_K bound, instead of 3 points previously. For the next higher bin the fractions are 30% instead of 7%. Due to this rise, we speak of a mitigation concerning the fine-tuning problem for ϵ_K in the Minimal RS model.

Still, our results are in some sense preliminary, since we have not worked out the scalar sector. The subsequent chapter deals with this topic.
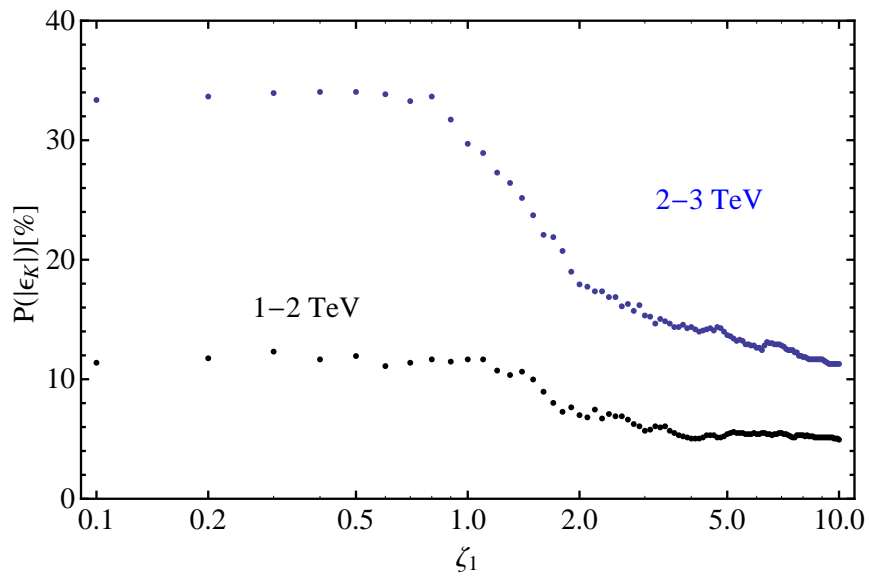
Figure 5.7.: Black (blue) points show the percentages in our extended model for the bin 1-2 TeV (2-3 Tev), when varying ζ_1 while $\zeta_\epsilon = 1/\epsilon$, $\vartheta = 45°$ are fixed. Apart from statistical fluctuations, the points fulfilling the ϵ_K bound for ζ_1 values larger than one decrease significantly.

6. Extension of the Higgs Sector

In literature, axial gluons have already been considered in the Standard Model, including discussions of the extended scalar sector, for instance in [66]. Until this stage, such an extension has not been worked out within the Randall-Sundrum framework so far. In the following, we are going to give a first treatment of the enlarged Higgs sector, containing the main properties in order to justify the numerical analysis of the previous chapter.

Motivation

The solution to the RS flavor problem relies on the (MM) boundary conditions for the pseudo-axial gluon $\mathcal{A}$. To generate the BCs, we need additional scalar fields localized at the UV and IR brane, that are charged under the symmetry group

$$G_c \equiv SU(3)_D \times SU(3)_S = \left\{ \left(U^D, U^S \right) \big| U^D \in SU(3)_D,\ U^S \in SU(3)_S \right\}, \qquad (6.1)$$

which will be gauged. The aim is then to find a realistic and minimal extension of the Higgs sector in the RS model, that spontaneously breaks the complete gauge group to the unbroken color $SU(3)_c$ and electromagnetic $U(1)_{Q_e}$,

$$G \equiv SU(3)_D \times SU(3)_S \times SU(2)_L \times U(1)_Y \xrightarrow{\text{SSB}} SU(3)_c \times U(1)_{Q_e}. \qquad (6.2)$$

We begin with the transformation behavior of the 5D quark fields under our extended gauge group G. They are listed in tab. 6.1 with the generation index $n = 1, 2, 3$

5D Quark Fields	$SU(3)_D$	$SU(3)_S$	$SU(2)_L$	I_3	$U(1)_Y$
$(Q^n)^i_\alpha = (u^n, d^n)^i_\alpha$	**3**	**1**	**2**	$(1/2, -1/2)$	$1/6$
$(u^{c,n})_{\bar{\alpha}}$	**1**	**3**	**1**	0	$2/3$
$(d^{c,n})_{\bar{\alpha}}$	**1**	**3**	**1**	0	$-1/3$
Gauge Fields	$(G_D)^a_M$	$(G_S)^a_M$	W^k_M		B_M

Table 6.1.: Quantum numbers of the 5D quark fields in our extended model.

and the weak isospin label $i = 1, 2$. To distinguish between both $SU(3)$'s, we choose Greek letters like $\alpha = 1, 2, 3$ for the $SU(3)_D$ triplet and letters with a bar like $\bar{\alpha} = 1, 2, 3$ in case of an $SU(3)_S$ triplet. Both additional symmetry groups $SU(3)_D$ and $SU(3)_S$ are gauged by the fields $(G_D)^a_M$ and $(G_S)^a_M$ with $a = 1, 2, ..., 8$.

Scalar Field Content

We see, that quark weak doublets and singlets transform in fundamental representations of $SU(3)_D$ and $SU(3)_S$, while the Higgs field Φ is not charged under these groups. As a consequence the Yukawa terms of the Minimal RS model in (2.52) are not gauge invariant any more. To solve this issue, we need at least two additional scalar fields $\Phi^{(1)}$ and $\Phi^{(2)}$ located at the IR brane, one for the up-sector and one for the down-sector, that transform as triplets under $SU(3)_D$ and as anti-triplets under $SU(3)_S$ respectively. Their transformation behavior is listed in tab. 6.2, where $\mathbf{3^*}$

Scalar Fields	$SU(3)_D$	$SU(3)_S$	$SU(2)_L$	$U(1)_Y$	localization
$\hat{\Phi}^i$	$\mathbf{1}$	$\mathbf{1}$	$\mathbf{2}$	$1/2$	IR brane
$\Phi^{(1)i}_{\alpha\bar{\alpha}}$	$\mathbf{3}$	$\mathbf{3^*}$	$\mathbf{2}$	$-1/2$	IR brane
$\Phi^{(2)i}_{\alpha\bar{\alpha}}$	$\mathbf{3}$	$\mathbf{3^*}$	$\mathbf{2}$	$1/2$	IR brane
$\Phi^{(0)}_{\alpha\bar{\alpha}}$	$\mathbf{3}$	$\mathbf{3^*}$	$\mathbf{1}$	0	UV brane

Table 6.2.: Scalar fields in our extended model.

denotes the complex conjugate fundamental representation of $SU(3)$. To clarify the notation introduced above, the scalar field $\Phi^{(1)}$ (analog for $\Phi^{(2)}$) transforms under G_c as

$$\Phi^{(1)i}_{\alpha\bar{\alpha}} \xrightarrow{SU(3)_D \times SU(3)_S} \Phi'^{(1)i}_{\alpha\bar{\alpha}} = U^D_{\alpha\beta} U^{S*}_{\bar{\alpha}\bar{\beta}} \Phi^{(1)i}_{\beta\bar{\beta}} = (U^D \Phi^{(1)i} U^{S\dagger})_{\alpha\bar{\alpha}}, \qquad (6.3)$$

with special unitary 3×3 matrices $U^D \in SU(3)_D$ and $U^S \in SU(3)_S$. Now we can write down the Yukawa terms for our extended model, that have to be singlets under G. The possible gauge invariant terms are contained in the Lagrangian

$$\mathcal{L}_{\text{FS},Y} = -\sqrt{|G|}\,\delta(x_5 - r\pi) \left[\boldsymbol{Y}^{(5)}_d \bar{Q}^i_\alpha \Phi^{(2)i}_{\alpha\bar{\alpha}} d^c_{\bar{\alpha}} + \boldsymbol{Y}^{(5)}_u \bar{Q}^i_\alpha \Phi^{(1)i}_{\alpha\bar{\alpha}} u^c_{\bar{\alpha}} + \text{h.c.} \right], \qquad (6.4)$$

where we have suppressed the generation index for clarity. Note there is no Yukawa term for the $\Phi^{(0)}$ field, since it is a singlet under $SU(2)_L$.

So far, we have motivated the need for $\Phi^{(1)}$ and $\Phi^{(2)}$. Later in section 6.2 it turns out, that we need a SM-like Higgs field $\hat{\Phi}$ in order to prevent physical Goldstone bosons in our theory. Furthermore, a bi-triplet field $\Phi^{(0)}$ has to be introduced in the UV to generate the mixed boundary condition of the pseudo-axial gluon at this brane. The complete scalar content is listed in table 6.2.

Scalar Action

All four fields $\hat{\Phi}$, $\Phi^{(0)}$, $\Phi^{(1)}$ and $\Phi^{(2)}$ build up the scalar sector of our extended model. Their action can be written as

$$S^{(5)}_{\text{HS}} = \int d^4x \int^{\pi r}_{-\pi r} dx_5 \left(\mathcal{L}_{\Phi,\text{UV}} + \mathcal{L}_{\Phi,\text{IR}} \right) \qquad (6.5)$$

with Lagrangians for the fields localized at the UV and at the IR brane,

$$\mathcal{L}_{\Phi,\text{UV}} = \delta(|\phi|)\left\{\text{Tr}\big[(D_\mu\Phi^{(0)})^\dagger(D^\mu\Phi^{(0)})\big] - V_{\text{UV}}(\Phi^{(0)})\right\}, \tag{6.6}$$

$$\mathcal{L}_{\Phi,\text{IR}} = \delta(|\phi|-\pi)\left\{(D_\mu\hat{\Phi})^\dagger(D^\mu\hat{\Phi}) + \text{Tr}\big[(D_\mu\Phi^{(1)})^{i\dagger}(D^\mu\Phi^{(1)})^i\big]\right.$$
$$\left. + \text{Tr}\big[(D_\mu\Phi^{(2)})^{i\dagger}(D^\mu\Phi^{(2)})^i\big] - V_{\text{IR}}(\hat{\Phi},\Phi^{(1)},\Phi^{(2)})\right\}. \tag{6.7}$$

Note that the δ-function in (6.6) is defined, similarly to the one in (2.30), by

$$\delta(|\phi|) \equiv \lim_{\theta\to0^+}\frac{1}{2}\left[\delta(\phi+\theta) + \delta(\phi-\theta)\right], \tag{6.8}$$

which shifts discontinuities at $\phi = 0$ into the bulk. Furthermore, we made use of the trace notation to simplify the kinetic terms for the colored fields, since

$$[(D_\mu\Phi^{(1)})^i_{\alpha\bar{\alpha}}]^*(D^\mu\Phi^{(1)})^i_{\alpha\bar{\alpha}} = [(D_\mu\Phi^{(1)})^{i\dagger}]_{\bar{\alpha}\alpha}(D^\mu\Phi^{(1)})^i_{\alpha\bar{\alpha}} = \text{Tr}\big[(D_\mu\Phi^{(1)})^{i\dagger}(D^\mu\Phi^{(1)})^i\big], \tag{6.9}$$

and analog for $\Phi^{(2)}$ and $\Phi^{(0)}$. The potential terms are included in V_{UV} and V_{IR}, we will deal with them in section 6.2. In relation to the transformation behavior in tab. 6.2, the covariant derivatives for the new scalar fields are given by

$$(D_\mu\Phi^{(0)})_{\alpha\bar{\alpha}} = \left(\delta_{\alpha\beta}\delta_{\bar{\alpha}\bar{\beta}}\partial_\mu - ig_{D5}\delta_{\bar{\alpha}\bar{\beta}}T^a_{\alpha\beta}(G_D)^a_\mu + ig_{S5}\delta_{\alpha\beta}(T^a_{\bar{\alpha}\bar{\beta}})^*(G_S)^a_\mu\right)\Phi^{(0)}_{\beta\bar{\beta}}, \tag{6.10}$$

$$(D_\mu\Phi^{(1)})^i_{\alpha\bar{\alpha}} = \left(\delta_{\alpha\beta}\delta_{\bar{\alpha}\bar{\beta}}\delta_{ij}\partial_\mu - ig_{D5}\delta_{\bar{\alpha}\bar{\beta}}\delta_{ij}T^a_{\alpha\beta}(G_D)^a_\mu + ig_{S5}\delta_{\alpha\beta}\delta_{ij}(T^a_{\bar{\alpha}\bar{\beta}})^*(G_S)^a_\mu\right.$$
$$\left. - ig_5\delta_{\alpha\beta}\delta_{\bar{\alpha}\bar{\beta}}W^k_\mu\tau^k_{ij} - ig_5'\delta_{\alpha\beta}\delta_{\bar{\alpha}\bar{\beta}}Y_u B_\mu\right)\Phi^{(1)j}_{\beta\bar{\beta}}, \tag{6.11}$$

with $Y_u = -1/2$. Concerning $\Phi^{(2)}$, replace u with d in (6.11) and insert $Y_d = 1/2$. Note the positive sign and the complex conjugate generator $(T^a)^*$ within the G_S-terms in (6.10) and (6.11), which is due to the conjugate representation **3*** under $SU(3)_S$. Regarding $\hat{\Phi}$, the covariant derivative is the same as for the Higgs field,

$$D_\mu\hat{\Phi} = (\partial_\mu - ig_5 W^k_\mu\tau^k - \frac{ig_5'}{2}B_\mu)\hat{\Phi}, \tag{6.12}$$

since they have identical quantum numbers.

Spontaneous Symmetry Breaking (SSB)

Next, we assume that the potentials V_{UV}, V_{IR} induce a breaking of G to the SM gauge group in (6.2). This implies a breakdown of $SU(3)_D \times SU(3)_S$ to its diagonal subgroup

$$H_c \equiv \left\{(U,U)\,\Big|\,U \equiv U^D = U^S,\, U^D \in SU(3)_D,\, U^S \in SU(3)_S\right\}, \tag{6.13}$$

which is isomorphic to $SU(3)$ and can be identified with the color group $SU(3)_c$. Comparing the transformation behavior with (6.3), the three colored scalars transform after SSB like

$$\Phi_{\alpha\bar{\alpha}}^{(0)} \xrightarrow{H_c} \Phi_{\alpha\bar{\alpha}}^{\prime(0)} = U_{\alpha\beta} U_{\bar{\alpha}\bar{\beta}}^* \Phi_{\beta\bar{\beta}}^{(0)} = (U\,\Phi^{(0)}\,U^\dagger)_{\alpha\bar{\alpha}}, \tag{6.14}$$

$$\Phi_{\alpha\bar{\alpha}}^{(x)i} \xrightarrow{H_c} \Phi_{\alpha\bar{\alpha}}^{\prime(x)i} = U_{\alpha\beta} U_{\bar{\alpha}\bar{\beta}}^* \Phi_{\beta\bar{\beta}}^{(x)i} = (U\,\Phi^{(x)i}\,U^\dagger)_{\alpha\bar{\alpha}} \qquad \text{for} \quad x = 1,2, \tag{6.15}$$

which states that $\Phi^{(0)}$, $\Phi^{(x)i}$ live in the $\mathbf{3} \otimes \mathbf{3^*}$ representation of $SU(3)_c$. From group theory, we know that this tensor product representation can be decomposed into the direct sum of two irreducible ones,

$$\mathbf{3} \otimes \mathbf{3^*} = \mathbf{1} \oplus \mathbf{8}, \tag{6.16}$$

which are denoted as the singlet $\mathbf{1}$ and octet $\mathbf{8}$ representations. To see this explicitly, we introduce a convenient parametrization[1]

$$\Phi_{\alpha\bar{\alpha}}^{(0)} = \phi_{(0)}^A T_{\alpha\bar{\alpha}}^A = \phi_{(0)}^0 T_{\alpha\bar{\alpha}}^0 + \phi_{(0)}^a T_{\alpha\bar{\alpha}}^a,$$
$$\Phi_{\alpha\bar{\alpha}}^{(x)i} = \phi_{(x)}^{i,A} T_{\alpha\bar{\alpha}}^A = \phi_{(x)}^{i,0} T_{\alpha\bar{\alpha}}^0 + \phi_{(x)}^{i,a} T_{\alpha\bar{\alpha}}^a \qquad \text{for} \quad x = 1,2, \tag{6.17}$$

where the range for capital letters $A = 0,1,...,8$ is supplemented by the zero with respect to $a = 1,2,...,8$. Each field $\Phi^{(0)}$, $\Phi^{(x)i}$ can be decomposed into a set of complex scalar fields $\left\{\phi_{(0)}^A\right\}$, $\left\{\phi_{(x)}^{i,A}\right\}$ and basis elements, defined via

$$T^A \equiv \begin{cases} \mathbb{1}/2 & , A = 0 \\ \lambda_A/2 & , A \in \{1,2,...,8\} \end{cases}, \tag{6.18}$$

with the 3×3 unit matrix $\mathbb{1}$ and the Gell-Mann matrices $\lambda_1, \lambda_2, ..., \lambda_8$. Now, when we consider an infinitesimal $SU(3)_c$ transformation

$$U = e^{i\delta^a T^a} = 1 + i\delta^a T^a + \mathcal{O}(\bar{\delta}^2), \tag{6.19}$$

with $\delta^a \ll 1$ and use the parametrization (6.17), the fields $\Phi^{(x)i}$ (likewise for $\Phi^{(0)}$) transform as

$$\begin{aligned}
\Phi^{\prime(x)i} &= \phi_{(x)}^{\prime i,0} T^0 + \phi_{(x)}^{\prime i,a} T^a \\
&= (1 + i\delta^b T^b + \mathcal{O}(\bar{\delta}^2)) \left[\phi_{(x)}^{i,0} T^0 + \phi_{(x)}^{i,a} T^a\right] (1 + i\delta^c T^c + \mathcal{O}(\bar{\delta}^2))^\dagger \\
&= \phi_{(x)}^{i,0} T^0 + \left[\phi_{(x)}^{i,a} + i(if_{abc})\,\delta^b\,\phi_{(x)}^{i,c}\right] T^a + \mathcal{O}(\bar{\delta}^2).
\end{aligned} \tag{6.20}$$

Comparing the last line with the first one, we can identify the symmetry invariant field $\phi_{(x)}^{i,0}$ with the singlet and the multiplet $\left\{\phi_{(x)}^{i,a}\,\middle|\,a = 1,2,...,8\right\}$ with the octet, which transforms in the adjoint representation

$$\phi_{(x)}^{i,a} \xrightarrow{H_c} \phi_{(x)}^{\prime i,a} = \left[e^{i\delta^b T_{\text{adj}}^b}\right]_{ac} \phi_{(x)}^{i,c} \qquad \text{with} \quad (T_{\text{adj}}^b)_{ac} \equiv if_{abc}, \tag{6.21}$$

---

[1]This parametrization can be inverted by $\phi_{(x)}^{i,A} = \frac{1}{C_A}\text{Tr}[\Phi^{(x)i}T^A]$ (analog for $\phi_{(0)}^A$), where $C_0 = 3/4$ and $C_1, ..., C_8 = 1/2$.

where δ^b need not be restricted here to small values. The point is, that we obtain after spontaneous symmetry breaking $SU(3)_c$ singlet and octet fields in our theory.

VEVs

As mentioned earlier, the SSB has to be generated by the potentials V_{UV} and V_{IR}, that will be discussed in section 6.2. However at this stage, we assume that the potentials allow for a non-zero minimum at the following vacuum expectation values for the scalar fields

$$\langle \Phi^{(0)}_{\alpha\bar\alpha} \rangle = \frac{v_0}{\sqrt{2N_c}} \delta_{\alpha\bar\alpha}, \qquad\qquad \langle \hat\Phi^i \rangle = \frac{\hat v}{\sqrt 2} \delta_{i2},$$

$$\langle \Phi^{(1)i}_{\alpha\bar\alpha} \rangle = \frac{v_1}{\sqrt{2N_c}} \delta_{i1}\delta_{\alpha\bar\alpha}, \qquad\qquad \langle \Phi^{(2)i}_{\alpha\bar\alpha} \rangle = \frac{v_2}{\sqrt{2N_c}} \delta_{i2}\delta_{\alpha\bar\alpha}\ . \qquad (6.22)$$

We chose the prefactors such, that we obtain convenient mass terms for the $W^\pm$ and Z bosons in the subsequent section. Then, the next step is to expand the scalar fields around their VEVs in (6.22) and to decompose them into color singlets and octets. We choose the following parametrization

$$\hat\Phi = \frac{1}{\sqrt 2} \begin{pmatrix} \sqrt 2\, \hat S^+ \\ \hat v + \hat S^0_R + i\hat S^0_I \end{pmatrix}, \qquad (6.23)$$

$$\Phi^{(0)}_{\alpha\bar\alpha} = \left(v_0 + S^0_{(0)R} + iS^0_{(0)I} \right) \frac{\delta_{\alpha\bar\alpha}}{\sqrt{2N_c}} + \left(O^{0,a}_{(0)R} + iO^{0,a}_{(0)I} \right) T^a_{\alpha\bar\alpha}, \qquad (6.24)$$

$$\Phi^{(1)}_{\alpha\bar\alpha} = \begin{pmatrix} v_1 + S^0_{(1)R} + iS^0_{(1)I} \\ \sqrt 2\, S^-_{(1)} \end{pmatrix} \frac{\delta_{\alpha\bar\alpha}}{\sqrt{2N_c}} + \begin{pmatrix} O^{0,a}_{(1)R} + iO^{0,a}_{(1)I} \\ \sqrt 2\, O^{-,a}_{(1)} \end{pmatrix} T^a_{\alpha\bar\alpha}, \qquad (6.25)$$

$$\Phi^{(2)}_{\alpha\bar\alpha} = \begin{pmatrix} \sqrt 2\, S^+_{(2)} \\ v_2 + S^0_{(2)R} + iS^0_{(2)I} \end{pmatrix} \frac{\delta_{\alpha\bar\alpha}}{\sqrt{2N_c}} + \begin{pmatrix} \sqrt 2\, O^{+,a}_{(2)} \\ O^{0,a}_{(2)R} + iO^{0,a}_{(2)I} \end{pmatrix} T^a_{\alpha\bar\alpha}, \qquad (6.26)$$

where the vector notation refers to the isospin space. We denote color singlets with S and octets with O, where the first superscript gives the sign of the electric charge $Q_e = I_3 + Y$ or is zero in case of neutral fields. The charged fields are complex scalars, while we directly decomposed the neutral fields into real and imaginary parts indicated by the subscripts R and I respectively. Factors of $\sqrt 2$ or $\sqrt{2N_c}$ in front of the fields are chosen such, that the kinetic terms for the singlets and octets are canonically normalized,

$$(\partial_\mu \hat\Phi)^\dagger (\partial^\mu \hat\Phi) = \frac{1}{2} \left[(\hat S^0_R)^2 + (\hat S^0_I)^2 \right] + \hat S^+ \hat S^-,$$

$$\mathrm{Tr}\left[(\partial_\mu \Phi^{(0)})^\dagger (\partial^\mu \Phi^{(0)}) \right] = \frac{1}{2} \left[(S^0_{(0)R})^2 + (S^0_{(0)I})^2 + (O^{0,a}_{(0)R})^2 + (O^{0,a}_{(0)I})^2 \right],$$

$$\mathrm{Tr}\left[(\partial_\mu \Phi^{(x)})^{i\dagger} (\partial^\mu \Phi^{(x)})^i \right] = \frac{1}{2} \left[(S^0_{(x)R})^2 + (S^0_{(x)I})^2 + (O^{0,a}_{(x)R})^2 + (O^{0,a}_{(x)I})^2 \right]$$
$$+ S^+_{(x)} S^-_{(x)} + O^{+,a}_{(x)} O^{-,a}_{(x)}, \qquad (6.27)$$

for $x = 1, 2$ and where $\hat{S}^- \equiv (\hat{S}^+)^\dagger$, $S^- \equiv (S^+)^\dagger$, $O_{(x)}^{-;a} \equiv (O_{(x)}^{+;a})^\dagger$.

Summarizing the field content, our scalar sector encompasses one charged and two neutral singlets (4 real DOF) at the UV brane, while we have six neutral and two charged singlets as well as octets (90 real DOF) at the IR brane.

Nambu-Goldstone Bosons

We need to clarify how many massless scalar particles we expect in our theory. Therefore, we use some general results, which link the number of broken generators to the number of massless scalar fields [5].

Starting with the Lagrangian at the UV Brane $\mathcal{L}_{\Phi,\text{UV}}$ in (6.6), we note that $\Phi^{(0)}$ transforms non-trivially only under G_c, which has 16 generators. Let us consider an infinitesimal symmetry transformation

$$\Phi_{\alpha\bar{\alpha}}^{(0)} \xrightarrow{G_c} \Phi_{\alpha\bar{\alpha}}^{\prime(0)a} = \Phi_{\alpha\bar{\alpha}}^{(0)} + i\epsilon_D^a T_{\alpha\beta}^a \Phi_{\beta\bar{\alpha}}^{(0)} - i\epsilon_S^a T_{\bar{\alpha}\bar{\beta}}^{a*} \Phi_{\alpha\bar{\beta}}^{(0)}, \qquad \text{with} \quad \epsilon_D^a, \epsilon_S^a \ll 1, \quad (6.28)$$

which can be inferred from (6.3) to leading order in ϵ_D^a, ϵ_S^a when setting $U_{\alpha\beta}^D = 1 + i\epsilon_D^a T_{\alpha\beta}^a$ and $U_{\bar{\alpha}\bar{\beta}}^S = 1 + i\epsilon_S^a T_{\bar{\alpha}\bar{\beta}}^a$. Inserting $\langle \Phi_{\beta\bar{\alpha}}^{(0)} \rangle$ into (6.28), the VEV is left invariant whenever the following term vanishes

$$\epsilon_D^a T_{\alpha\beta}^a \langle \Phi_{\beta\bar{\alpha}}^{(0)} \rangle - \epsilon_S^a T_{\bar{\alpha}\bar{\beta}}^{a*} \langle \Phi_{\alpha\bar{\beta}}^{(0)} \rangle = \frac{v_0}{\sqrt{2N_c}} T_{\alpha\bar{\alpha}}^a (\epsilon_D^a - \epsilon_S^a), \qquad \text{for} \quad \alpha, \bar{\alpha} = 1, 2, 3 \,. \quad (6.29)$$

Taking $\epsilon_D = \epsilon_S$, this is obviously fulfilled and just states that the theory is still invariant under the diagonal subgroup $SU(3)_c$ after SSB. When $\epsilon_D^a \neq \epsilon_S^a$ for some $a \in \{1, 2, ..., 8\}$, (6.29) does not vanish. There are eight broken generators, that give rise to eight massless scalar fields, when we calculate the mass matrix of the potential V_{UV}. Since G_c is a gauge symmetry, their degrees of freedom are related to the longitudinal components of the pseudo-axial gluon. This can be seen from the matching calculation in section 6.1.

At the IR brane, we have to consider the fields $\Phi^{(1)}$, $\Phi^{(2)}$ and $\hat{\Phi}$ which transform under the full gauge group G, that has 16 symmetry generators from G_c and four from $SU(2)_L \times U(1)_Y$. After SSB, the remaining symmetry $SU(3)_c \times U(1)_{Q_e}$ has 9 generators, therefore we expect 11 massless scalar fields. Eight of them contribute to the longitudinal degrees of freedom of the pseudo-axial gluon[2], while three scalars are absorbed by the zero-modes of the $W^\pm$ and Z bosons.

---

[2]In fact, this point is subtle. Due to the breaking at the UV and IR brane, we have a total amount of 16 DOF, where eight of them must be absorbed by the zero-mode of the pseudo-axial gluon. Concerning the remaining eight degrees of freedom, we expect that they lead to a (physical) zero-mode of the scalar component $\mathcal{A}_5^a$.

There is another important aspect, concerning the symmetry of the potentials. It may be possible, that a potential admits a larger global symmetry than the gauge symmetry of the fields. In that case, we obtain for each additional generator of the larger group a massless scalar field.

Estimating the Scalar Contributions for K^0-$\bar{K}^0$ Mixing

At this stage, it is necessary to check that the newly introduced singlet and octet fields will not give significant contributions to ϵ_K, thus keeping the analysis of the previous chapter valid. To estimate their size, we insert the decomposition of $\Phi^{(2)}$ into the Yukawa terms in (6.4) and extract the relevant interactions involving vertices that couple singlets and octets to down-type quarks. The corresponding 5D action reads

$$
S_{\text{FS},Y}^{(5)} \ni - \int d^4x \int_{-\pi r}^{\pi r} dx_5 \, e^{-3\sigma(\phi)} \, \delta(x_5 - r\pi) \frac{2}{k}
$$
$$
\times \left[\frac{1}{\sqrt{2N_c}} (S_{(2)R}^0 + iS_{(2)I}^0) \, \bar{d}_\alpha \boldsymbol{Y}_d d_\alpha^c + (O_{(2)R}^{0,a} + iO_{(2)I}^{0,a}) \, \bar{d}_\alpha T_{\alpha\bar{\alpha}}^a \boldsymbol{Y}_d d_{\bar{\alpha}}^c + \text{h.c.} \right],
$$
(6.30)

where we replaced the 5D by the 4D Yukawa matrices via $\boldsymbol{Y}_d^{(5)} = \boldsymbol{Y}_d \, 2/k$. Due to the δ-function in (6.30), we can directly perform the integration along x_5 meaning to evaluate the quark profiles at $\phi = -\pi^+, \pi^-$. In the same manner as for the Higgs particle in the Minimal RS model, one can reformulate the profiles at the IR boundary by making use of orhonormality relations for the quarks. Following the steps performed in [28], [27] and adapting their results to our case, we can rewrite (6.30) as[3]

$$
S_{\text{FS},Y}^{(5)} \ni - \int d^4x \sum_{m,n} \left[\frac{m_m^d}{v} \delta_{mn} - \frac{m_m^d}{v} (\delta_d)_{mn} - \frac{m_m^d}{v} (\delta_D)_{mn} - (\Delta\tilde{g}_h^d)_{mn} \right]
$$
$$
\times \left[\frac{1}{\sqrt{N_c}} (S_{(2)R}^0 + iS_{(2)I}^0) \, \bar{d}_L^{(m)} d_R^{(n)} + \sqrt{2}(O_{(2)R}^{0,a} + iO_{(2)I}^{0,a}) \, \bar{d}_L^{(m)} \boldsymbol{T}^a d_R^{(n)} + \text{h.c.} \right],
$$
(6.31)

where

$$
(\Delta\tilde{g}_h^d)_{mn} \equiv - \frac{\sqrt{2}\pi}{L\epsilon} \, a_m^{(d)\dagger} \boldsymbol{S}_m^{(d)}(\pi^-) \boldsymbol{Y}_d^\dagger \boldsymbol{S}_n^{(D)}(\pi^-) a_n^{(D)} \,.
$$
(6.32)

Based on the first bracket in (6.31), we see that flavor-changing transitions can only be induced by the quantities $\delta_{d,D}$ and $\Delta\tilde{g}_h^d$, whose size is of $\mathcal{O}(v^2/M_{\text{KK}}^2)$. When we calculate a diagram exchanging one of the scalar fields and perform the low energy limit, the Wilson coefficient can be estimated to be of order $v^4/(m_S^2 M_{\text{KK}}^4)$, where m_S denotes the scalar mass coming from the internal propagator. Hence, we expect the scalar contributions to be numerically insignificant, when compared with the strong and electroweak ones.

---

[3]Note that the result ignores the rescaling of the Yukawa matrices in (2.62). Still, this approximation is sufficient for our purpose here.

Constraints for v_1 and v_2

Returning to the Yukawa terms (6.4) in our extended model, we can insert the VEVs for $\Phi^{(1)}$, $\Phi^{(2)}$ and obtain

$$\mathcal{L}_{\text{FS},Y} \ni -\sqrt{|G|}\,\delta(x_5 - r\pi)\left[\frac{v_2}{\sqrt{2N_c}}\,\bar{d}\,\boldsymbol{Y}_d^{(5)}d^c + \frac{v_1}{\sqrt{2N_c}}\,\bar{u}\,\boldsymbol{Y}_u^{(5)}u^c + \text{h.c.}\right], \qquad (6.33)$$

showing that v_1 sets the mass scale for the up- and v_2 for the down-type quarks. We can achieve agreement with the Minimal model, see (2.52), by imposing

$$v_1 = v_2 = \sqrt{N_c}\,v \approx 426\,\text{GeV} . \qquad (6.34)$$

But this turns out to be in conflict with the demand to reproduce the correct $W^\pm$ and Z masses, as will be shown in the next section 6.1, where v_1 and v_2 must at least fulfill the following inequality

$$v_1^2 + v_2^2 \leq v^2 . \qquad (6.35)$$

While we can not circumvent this condition (6.35), the quark masses are not determined singly by the Yukawa terms in (6.33), but also by the bulk parameters. In our model, their ZMA expressions are given by (compare with (2.80))

$$m_{u_i} \approx \frac{v_1 Y_\star}{\sqrt{2N_c}}|F(c_{Q_i})F(c_{u_i})|, \qquad m_{d_i} \approx \frac{v_2 Y_\star}{\sqrt{2N_c}}|F(c_{Q_i})F(c_{d_i})|, \qquad (6.36)$$

where we have abbreviated the Yukawa entries with $Y_\star$ for simplification. So, instead of imposing condition (6.34), we can also obtain the correct quark masses by properly redefining the zero-mode wavefunctions,

$$F(c_{u_i}) \to \sqrt{N_c}\frac{v}{v_1}F(c_{u_i}) \equiv F(\tilde{c}_{u_i}), \qquad F(c_{d_i}) \to \sqrt{N_c}\frac{v}{v_2}F(c_{d_i}) \equiv F(\tilde{c}_{d_i}), \qquad (6.37)$$

which results in a shift of the (singlet) c-parameters, denoted by $\tilde{c}_{u_i,d_i}$, towards larger values. Hence, the quark profiles get pushed in direction towards the IR brane. But, this may mitigate the RS GIM suppression and therefore would affect our numerical analysis in section 5.2. However, to see how strong the impact on ϵ_K really is, one has to repeat the analysis with new parameter sets, containing the shifted bulk parameters $\tilde{c}_{u_i}$ and $\tilde{c}_{d_i}$.

6.1. Gauge Boson Masses

To calculate the mass terms for the gauge bosons, we need to consider the kinetic terms of the scalar fields, that have a nontrivial transformation behavior under G_c, yielding

$$S_{\text{HS}}^{(5)} \ni \int d^4x \int_{-r\pi}^{r\pi} dx_5 \left\{ \delta(|x_5|)\text{Tr}\left[(D_\mu\Phi^{(0)})^\dagger(D^\mu\Phi^{(0)})\right] \right.$$
$$\left. + \delta(|x_5| - \pi r)\sum_{x=1,2}\text{Tr}\left[(D_\mu\Phi^{(x)})^{i\dagger}(D^\mu\Phi^{(x)})^i\right] \right\} . \qquad (6.38)$$

It is convenient to rewrite the appearing covariant derivatives, see (6.10) and (6.11), by rotating $W^\pm$, Z, A to their known mass eigenstates in (2.31) and by replacing G_D and G_S with the gluon and pseudo-axial gluon combinations via

$$\begin{pmatrix} G \\ \mathcal{A} \end{pmatrix} = \frac{1}{\sqrt{g_{D5}^2 + g_{S5}^2}} \begin{pmatrix} g_{S5} & g_{D5} \\ -g_{D5} & g_{S5} \end{pmatrix} \begin{pmatrix} G_D \\ G_S \end{pmatrix}, \qquad (6.39)$$

where $g_{s5} = g_{D5}\cos\vartheta = g_{S5}\sin\vartheta$ and which agrees with (5.10). Up to terms mixing two fields, we find

$$(D_\mu \Phi^{(0)})_{\alpha\bar\alpha} = \frac{ig_{s5}v_0 T^a_{\alpha\bar\alpha}}{\sqrt{2N_c}\sin\vartheta\cos\vartheta} \mathcal{A}^a_\mu + \partial_\mu \Phi^{(0)}_{\alpha\bar\alpha} + \text{ bilinear terms,}$$

$$(D_\mu \hat\Phi) = \begin{pmatrix} \frac{-ig_5\hat v}{2} W^+_\mu \\ \frac{ig_5\hat v}{2\sqrt{2}\cos\theta_W} Z_\mu \end{pmatrix} + \partial_\mu \hat\Phi + \text{ bilinear terms,}$$

$$(D_\mu \Phi^{(1)})_{\alpha\bar\alpha} = \begin{pmatrix} \frac{-ig_5 v_1 \delta_{\alpha\bar\alpha}}{2\cos\theta_W\sqrt{2N_c}} Z_\mu + \frac{ig_{s5}v_1 T^a_{\alpha\bar\alpha}}{\sqrt{2N_c}\sin\vartheta\cos\vartheta} \mathcal{A}^a_\mu \\ \frac{-ig_5 v_1 \delta_{\alpha\bar\alpha}}{2\sqrt{N_c}} W^-_\mu \end{pmatrix} + \partial_\mu \Phi^{(1)}_{\alpha\bar\alpha} + \text{ bilinear terms,}$$

$$(D_\mu \Phi^{(2)})_{\alpha\bar\alpha} = \begin{pmatrix} \frac{-ig_5 v_2 \delta_{\alpha\bar\alpha}}{2\sqrt{N_c}} W^+_\mu \\ \frac{ig_5 v_2 \delta_{\alpha\bar\alpha}}{2\cos\theta_W\sqrt{2N_c}} Z_\mu + \frac{ig_{s5}v_2 T^a_{\alpha\bar\alpha}}{\sqrt{2N_c}\sin\vartheta\cos\vartheta} \mathcal{A}^a_\mu \end{pmatrix} + \partial_\mu \Phi^{(2)}_{\alpha\bar\alpha} + \text{ bilinear terms,}$$

$$(6.40)$$

where again the vector notation refers to the isospin. Using these expression in (6.38), we can read off the 5D mass terms, yielding

$$S^{(5)}_{\text{HS}} \ni \int d^4x \int_{-\pi r}^{\pi r} dx_5 \left\{ \delta(|\phi|) \frac{(M_{\mathcal{A}}^{\text{UV}})^2}{2} \mathcal{A}^a_\mu \mathcal{A}^{a\mu} \right.$$
$$\left. + \delta(|\phi| - \pi) \left[\frac{(M_{\mathcal{A}}^{\text{IR}})^2}{2} \mathcal{A}^a_\mu \mathcal{A}^{a\mu} + M_W^2 W^+_\mu W^{-\mu} + \frac{M_Z^2}{2} Z_\mu Z^\mu \right] \right\}, \quad (6.41)$$

with

$$M_{G,A} = 0, \qquad M_W = \frac{g_5\sqrt{v_1^2 + v_2^2 + \hat v^2}}{2}, \qquad M_Z = \frac{M_W}{\cos\theta_W}, \qquad (6.42)$$

$$M_{\mathcal{A}}^{\text{UV}} = \frac{g_{s5}\, v_0}{\sqrt{2N_c}\sin\vartheta\cos\vartheta}, \qquad M_{\mathcal{A}}^{\text{IR}} = \frac{g_{s5}\sqrt{v_1^2 + v_2^2}}{\sqrt{2N_c}\sin\vartheta\cos\vartheta}. \qquad (6.43)$$

We can compare M_W and M_Z with the expressions of the Minimal RS model in (2.32). Since we have to reproduce the correct masses, the following condition must be fulfilled

$$v_1^2 + v_2^2 + \hat v^2 = v^2, \qquad (6.44)$$

which led to the inequality mentioned before in (6.35). Concerning the pseudo-axial gluon, there is a mass term on each of the two branes. While $M_{\mathcal{A}}^{\text{UV}}$ stems from the vacuum expectation value of the $\Phi^{(0)}$ field, $M_{\mathcal{A}}^{\text{IR}}$ includes the contributions from the VEVs of $\Phi^{(1)}$ and $\Phi^{(2)}$.

Matching and EOM for the Pseudo-Axial Gluon

In order to link the mass terms to the boundary conditions of the pseudo-axial gluon, we have to perform a matching calculation and derive the EOM for its profile functions. We start by considering at most quadratic fields, that contain the pseudo-axial gluon, yielding

$$
-\frac{1}{4}(\partial_{[\mu} A^a_{\nu]})^2 + \frac{1}{2} e^{-2\sigma}(\partial_\mu A^a_5)^2 - \frac{1}{2} A^a_\mu (\partial_5 e^{-2\sigma} \partial_5 A^{a\mu}) - (\partial_\mu A^{a\mu})(\partial_5 e^{-2\sigma} A^a_5)
$$
$$
+ \delta(|x_5|)\left[M^{\mathrm{UV}}_{\mathcal{A}}(\partial_\mu O^{0,a}_{(0)I})\mathcal{A}^{a\mu} + \frac{1}{2}(M^{\mathrm{UV}}_{\mathcal{A}})^2 \mathcal{A}^a_\mu \mathcal{A}^{a\mu} \right]
$$
$$
+ \delta(|x_5| - \pi)\left[M^{(1)}_{\mathcal{A}}(\partial_\mu O^{0,a}_{(1)I})\mathcal{A}^{a\mu} + M^{(2)}_{\mathcal{A}}(\partial_\mu O^{0,a}_{(2)I})\mathcal{A}^{a\mu} + \frac{1}{2}(M^{\mathrm{IR}}_{\mathcal{A}})^2 \mathcal{A}^a_\mu \mathcal{A}^{a\mu} \right] . \quad (6.45)
$$

The terms in the first line stem from $\mathcal{L}_{\mathcal{A}}$ in appendix A.17, when one writes out the μ- and 5-components of $\mathcal{A}^a_M$ (including partial integrations). The remaining two lines are obtained from the kinetic terms in (6.38). Concerning the brane localized terms, we see that $\mathcal{A}$ couples to three neutral octet fields. We further defined

$$
M^{(x)}_{\mathcal{A}} \equiv \frac{g_{s5} v_x^2}{\sqrt{2N_c}\sin\vartheta\cos\vartheta} \qquad \text{for} \quad x = 1, 2, \quad (6.46)
$$

which are the single mass terms stemming from $\Phi^{(1)}$ and $\Phi^{(2)}$. Adding their squared values gives

$$
(M^{\mathrm{IR}}_{\mathcal{A}})^2 = (M^{(1)}_{\mathcal{A}})^2 + (M^{(2)}_{\mathcal{A}})^2 . \quad (6.47)
$$

The problematic terms in (6.45) mix $\mathcal{A}^a_\mu$ with $\mathcal{A}^a_5$ or with one of the octets. As in the Minimal RS model (2.33), we can choose a suitable gauge-fixing Lagrangian to eliminate those terms,

$$
\mathcal{L}^{\mathcal{A}}_{\mathrm{GF}} = -\frac{1}{2\xi_{\mathcal{A}}}\Bigg(\partial_\mu A^{a\mu} - \xi_{\mathcal{A}}\Big[\delta(|x_5|)M^{\mathrm{UV}}_{\mathcal{A}} O^{0,a}_{(0)I} + \delta(|x_5| - \pi)\big\{ M^{(1)}_{\mathcal{A}} O^{0,a}_{(1)I} + M^{(2)}_{\mathcal{A}} O^{0,a}_{(2)I} \big\}
$$
$$
+ \partial_5 e^{-2\sigma} \mathcal{A}^a_5 \Big]\Bigg)^2 . \quad (6.48)
$$

Adding $\mathcal{L}^{\mathcal{A}}_{\mathrm{GF}}$ to (6.45) and including also the kinetic terms for the relevant octets, see (6.27), we find

$$
-\frac{1}{4}(\partial_{[\mu} A^a_{\nu]})^2 - \frac{1}{2\xi_{\mathcal{A}}}(\partial_\mu \mathcal{A}^{a\mu})^2 + \frac{1}{2} e^{-2\sigma}(\partial_\mu A^a_5)^2
$$
$$
-\frac{1}{2} A^a_\mu (\partial_5 e^{-2\sigma} \partial_5 A^{a\mu}) + \delta(|x_5|)\frac{1}{2}(M^{\mathrm{UV}}_{\mathcal{A}})^2 \mathcal{A}^a_\mu \mathcal{A}^{a\mu} + \delta(|x_5| - \pi)\frac{1}{2}(M^{\mathrm{IR}}_{\mathcal{A}})^2 \mathcal{A}^a_\mu \mathcal{A}^{a\mu}
$$
$$
-\frac{\xi_{\mathcal{A}}}{2}\left[\delta(|x_5|)M^{\mathrm{UV}}_{\mathcal{A}} O^{0,a}_{(0)I} + \delta(|x_5| - \pi)\big\{ M^{(1)}_{\mathcal{A}} O^{0,a}_{(1)I} + M^{(2)}_{\mathcal{A}} O^{0,a}_{(2)I} \big\} + \partial_5 e^{-2\sigma} \mathcal{A}^a_5 \right]^2
$$
$$
+ \delta(|x_5|)\frac{1}{2}(\partial_\mu O^{0,a}_{(0)I})^2 + \delta(|x_5| - \pi)\frac{1}{2}\left[(\partial_\mu O^{0,a}_{(1)I})^2 + (\partial_\mu O^{0,a}_{(2)I})^2 \right] . \quad (6.49)
$$

Inserting the KK decompositions for the pseudo-axial gluon in (5.14), we can integrate (6.49) along x_5 and try to match it on a sensible 4D theory. We do not give the calculation steps here, but refer to [29], where the general procedure is discussed in detail for the Z boson within the Minimal RS model. Adapted to our case, we can infer the equation of motion of the pseudo-axial gluon from the second line in (6.49), yielding

$$-\partial_5 e^{-2\sigma} \partial_5 \chi_n^{\mathcal{A}} = (m_n^{\mathcal{A}})^2 \chi_n^{\mathcal{A}} - \delta(|x_5|)(M_{\mathcal{A}}^{\mathrm{UV}})^2 \chi_n^{\mathcal{A}} - \delta(|x_5| - \pi)(M_{\mathcal{A}}^{\mathrm{IR}})^2 \chi_n^{\mathcal{A}} \,. \quad (6.50)$$

For the remaining terms, it is convenient to decompose the octet fields in terms of the basis fields $\varphi_{\mathcal{A}}^{(n)a}$, that are the 4D modes when decomposing $\mathcal{A}_5$ as in (5.14). So, we can write

$$O_{(0)I}^{0,a} = \sum_n b_n^{\mathcal{A},0} \varphi_{\mathcal{A}}^{(n)a}, \qquad O_{(1)I}^{0,a} = \sum_n b_n^{\mathcal{A},1} \varphi_{\mathcal{A}}^{(n)a}, \qquad O_{(2)I}^{0,a} = \sum_n b_n^{\mathcal{A},2} \varphi_{\mathcal{A}}^{(n)a}, \quad (6.51)$$

with coefficients $b_n^{\mathcal{A},0}$, $b_n^{\mathcal{A},1}$ and $b_n^{\mathcal{A},2}$ to be determined by the matching procedure. Performing all steps, we finally obtain the conditions

$$a_n^{\mathcal{A}} = -\frac{1}{m_n^{\mathcal{A}}}, \qquad b_n^{\mathcal{A},0} = \frac{M_{\mathcal{A}}^{\mathrm{UV}}}{\sqrt{r}} \frac{\chi_n^{\mathcal{A}}(0^+)}{m_n^{\mathcal{A}}}, \qquad b_n^{\mathcal{A},x} = \frac{M_{\mathcal{A}}^{(x)}}{\sqrt{r}} \frac{\chi_n^{\mathcal{A}}(\pi^-)}{m_n^{\mathcal{A}}}, \quad (6.52)$$

for $x = 1, 2$. Thus, on the basis of these conditions we can integrate (6.49) along the extra-dimension leading to the following 4D action

$$\int d^4x \sum_n \left\{ -\frac{1}{4} (\partial_{[\mu} \mathcal{A}_{\nu]}^{(n)a})^2 - \frac{1}{2\xi_{\mathcal{A}}} (\partial_\mu \mathcal{A}^{(n)a\mu})^2 + \frac{(m_n^{\mathcal{A}})^2}{2} \mathcal{A}_\mu^{(n)a} \mathcal{A}^{(n)a\mu} \right.$$

$$\left. + \frac{1}{2} (\partial_\mu \varphi_{\mathcal{A}}^{(n)a})^2 - \frac{\xi_{\mathcal{A}} (m_n^{\mathcal{A}})^2}{2} \varphi_{\mathcal{A}}^{(n)a} \varphi_{\mathcal{A}}^{(n)a} \right\}, \quad (6.53)$$

where the field $\varphi_{\mathcal{A}}^{(n)a}$ represents for each mode the longitudinal degree of freedom of the pseudo-axial gluon mode $\mathcal{A}^{(n)a\mu}$.

Boundary Conditions for the Pseudo-Axial Gluon

Switching to t-notation, we can integrate the EOM in (6.50) along small intervals around the branes. Making use of the relations (A.11) and (A.9), we obtain the following BCs

$$\partial_t \chi_n^{\mathcal{A}}(t)\big|_{t=\epsilon^+} = \frac{v_0^2 \epsilon}{M_{\mathrm{KK}}^2} \frac{L g_s^2}{2N_c \sin^2 \vartheta \cos^2 \vartheta} \chi_n^{\mathcal{A}}(\epsilon^+), \quad (6.54)$$

$$\partial_t \chi_n^{\mathcal{A}}(t)\big|_{t=1^-} = -\frac{(v_1^2 + v_2^2)}{M_{\mathrm{KK}}^2} \frac{L g_s^2}{2N_c \sin^2 \vartheta \cos^2 \vartheta} \chi_n^{\mathcal{A}}(1^-) \,. \quad (6.55)$$

In section (5.1), we discussed the boundary parameters (5.33), that were parametrized through ζ_ϵ and ζ_1. Comparing them with (6.54) and (6.55), we can identify

$$\zeta_\epsilon \equiv \frac{v_0\,\epsilon}{M_{\mathrm{KK}}}, \qquad\qquad \zeta_1 \equiv \sqrt{\frac{v_1^2 + v_2^2}{v^2}}\ . \qquad (6.56)$$

We see that ζ_1 must be smaller than one, due to the condition (6.44). This justifies the parameter range $[0.1, 10]$ for ζ_1, that had been assumed in the numerical section 5.2.3. There, we also recognized that the exact value of ζ_ϵ is not of relevance, as long as it is not of order ϵ. Due to (6.56), this will not be the case for natural values $v_0 \sim M_{\mathrm{Pl}} \sim M_{\mathrm{EW}}/\epsilon$.

6.2. Scalar Potentials

For the potentials V_{UV} and V_{IR} in (6.6) and (6.7), one has to write down all possible terms, that are hermitian, Lorentz invariant and that respect the symmetry under the complete gauge group G in (6.2). We further limit ourselves to operator terms up to mass dimension four.

UV Brane

Let us start with the potential at the UV brane, which is made up of one field $\Phi^{(0)}$, that is only charged under $SU(3)_D \times SU(3)_S$. With respect to the symmetries, the most general potential reads

$$\begin{aligned}
V_{\mathrm{UV}}(\Phi^{(0)}) = &-\mu_c^{(0)}\mathrm{Tr}\big[\Phi^{(0)\dagger}\Phi^{(0)}\big] + \lambda_{c1}^{(0)}\mathrm{Tr}\big[\Phi^{(0)\dagger}\Phi^{(0)}\big]\,\mathrm{Tr}\big[\Phi^{(0)\dagger}\Phi^{(0)}\big] \\
&+ \lambda_{c2}^{(0)}\mathrm{Tr}\big[\Phi^{(0)\dagger}\Phi^{(0)}\Phi^{(0)\dagger}\Phi^{(0)}\big] \\
&+ \big(e^{(0)}\,\epsilon_{\alpha\beta\gamma}\epsilon_{\bar\alpha\bar\beta\bar\gamma}\,\Phi^{(0)}_{\alpha\bar\alpha}\Phi^{(0)}_{\beta\bar\beta}\Phi^{(0)}_{\gamma\bar\gamma}\ + \mathrm{h.c.}\big)
\end{aligned} \qquad (6.57)$$

with real parameters $\mu_c^{(0)}$, $\lambda_{c1}^{(0)}$, $\lambda_{c2}^{(0)}$ and one complex parameter $e^{(0)}$. Note that the trace notation is again just a convenient way to pair the $SU(3)_D$ ($SU(3)_S$) indices α ($\bar\alpha$), analog to (6.9). The last term in (6.57) represents a fully antisymmetric product of $SU(3)_D$ ($SU(3)_S$) indices and is an invariant scalar under G_c, since

$$\begin{aligned}
\epsilon_{\alpha\beta\gamma}\epsilon_{\bar\alpha\bar\beta\bar\gamma}\,\Phi^{(0)}_{\alpha\bar\alpha}\Phi^{(0)}_{\beta\bar\beta}\Phi^{(0)}_{\gamma\bar\gamma}\ &\xrightarrow{\ G_c\ }\ \epsilon_{\alpha\beta\gamma}\epsilon_{\bar\alpha\bar\beta\bar\gamma}U^D_{\alpha\alpha'}U^D_{\beta\beta'}U^D_{\gamma\gamma'}U^{S*}_{\bar\alpha\bar\alpha'}U^{S*}_{\bar\beta\bar\beta'}U^{S*}_{\bar\gamma\bar\gamma'}\Phi^{(0)}_{\alpha'\bar\alpha'}\Phi^{(0)}_{\beta'\bar\beta'}\Phi^{(0)}_{\gamma'\bar\gamma'} \\
&= \det(U^D)\det(U^{S*})\epsilon_{\alpha'\beta'\gamma'}\epsilon_{\bar\alpha'\bar\beta'\bar\gamma'}\Phi^{(0)}_{\alpha'\bar\alpha'}\Phi^{(0)}_{\beta'\bar\beta'}\Phi^{(0)}_{\gamma'\bar\gamma'}, \quad (6.58)
\end{aligned}$$

and $\det(U^D) = \det(U^{S*}) = 1$. Actually this term is important, since it prevents an additional global $U(1)$ symmetry invariance of the potential, which would have been allowed otherwise. This means that V_{UV} does not admit a larger symmetry group than G_c and we do not expect additional (physical) massless scalar fields.

IR Brane

The potential at the IR brane is more complicated, since it involves the three distinct scalar fields $\Phi^{(1)}$, $\Phi^{(2)}$ and $\hat{\Phi}$. We can split V_{IR} into seven sub-potentials, each including only terms made out of the fields that are given as arguments,

$$
\begin{aligned}
V_{\mathrm{IR}}(\Phi^{(1)}, \Phi^{(2)}, \hat{\Phi}) = {} & \hat{V}(\hat{\Phi}) + V^{(1)}(\Phi^{(1)}) + V^{(2)}(\Phi^{(2)}) + V_{\mathrm{mix}}^{(1,2)}(\Phi^{(1)}, \Phi^{(2)}) \\
& + \hat{V}_{\mathrm{mix}}^{(1)}(\Phi^{(1)}, \hat{\Phi}) + \hat{V}_{\mathrm{mix}}^{(2)}(\Phi^{(2)}, \hat{\Phi}) + \hat{V}_{\mathrm{mix}}^{(1,2)}(\Phi^{(1)}, \Phi^{(2)}, \hat{\Phi}) \,.
\end{aligned} \tag{6.59}
$$

Concerning the sub-potentials, that do not mix different fields, we find

$$
\hat{V}(\hat{\Phi}) = -\hat{\mu}^2 |\hat{\Phi}|^2 + \hat{\lambda}|\hat{\Phi}|^4, \tag{6.60}
$$

$$
\begin{aligned}
V^{(x)}(\Phi^{(x)}) = {} & -(\mu_c^{(x)})^2 \mathrm{Tr}\big[\Phi^{(x)i\dagger}\Phi^{(x)i}\big] + \lambda_{c1}^{(x)} \mathrm{Tr}\big[\Phi^{(x)i\dagger}\Phi^{(x)i}\big]\mathrm{Tr}\big[\Phi^{(x)j\dagger}\Phi^{(x)j}\big] \\
& + \lambda_{c2}^{(x)} \mathrm{Tr}\big[\Phi^{(x)i\dagger}\Phi^{(x)j}\big]\mathrm{Tr}\big[\Phi^{(x)j\dagger}\Phi^{(x)i}\big] \\
& + \lambda_{c3}^{(x)} \mathrm{Tr}\big[\Phi^{(x)i\dagger}\Phi^{(x)j}\Phi^{(x)i\dagger}\Phi^{(x)j}\big] \\
& + \lambda_{c4}^{(x)} \mathrm{Tr}\big[\Phi^{(x)i\dagger}\Phi^{(x)j}\Phi^{(x)j\dagger}\Phi^{(x)i}\big],
\end{aligned} \tag{6.61}
$$

for $x = 1, 2$ and where all appearing parameters are real. Comparing (6.61) with (6.57), there are further terms due to different combinations of the $SU(2)_L$ indices i and j. On the other hand, a fully antisymmetric term is not allowed, since $\Phi^{(x)}$ is charged under $U(1)_Y$. Proceeding with the remaining sub-potentials, the allowed terms mixing $\Phi^{(1)}$ with $\Phi^{(2)}$ and $\Phi^{(x)}$ with $\hat{\Phi}$ are included in

$$
\begin{aligned}
V_{\mathrm{mix}}^{(1,2)}(\Phi^{(1)}, \Phi^{(2)}) = {} & f_1 \mathrm{Tr}\big[\Phi^{(1)i\dagger}\Phi^{(1)i}\big]\mathrm{Tr}\big[\Phi^{(2)i\dagger}\Phi^{(2)i}\big] \\
& + f_2 \mathrm{Tr}\big[\Phi^{(1)i\dagger}\Phi^{(1)j}\big]\mathrm{Tr}\big[\Phi^{(2)j\dagger}\Phi^{(2)i}\big] \\
& + f_3 \mathrm{Tr}\big[\Phi^{(1)i\dagger}\Phi^{(2)i}\big]\mathrm{Tr}\big[\Phi^{(2)j\dagger}\Phi^{(1)j}\big] \\
& + f_4 \mathrm{Tr}\big[\Phi^{(1)i\dagger}\Phi^{(2)j}\big]\mathrm{Tr}\big[\Phi^{(2)j\dagger}\Phi^{(1)i}\big] \\
& + f_5 \mathrm{Tr}\big[\Phi^{(1)i\dagger}\Phi^{(1)i}\Phi^{(2)j\dagger}\Phi^{(2)j}\big] + f_6 \mathrm{Tr}\big[\Phi^{(1)i\dagger}\Phi^{(1)j}\Phi^{(2)j\dagger}\Phi^{(2)i}\big] \\
& + f_7 \mathrm{Tr}\big[\Phi^{(1)i\dagger}\Phi^{(2)i}\Phi^{(2)j\dagger}\Phi^{(1)j}\big] + f_8 \mathrm{Tr}\big[\Phi^{(1)i\dagger}\Phi^{(2)j}\Phi^{(2)j\dagger}\Phi^{(1)i}\big] \\
& + f_9\, \epsilon_{ik}\epsilon_{jl} \mathrm{Tr}\big[\Phi^{(1)i\dagger}\Phi^{(1)j}\big]\mathrm{Tr}\big[\Phi^{(2)k\dagger}\Phi^{(2)l}\big] \\
& + f_{10}\, \epsilon_{ik}\epsilon_{jl} \mathrm{Tr}\big[\Phi^{(1)i\dagger}\Phi^{(2)j}\big]\mathrm{Tr}\big[\Phi^{(2)k\dagger}\Phi^{(1)l}\big] \\
& + f_{11}\, \epsilon_{ik}\epsilon_{jl} \mathrm{Tr}\big[\Phi^{(1)i\dagger}\Phi^{(1)j}\Phi^{(2)k\dagger}\Phi^{(2)l}\big] \\
& + f_{12}\, \epsilon_{ik}\epsilon_{jl} \mathrm{Tr}\big[\Phi^{(1)i\dagger}\Phi^{(2)j}\Phi^{(2)k\dagger}\Phi^{(1)l}\big],
\end{aligned} \tag{6.62}
$$

$$
\begin{aligned}
\hat{V}_{\mathrm{mix}}^{(x)}(\Phi^{(x)}, \hat{\Phi}) = {} & c_1^{(x)}|\hat{\Phi}|^2 \mathrm{Tr}\big[\Phi^{(x)i\dagger}\Phi^{(x)j}\big] + c_2^{(x)}\hat{\Phi}^{i\dagger}\hat{\Phi}^j \mathrm{Tr}\big[\Phi^{(x)j\dagger}\Phi^{(x)i}\big] \\
& + c_3^{(x)}\, \epsilon_{ik}\epsilon_{jl}\hat{\Phi}^{i\dagger}\hat{\Phi}^j \mathrm{Tr}\big[\Phi^{(x)k\dagger}\Phi^{(x)l}\big],
\end{aligned} \tag{6.63}
$$

where all appearing coefficients are real numbers. Up to now, the potential V_{IR} admits an enlarged symmetry, since each field $\Phi^{(1)}$, $\Phi^{(2)}$, $\hat{\Phi}$ can transform under its

own $U(1)$ group while still keeping all terms invariant. This issue gets resolved, when we add the remaining sub-potential $V_{\text{mix}}^{(1,2)}$ restricting the global symmetry of V_{IR} to the complete group G. It is given by

$$
\begin{aligned}
\hat{V}_{\text{mix}}^{(1,2)}\big(\Phi^{(1)}, \Phi^{(2)}, \hat{\Phi}\big) = {}& d\,\epsilon_{ik}\,\hat{\Phi}^{i\dagger}\hat{\Phi}^{j\dagger}\text{Tr}\big[\Phi^{(1)k\dagger}\Phi^{(2)j}\big] \\
& + e_1\,\epsilon_{ij}\epsilon_{kl}\epsilon_{\alpha\beta\gamma}\epsilon_{\bar{\alpha}\bar{\beta}\bar{\gamma}}\,\hat{\Phi}^i\Phi_{\alpha\bar{\alpha}}^{(1)j}\Phi_{\beta\bar{\beta}}^{(1)k}\Phi_{\gamma\bar{\gamma}}^{(2)l} \\
& + e_2\,\epsilon_{kl}\epsilon_{\alpha\beta\gamma}\epsilon_{\bar{\alpha}\bar{\beta}\bar{\gamma}}\,\hat{\Phi}^{i\dagger}\Phi_{\alpha\bar{\alpha}}^{(2)i}\Phi_{\beta\bar{\beta}}^{(2)k}\Phi_{\gamma\bar{\gamma}}^{(1)l} \;+\; \text{h.c.}, \quad\quad (6.64)
\end{aligned}
$$

where d, e_1 and e_2 are in general complex numbers.

Concerning the count of parameters, the UV potential involves 1 complex and 3 real parameters, while we encounter 3 complex and 30 real parameters in case of the IR potential.

Requirements for SSB

Now, that we have the potential terms, the next step is to check if it can admit a spontaneous symmetry breakdown at the VEVs given in (6.22). In general, there are four conditions realistic potentials must comply [8]:

(1) Potential Value: In order to allow for a symmetry breakdown, the potential value at the assumed VEV must lie below the corresponding value when the fields are taken to be zero. In our case, this means

$$
V_{\text{UV}}\big(\langle\Phi^{(0)}\rangle\big) < V_{\text{UV}}(0), \quad\quad V_{\text{IR}}\big(\langle\Phi^{(1)}\rangle, \langle\Phi^{(2)}\rangle, \langle\hat{\Phi}\rangle\big) < V_{\text{IR}}(0,0,0), \quad\quad (6.65)
$$

which will lead to inequalities for the coefficient of both potentials.

(2) Extreme Value: To achieve a minimum at a VEV, it is necessary that the derivatives of the potential vanish at this point (critical point). Using the parametrization (6.17), this can be stated in our case as

$$
\frac{\partial V_{\text{UV}}}{\partial \phi_{(0)}^{i,A*}}\bigg|_0 = 0, \quad\quad\quad \frac{\partial V_{\text{IR}}}{\partial \hat{\Phi}^{i*}}\bigg|_0 = 0, \quad\quad\quad \frac{\partial V_{\text{IR}}}{\partial \phi_{(x)}^{i,A*}}\bigg|_0 = 0 \,. \quad\quad (6.66)
$$

where $i, x = 1, 2$ and $A = 0, 1, ..., 8$ and the subscript 0 denotes the evaluation at the VEVs in (6.22). With these equations, we can fix further parameters of the potentials.

(3) Minimum: We locally obtain a minimum at a critical point, when the Hessian matrix is positive-definite, meaning that all eigenvalues are larger than zero. But in our case, we expect some eigenvalues to be zero, due to the Goldstone bosons. This leads to a positive semi-definite Hessian and we can not use a simple criteria to decide whether it is a minimum or not.

(4) Boundedness from Below: To achieve a stable ground state, the potential must be bounded from below. This will further restrict certain parameter ranges for the coefficients.

While writing this thesis, we have completed the first two requirements and determined the Hessian matrix. Indeed we have found the expected eight zero-eigenvalues for V_{UV} as well as the eleven zero-eigenvalues for V_{IR}.

Summary & Outlook

This thesis deals with the ϵ_K obervable in the Randall-Sundrum model, that pushes new physics effects into high energy regions, making the model phenomenologically less attractive. We proposed an extension of the model by a pseudo-axial gluon that could mitigate the tension between the theoretical and the experimental value from a fine-tuning of $\mathcal{O}(1\%)$ to $\mathcal{O}(10\%)$ in the low M_{KK} range of 1-2 TeV. Since the results were not universal but relied on properties of the new gauge boson, we presented a basic treatment of the enlarged Higgs sector. The discussion was divided in the following way.

In the context of an effective field theory, we introduced the Standard Model and elaborated on the Gauge and Yukawa Hierarchy Problems that arise due to the naturalness principle (chapter 1). Being capable of solving both HPs by a warped extra dimension and by promoting the SM fields to five-dimensional bulk fields (except for the Higgs), we gave a detailed description of the Minimal Randall-Sundrum model (chapter 2). Within this framework, we derived a general expression for the five-dimensional gauge boson propagator, depending on the boundary conditions of the considered particle at the UV and IR brane (chapter 3). Thus equipped, we defined and explained the observable ϵ_K measuring indirect CP violation in the neutral Kaon sector (chapter 4). Within the SM, we calculated eight box diagrams for K^0-$\bar{K}^0$ mixing and justified the small theoretical value of $|\epsilon_K^{\mathrm{SM}}| \sim 10^{-3}$ with the GIM mechanism. Switching to the Randall-Sundrum model, we showed that the contributions to ϵ_K are dominated by the exchange of the complete gluon tower. Although the RS GIM mechanism was at work, the Wilson coefficients C_4^{RS} and C_5^{RS} received an additional strong chiral enhancement spoiling the suppression effect. In order to minimize these "dangerous" coefficients, we extended the strong gauge sector of the Minimal RS model by replacing the color gauge group with $G_c \equiv SU(3)_D \times SU(3)_S$, such that $SU(2)_L$ doublet and singlet fields transformed under different triplet representations (chapter 5). By rotating the gauge fields of G_c, we obtained mass eigenstates forming the known gluon and an additional massive pseudo-axial gluon, whose relative sign coupling to mixed chirality quarks played the key role for minimizing the gluon contributions in C_4^{RS} and C_5^{RS}. We calculated the combined effective Hamiltonian showing indeed that the leading contributions up to $\mathcal{O}(v^2/M_{KK}^2)$ cancel independently of the boundary conditions. Still, the BC types could not be chosen arbitrarily. While the (NN) case, leading to a massless pseudo-axial gluon, was directly discarded we further focused on the remaining (NM), (MN) and (MM) boundary conditions. The (NM) type implied a maximal mass of $m_0^{\mathcal{A}} \leq 0.235\, M_{KK}$ for the lowest mode, which is in contradiction with experimental measurements. On

the other hand, the (MN) BCs had to be excluded too, since it had forbidden to write down any Yukawa terms at the IR brane. The remaining (MM) case was a priori allowed and we parametrized the non-zero boundary conditions at the UV and IR brane by ζ_ϵ and ζ_1 respectively. Therewith we performed the numerical analysis and calculated for each of the 10000 physical parameter sets the ϵ_K values in the Minimal RS model as well as in the extended version of it. For a mixing angle of $\vartheta = 45°$ and $\zeta_\epsilon = 1/\epsilon$, we encountered a mitigation of the ϵ_K fine-tuning from $3\%\,(7\%)$ to $12\%\,(37\%)$ in the M_{KK} range of 1-2 TeV (2-3 TeV) . While the results stayed rather robust under variations of ϑ and ζ_ϵ, it demanded for ζ_1 a value near by or smaller than one: $\zeta_1 \lesssim 1$. To investigate allowed boundary conditions, we considered a minimal implementation of the new Higgs sector of our enlarged model (chapter 6). Due to the extended strong gauge group and the (MM) BCs of the pseudo-axial gluon, we needed at least three scalar fields located at the IR brane and one at the UV brane. We assumed sensible VEVs for these fields, that allowed for a breakdown of G_c to its diagonal subgroup, the color group $SU(3)_c$. Based on this, we calculated the $W^\pm$, Z boson mass terms and inferred the condition $\zeta_1 \leq 1$, which was consistent with the mitigation demand. At the end of the chapter we listed the potentials at the UV and IR brane, including all symmetry invariant terms up to mass dimension four. Finally we mentioned the criteria both potentials had to fulfill in order to allow for the assumed SSB and to turn our scalar sector into a realistic implementation.

As we have already mentioned in chapter 6, there are several questions that could not be settled yet and need for a further investigation:

- In our extended RS model, the mass terms of the up- and down-type quarks are smaller compared to the ones in the Minimal RS version. While this difference can be absorbed into the bulk parameters, resulting in a shift of the quark profiles towards the IR brane, the question raises how strong does this affect the contributions to ϵ_K.

- Concerning the potentials at the UV and IR brane, one has to determine the parameter ranges that allow for the spontaneous symmetry breakdown with the VEVs we have been assuming. Furthermore, one has to ensure that the new massive scalar octets and singlets are in agreement with current experimental exclusion bounds.

- While performing the matching calculation for the pseudo-axial gluon, we have seen that linear combinations of octets and singlets on the IR and UV brane were eaten to provide the longitudinal degrees of freedom for the pseudo-axial gluon. In this context, it is of general interest to understand how the degrees of freedom are distributed among the massless scalars of the potentials and the five-component of the gauge boson.

It is surely worthwhile to gain more insight into these subjects.

A. Collection of Calculations & Formulas

A.1. Randall-Sundrum Metric

Starting point is the gravity part of the classical Randall-Sundrum action in 2.19, which gives rise to the following 5D Einstein equation

$$\sqrt{|G|} \underbrace{\left(\frac{1}{2} R_{MN}^{(5)} R^{(5)} - R_{MN}^{(5)} \right)}_{G_{MN}^{(5)}} = \frac{1}{4 M_{\text{Pl}(5)}^3} \left(\Lambda^{(5)} \sqrt{|G|} G_{MN} + V_{\text{UV}} \sqrt{G^{\text{UV}}} G_{\mu\nu}^{\text{UV}} \delta_M^\mu \delta_N^\nu \delta(x_5) \right.$$

$$\left. + V_{\text{IR}} \sqrt{G^{\text{IR}}} G_{\mu\nu}^{\text{IR}} \delta_M^\mu \delta_N^\nu \delta(x_5 - r\pi) \right) . \qquad (A.1)$$

Using the ansatz 2.18 to calculate the Christoffel symbols $\Gamma_{MN}^P = \frac{1}{2} G^{PR}(\partial_M G_{NR} + \partial_N G_{RM} - \partial_R G_{MN})$, one finds only two non-vanishing types

$$\Gamma_{\mu\nu}^5 = -(\partial_5 \sigma) e^{-2\sigma} \eta_{\mu\nu} \qquad \text{and} \qquad \Gamma_{\mu 5}^\nu \equiv \Gamma_{5\mu}^\nu = -(\partial_5 \sigma) \delta_\mu^\nu . \qquad (A.2)$$

Straightforwardly, we can calculate the Ricci-tensor $R_{MN}^{(5)} = \partial_P \Gamma_{MN}^P - \partial_N \Gamma_{MP}^P + \Gamma_{PQ}^P \Gamma_{MN}^Q - \Gamma_{MN}^P \Gamma_{MP}^Q$ and derive the Ricci-scalar $R^{(5)} = R_{MN} G^{MN}$, to obtain the nonzero components of the 5D Einstein tensor $G_{MN}^{(5)}$,

$$G_{\mu\nu} = \left[3\partial_5^2 \sigma - 6(\partial_5 \sigma)^2 \right] \eta_{\mu\nu} \qquad \text{and} \qquad G_{55} = 6 (\partial_5 \sigma)^2 . \qquad (A.3)$$

Evaluating (A.1) for the (55)-component yields the solution

$$\sigma(\phi) = r|\phi| \sqrt{-\frac{\Lambda^{(5)}}{24 M_{\text{Pl}(5)}^3}}, \qquad (A.4)$$

which enforces a negative 5D cosmological constant. The above expression can only be considered as a solution, if equation (A.1) is also fulfilled for the remaining $(\mu\nu)$ components. Therefore one needs the first and second derivatives of $\sigma(\phi)$,

$$\partial_\phi \sigma(\phi) = \text{sgn}\phi \, k \qquad \text{and} \qquad \partial_\phi^2 \sigma(\phi) = 2rk \left[\delta(\phi) - \delta(\phi - \pi) \right], \qquad (A.5)$$

where we introduced the scale $k \equiv \sqrt{-\frac{\Lambda^{(5)}}{24 M_{\text{Pl}(5)}^3}}$ and took account of the 2π-periodicity in ϕ. Inserting the derivatives into (A.3) and finally into the Einstein equations fixes the "vacuum" energies to

$$V_{\text{UV}} = -V_{\text{IR}} = 24 M_{\text{Pl}(5)}^3 k . \qquad (A.6)$$

A.2. Useful Relations between ϕ and t

Based on the definition $t \equiv \epsilon e^{kr|\phi|}$, we can relate the differentials by

$$dt = \text{sgn}\phi \, krt \, d\phi = \text{sgn}\phi \, \frac{Lt}{\pi} \, d\phi \, . \tag{A.7}$$

When performing integrations over the fifth dimension, we can substitute t for ϕ, leading to

$$\int_{-\pi}^{\pi} d\phi \quad \longrightarrow \quad \frac{2\pi}{L} \int_{\epsilon}^{1} \frac{dt}{t} \qquad \text{and} \qquad \int_{-\pi}^{\pi} d\phi \, e^{\sigma(\phi)} \quad \longrightarrow \quad \frac{2\pi}{L\epsilon} \int_{\epsilon}^{1} dt \, . \tag{A.8}$$

Another convenient relation concerns the conversion of the boundary conditions

$$\partial_\phi \chi(\phi) \Big|_{0^+} = a \, \chi(0^+) \qquad \Longleftrightarrow \qquad \partial_t \chi(t) \Big|_{\epsilon^+} = \frac{a\pi}{L\epsilon} \, \chi(\epsilon^+), \tag{A.9}$$

$$\partial_\phi \chi(\phi) \Big|_{\pi^-} = b \, \chi(\pi^-) \qquad \Longleftrightarrow \qquad \partial_t \chi(t) \Big|_{1^-} = \frac{b\pi}{L} \, \chi(1^-), \tag{A.10}$$

where $\chi(\phi)$ is a general orbifold-even profile. Furthermore, such boundary conditions can be inferred from the following equation of motion

$$-\partial_5 e^{-2\sigma} \partial_5 \chi(\phi) = m_n^2 \chi(\phi) - \delta(|x_5|)\frac{2a}{r}\chi_n(\phi) + \delta(|x_5| - r\pi)\frac{2b\epsilon^2}{r}\chi(\phi), \tag{A.11}$$

by integrating (A.11) along small intervals around the UV and IR brane.

A.3. Kinetic Part of the Gluon and the Pseudo-Axial Gluon

In our extended RS model, the strong sector involves the gauge bosons G_D and G_S, whose field tensors are given by

$$(G_D^a)_{MN} = \partial_{[M}(G_D^a)_{N]} + g_{D5} \, f^{abc} \, (G_D^b)_M (G_D^c)_N, \tag{A.12}$$

$$(G_S^a)_{MN} = \partial_{[M}(G_S^a)_{N]} + g_{S5} \, f^{abc} \, (G_S^b)_M (G_S^c)_N. \tag{A.13}$$

Based on these, we can construct the kinetic action (without gauge fixing terms)

$$S_{\text{GBS}}^{(5)} \ni \int d^5x \sqrt{|G|} G^{KM} G^{LN} \left[-\frac{1}{4}(G_D^a)_{KL}(G_D^a)_{MN} - \frac{1}{4}(G_S^a)_{KL}(G_S^a)_{MN} \right], \tag{A.14}$$

and rotate to the mass eigenstates $G, \mathcal{A}$ via (6.39). After several steps, we obtain

$$S_{\text{GBS}}^{(5)} \ni \int d^5x \left[\mathcal{L}_G + \mathcal{L}_\mathcal{A} + \mathcal{L}_{G\mathcal{A}} \right], \tag{A.15}$$

105

with

$$\mathcal{L}_G = \sqrt{|G|}G^{KM}G^{LN}\left[-\frac{1}{4}G^a_{KL}G^a_{MN}\right], \tag{A.16}$$

$$\mathcal{L}_\mathcal{A} = \sqrt{|G|}G^{KM}G^{LN}\left[-\frac{1}{4}\partial_{[K}\mathcal{A}^a_{L]}\partial_{[M}\mathcal{A}^a_{N]} - g_{s5}(ct_\vartheta - tn_\vartheta)f^{abc}(\partial_K\mathcal{A}^a_L)\mathcal{A}^b_M\mathcal{A}^c_N\right.$$
$$\left.-\frac{g^2_{s5}}{4}(tn^2_\vartheta + ct^2_\vartheta)f^{abc}f^{ade}\mathcal{A}^b_K\mathcal{A}^c_L\mathcal{A}^d_M\mathcal{A}^e_N\right], \tag{A.17}$$

$$\mathcal{L}_{G\mathcal{A}} = \sqrt{|G|}G^{KM}G^{LN}\left[-g_{s5}f^{abc}(\partial_K G^a_L)\mathcal{A}^b_M\mathcal{A}^c_N - \frac{g_{s5}}{2}f^{abc}\partial_{[K}\mathcal{A}^a_{L]}G^b_{[M}\mathcal{A}^c_{N]}\right.$$
$$-\frac{1}{4}g^2_{s5}f^{abc}f^{ade}G^b_{[K}\mathcal{A}^c_{L]}G^d_{[M}\mathcal{A}^e_{N]}$$
$$-\frac{1}{2}g^2_{s5}f^{abc}f^{ade}G^b_K G^c_L\mathcal{A}^d_M\mathcal{A}^e_N$$
$$\left.-\frac{1}{2}g^2_{s5}(ct_\vartheta - tn_\vartheta)f^{abc}f^{ade}(G^b_{[K}\mathcal{A}^c_{L]})\mathcal{A}^d_M\mathcal{A}^e_N\right], \tag{A.18}$$

where $tn_\vartheta \equiv \tan\vartheta$ and $ct_\vartheta \equiv \cot\vartheta$.

B. Input Parameter

B.1. Standard Model Values

For the numerical analysis in section 5.2, we need the SM parameters listed below in table B.1. The stated quark masses are obtained from the experimental masses, which are given within the references in the $\overline{\text{MS}}$ scheme, by evolving them to the renormalization scale of 1.5 TeV.

Parameter	Value	Reference
m_u	(1.5 ± 1.0) MeV	[11]
m_c	(550 ± 40) MeV	[11]
m_t	(140 ± 5) GeV	[11]
m_d	(3.0 ± 2.0) MeV	[11]
m_s	(50 ± 15) MeV	[11]
m_b	(2.2 ± 0.1) GeV	[11]
λ	0.2253 ± 0.0007	[11]
A	$0.808^{+0.022}_{-0.015}$	[11]
$\bar{\rho}$	$0.132^{+0.022}_{-0.014}$	[11]
$\bar{\eta}$	0.341 ± 0.013	[11]
M_W	(80.399 ± 0.023) GeV	[11]
M_Z	(91.1876 ± 0.0021) GeV	[11]

Table B.1.: SM values.

B.2. Magic Numbers

The parameters are taken from [51],

$$a_i = (0.29, 0.69, 0.79, 1.1, 0.14)$$

$$b_i^{11} = (0.82, 0, 0, 0, 0), \qquad\qquad c_i^{11} = (0.016, 0, 0, 0, 0),$$

$$b_i^{22} = (0, 2.4, 0.011, 0, 0),$$
$$b_i^{23} = (0, 0.63, 0.17, 0, 0),$$
$$b_i^{32} = (0, 0.019, 0.028, 0, 0),$$
$$b_i^{33} = (0, 0.0049, 0.43, 0, 0),$$
$$b_i^{44} = (0, 0, 0, 4.4, 0),$$
$$b_i^{45} = (0, 0, 0, 1.5, 0.17),$$
$$b_i^{54} = (0, 0, 0, 0.18, 0),$$
$$b_i^{55} = (0, 0, 0, 0.061, 0.82),$$

$$c_i^{22} = (0, 0.23, 0.002, 0, 0),$$
$$c_i^{23} = (0, 0.018, 0.0049, 0, 0),$$
$$c_i^{32} = (0, 0.0028, 0.0093, 0, 0),$$
$$c_i^{33} = (0, 0.00021, 0.023, 0, 0),$$
$$c_i^{44} = (0, 0, 0, 0.68, 0.0055),$$
$$c_i^{45} = (0, 0, 0, 0.35, 0.0062),$$
$$c_i^{54} = (0, 0, 0, 0.026, 0.016),$$
$$c_i^{55} = (0, 0, 0, 0.013, 0.018) \,.$$

Bibliography

[1] L. Randall and R. Sundrum. Phys.Rev.Lett. **83** (1999) 3370–3373.

[2] S. Weinberg, *The Quantum Theory of Fields (Volume 1)*. Cambridge University Press, 1995.

[3] S. Weinberg, "What is Quantum Field Theory, and what did we think it is?", 1996. `arXiv:hep-th/9702027`.

[4] L. H. Ryder, *Quantum Field Theory*. Cambridge University Press, 1996.

[5] T.-P. Cheng and L.-F. Li, *Gauge theory of elementary particle physics*. Oxford University Press, 1984.

[6] M. Dine, "TASI Lectures on the Strong CP Problem", 2000. `arXiv:hep-ph/0011376`.

[7] L. Faddeev and V. Popov. Phys.Lett. **B25** (1967) 29–30.

[8] P. Langacker, *The Standard Model and Beyond*. CRC Press, 2010.

[9] N. Cabibbo. Phys.Rev.Lett. **10** (1963) 531–533.

[10] K. Makoto and M. Toshihide. Prog.Theo.Phys. **49** (1973) 652–657.

[11] K. Nakamura *et al.* J.Phys. **G37** (2010) 075021.

[12] L. Wolfenstein. Phys.Rev.Lett. **51** (1983) 1945–1947.

[13] Y. Grossman, "Introduction to Flavor Physics", 2010. `arXiv:1006.3534`.

[14] J. Berger and Y. Grossman. Phys.Lett. **B675** (2009) 365–370.

[15] M. Neubert, "Effective Field Theory and Heavy Quark Physics", 2005. `arXiv:hep-ph/0512222`.

[16] J. Polchinski, "Effective Field Theory and the Fermi Surface", 1992. `arXiv:hep-th/9210046`.

[17] G. P. Lepage, "What is Renormalization?", 1989. `arXiv:hep-ph/0506330`.

[18] G. Ecker, "Effective Field Theories", 2005. `arXiv:hep-ph/0507056`.

[19] M. E. Peskin and D. V. Schroeder, *An Introduction To Quantum Field Theory (Frontiers in Physics)*. Westview Press, 1995.

[20] R. Barbieri and G. Giudice. Nucl.Phys. **B306** (1988) 63.

[21] G. Nordström. Physikalische Zeitschrift **15** (1914) 504–506.

[22] T. Kaluza. Preussische Akademie der Wissenschaften. Berlin (1921) 966–972.

[23] O. Klein. Zeitschrift für Physik **A37** (1926) 895906.

[24] N. Arkani-Hamed, S. Dimopoulos, and G. Dvali. Phys.Lett. **B429** (1998) 263–272.

[25] E. Adelberger, J. Gundlach, B. Heckel, S. Hoedl, and S. Schlamminger. Prog.Part.Nucl.Phys. **62** (2009) 102–134.

[26] W. D. Goldberger and M. B. Wise. Phys.Rev.Lett. **83** (1999) 4922–4925.

[27] S. Casagrande, F. Goertz, U. Haisch, M. Neubert, and T. Pfoh. JHEP **2008** (2008) 094.

[28] S. Casagrande, "Flavor Physics and Electroweak Precision Tests in Randall-Sundrum Models", Master's thesis, Johannes-Gutenberg Universität Mainz, 2008.

[29] M. Bauer, "The Randall-Sundrum Model and its Effects on Meson Mixing and Rare B-Decays", Master's thesis, Johannes-Gutenberg Universität Mainz, 2009.

[30] K. Hwang and J. E. Kim, "Orbifold Compactification and Related Phenomenology", 2004. `arXiv:hep-ph/0411286`.

[31] M. Quiros, "New Ideas in Symmetry Breaking", 2003. `arXiv:hep-ph/0302189`.

[32] R. Sundrum, "Tasi 2004 Lectures: To the Fifth Dimension and Back", 2005. `arXiv:hep-th/0508134`.

[33] Y. Grossman and M. Neubert. Phys.Lett. **B474** (2000) 361–371.

[34] S. Chang, J. Hisano, H. Nakano, N. Okada, and M. Yamaguchi. Phys.Rev. **D62** (2000) 084025.

[35] R. Bertlmann, *Anomalies in Quantum Field Theory*. Clarendon Press, 1996.

[36] C. Csaki, Y. Grossman, P. Tanedo, and Y. Tsai. Phys.Rev. **D83** (2011) 073002.

[37] F. Goertz, *Warped Extra Dimensions: Flavor, Precision Tests and Higgs Physics*. PhD thesis, 2011. `arXiv:1112.6387`.

[38] C. Froggatt and H. B. Nielsen. Nucl.Phys. **B147** (1979) 277.

[39] K. Agashe, G. Perez, and A. Soni. Phys.Rev. **D71** (2005) 016002.

[40] C. Schmell, "The Inclusive Radiative Decay $\bar{B} \to X_s\gamma$ in the Randall-Sundrum Model", Master's thesis, Johannes-Gutenberg Universität Mainz, 2008.

[41] J. Mutschall, "Radiative B-Meson Decays in Warped Extra Dimensions", Master's thesis, Johannes-Gutenberg Universität Mainz, 2011.

[42] L. Randall and M. D. Schwartz. JHEP **0111** (2001) 003.

[43] O. Gedalia, G. Isidori, and G. Perez. Phys.Lett. **B682** (2009) 200–206.

[44] C. Delaunay, O. Gedalia, S. J. Lee, G. Perez, and E. Ponton. Phys.Lett. **B703** (2011) 486–490.

[45] M. Bauer, S. Casagrande, U. Haisch, and M. Neubert. JHEP **1009** (2010) 017.

[46] Y. Nir, "CP Violation - A New Era", 2001. `arXiv:hep-ph/0109090`.

[47] V. Weisskopf and E. P. Wigner. Zeitschrift für Physik **63** (1930) 54–73.

[48] L.-L. Chau. Phys.Rept. **95** (1983) 1–94.

[49] A. J. Buras, "Weak Hamiltonian, CP Violation and Rare Decays", 1998. `arXiv:hep-ph/9806471`.

[50] A. J. Buras and D. Guadagnoli. Phys.Rev. **D78** (2008) 033005.

[51] M. Ciuchini, V. Lubicz, L. Conti, A. Vladikas, A. Donini, *et al.* JHEP **9810** (1998) 008.

[52] M. Ciuchini, E. Franco, V. Lubicz, G. Martinelli, I. Scimemi, and L. Silvestrini. Nucl.Phys. **B523** (1998) 501–525.

[53] S. L. Glashow, J. Iliopoulos, and L. Maiani. Phys.Rev. **D2** (1970) 1285–1292.

[54] T. Inami and C. Lim. Prog.Theor.Phys. **65** (1981) 297.

[55] A. J. Buras, M. Jamin, and P. Weisz. Nucl.Phys. **B347** (1990) 491–536.

[56] J. Urban, F. Krauss, U. Jentschura, and G. Soff. Nucl.Phys. **B523** (1998) 40–58.

[57] J. Charles, O. Deschamps, S. Descotes-Genon, R. Itoh, H. Lacker, *et al.* Phys.Rev. **D84** (2011) 033005.

[58] M. Bauer, S. Casagrande, L. Gründer, U. Haisch, and M. Neubert. Phys.Rev. **D79** (2009) 076001.

[59] H. Davoudiasl, G. Perez, and A. Soni. Phys.Lett. **B665** (2008) 67–71.

[60] J. Santiago. JHEP **0812** (2008) 046.

[61] M. Bauer, R. Malm, and M. Neubert. Phys.Rev.Lett. **108** (2012) 081603.

[62] V. Khachatryan *et al.* Phys.Rev.Lett. **105** (2010) 211801.

[63] G. Aad *et al.* Phys.Lett. **B708** (2012) 37–54.

[64] C. Aubin, J. Laiho, and R. S. Van de Water. Phys.Rev. **D81** (2010) 014507.

[65] V. Lubicz and C. Tarantino. Nuov.Cim. **B123** (2008) 674–688.

[66] M. Martynov and A. Smirnov. Mod.Phys.Lett. **A24** (2009) 1897–1905.

Acknowledgments

First of all I would like to thank my advisor Matthias Neubert for giving me the opportunity to work on such an interesting topic and to be part of a very active research group. Very special thanks go to my roommate Martin Bauer, with whom I could work together and who is a very helpful and encouraging person. I am also thankful to Christoph Schmell, Daniel Wilhelm, Andreas Nink, Tobias Weiler, Till Martini and Paul Archer for proofreading. Furthermore, I want to express my gratitude to all members of the THEP group, who contributed their share in a pleasant atmosphere.

In connection to my talk about neutrinos, I am very thankful to Tobias Hurth for his support and interesting discussions.

I'm deeply thankful to Anna-Lisa Theisen, just for being herself.

This thesis is dedicated to my parents for their emotional and financial support throughout my studies.